THE UNIVERSITY *of* EDINBURGH

Foundation Technologies in Synthetic Biology: Tools for Use in Understanding Plant Immunity

John W. Moore

Doctor of Philosophy

The University of Edinburgh

2012

Abstract

The plant hormone salicylic acid (SA) is an essential activator of plant immune responses directed against biotrophic pathogens. The transcription cofactor NPR1 (Nonexpressor of *pathogenesis- related* (*PR*) genes 1) functions to transduce the SA signal into an operational response directed to limited pathogen damage. In the absence of pathogen, NPR1 protein resides in the cytoplasm as a large molecular weight oligomer held together by disulphide bonding. Initiation of defence signalling leads to changes in intracellular redox conditions that promote NPR1 momomer release. Translocation of monomeric NPR1 to the nucleus results in the activation of over 2200 immune-related genes in *Arabidopsis*. NPR1 lacks a canonical DNA-binding domain but is known to perform part of its regulatory function through engagement of TGA factors (bZIP transcription factor). Induction of SA-dependent signalling is invariably associated with *PR-1* gene expression and accumulation of mRNA for this gene serves as a useful marker of defence activation. However, both functional redundancy and stochastic factors limit the effectiveness of standard genetic approaches used in plant research, and thus much of the hierarchal processes surrounding NPR1-dependent gene activation are not fully understood.

Using a synthetic biology approach we aim to complete exploratory work and set the foundations for the development of a yeast tool that can be used to manipulate and subsequently understand NPR1 function in relation to interacting partners and gene activation. Accordingly, using this tool we sought to create a conceptual protein circuit based on theoretical plant immunity.

In completing this work we have developed a *Saccharomyces cerevisiae* strain that exhibits a highly oxidising intracellular redox environment. This was achieved by knocking out genes encoding *S*-nitrosoglutathione reductase (*SFA1*), flavohemoglobin (*YHB1*) and *YAP1* (bZIP transcription factor), all important components in regulating cellular redox homeostasis and protein *S*-nitrosylation state in *S. cerevisiae*. Characterisation of this cell (designated *Δsfa1yap1yhb1*) reveals a high tolerance to such redox perturbations. Importantly, NPR1 is by default, assembled predominantly in the oligomeric form in this biological chassis.

By activating two inducible inputs in the form of *Arabidopsis S*-nitrosoglutathione reductase (AtGSNOR) and Thioredoxin (AtTRXh5) which both function to promote NPR1 monomerisation, we have created a switch to selectively control NPR1 oligomer-monomer equilibrium. To complete the synthetic circuit, TGA3 was included, along with a modified yeast MEL1 promoter that has been customised to contain the TGA-responsive upstream activation sequence (termed the *as-1* element) present in the promoter region of the *PR-1* gene.

Using FRET tools we were able to confirm nuclear interaction between monomeric NPR1 and TGA3, with this association appearing to induce *as-1* element binding. However this process is not sufficient to activate a Luciferase (LUC) reporter gene, even when the GAL4 activation domain (GAL4 AD) is fused to NPR1. Ordinarily, a CUL3-dependent proteolysis-coupled transcription cycle is necessary to maintain efficient NPR1-dependent gene transcription in *Arabidopsis*. Although *S. cerevisiae* encodes an evolutionarily related CUL3 ortholog, examination by western blot demonstrates that NPR1 protein is stable in this cell, indicating an endogenous mechanism to degrade NPR1 is either not present or not functional in yeast. As such, this synthetic yeast tool represents a completely novel approach to identify missing components functioning in NPR1-mediated transcriptional regulation.

Furthermore, in collaboration with a skilled bioinformatician, and using a rule-based stochastic modeling tool known as Kappa, we have been able to develop, for the first time, a preliminary mathematical simulation representative of NPR1-dependent gene activation that can be used as a foundation for future works.

Declaration

I hereby declare that the work presented here is my own and has not been submitted in any form for any degree at this or any other university.

John W. Moore

Acknowledgements

Firstly, I would like to thank the EPSRC for providing the financial support for me to undertake this Ph.D.

I am incredibly grateful to my supervisors Prof. Gary Loake and Dr. Alistair Elfick.

To Gary; you have been hugely influential in moulding my career. It was through your lectures that I was introduced to the subject of molecular plant-pathogen interactions. You gave me the chance to complete an undergraduate summer placement in your lab, and it was this experience that reinforced my desire to pursue a career in academic research. You then gave me the opportunity to complete a Ph.D and for this I am forever indebted to you! I am now starting a career in a scientific field that I adore. I am especially grateful for the freedom you have given me and the support provided in allowing me to develop my own ideas.

To Alistair; thank you for allowing me to develop an appreciation of science from a synthetic biology perspective. It was because of your enthusiasm and encouragement that I was able to spend time in Beijing, San Francisco and of course the glamorous Glasgow.

A BIG thank you to Steven Spoel for taking me under his wing and teaching me the necessary attribute required for scientific endeavour and innovation. It was a real privilege to work under your technical excellence. You are the most incredible scientist I have ever met and I hope very much to work with you again in the future.

Thanks to Prof. Chengcai Chu, Dr. Yiqin Wang and the rest of the lab at the Chinese Academy of Sciences for allowing me to learn science the Chinese way! You are the kindest, most welcoming people I have met and I thoroughly enjoyed my few months working in the lab. I hope to return one day to see all of your smiling faces.

Thanks to Dr. David Kelly in the COIL facilities for your assistance with completing the microscope work. You might support a terrible football team but I'm hoping one day you will see the (black and white) light. Also thank you to the very efficient John Wilson-Kanamori for the help in devising the mathematical model.

Thank you to all past and present members of the lab for making day-to-day work thoroughly enjoyable and entertaining. A special thanks to my main men Byung-Wook Yun and Krieng Kanchanawatee for the many laughs.

I would especially like to thank my mutant Eunjung for your love, support and patience. You have a natural ability to make people happy and I consider myself to be a very lucky guy.

Last, but by no means least, I would like to thank my family for the continual encouragement over the years. I took the decision to better myself and you have all staunchly supported me along the way.

Thank you all for everything!

Table of Content

Contents

List of Figures

List of Tables

Abbreviations

AD	Activation Domain
ANK	Ankyrin repeat
as-1	activating sequence 1
Avr	Avirulence/avirulent
BAK1	BRI1 associated receptor kinase 1
BRCA2	Ortholog of BREAST CANCER SUSCEPTIBILITY PROTEIN 2
BTB	Broad-Complex, Tramtrack, Bric-a-brac
BTH	benzol (1,2,3) thiadiazole-7-cabothionic acid S-methyl ester
bZIP	Basic domain/leucine zipper
CC	Coiled-coil
CUL	Cullin
Cys	Cysteine
DTT	Dithiotreitol
ECFP	Enhanced Cyan Fluorescent Protein
EDS	Enhanced disease susceptibility
ET	Ethylene
ETI	Effector-triggered immunity
EYFP	Enhanced Yellow Fluorescent Protein
GFP	Green fluorescent protein
GRX	Glutaredoxin
GSH	Reduced glutathione
GSSG	Oxidised glutathione
GSNO	*S*-nitrosoglutathione
GSNOR	*S*-nitrosoglutathione reductase
H_2O_2	Hydrogen peroxide
HR	Hypersensitive response
ICS	Isochorismate synthase
INA	2,6-dichloroisonicotinic acid
JA	Jasmonic acid
Leu	leucine
LS	linker-scan
LUC	Luciferase
MAPK	Mitogen activated protein kinase
MeJA	Methyl jasmonate
MeSA	Methyl salicylate
MET	Methionine
NADPH	Nicotinamide adenine dinucleotide phosphate
NahG	Salicylate hydroxylase
NB-LRR	nucleotide binding, leucine-rich repeat
NDR1	SPECIFIC DISEASE RESISTANCE 1

NLS	Nuclear localization signal
NO	Nitric oxide
NPR1	Non-expressor of *PR* genes
NTRA	NADPH-dependent thioredoxin reductase
PAD	Phytoalexin deficient
PAMP	Pathogen-associated molecular pattern
PEG	Polyethylene glycol
POZ	Poxvirus, Zinc finger
Pst	*Pseudomonas syringae* pv. *tomato*
PR	Pathogenesis related
PRR	Pattern recognition receptor
PTI	PAMP-triggered immunity
R	Resistance
RAD51D	RAS ASSOCIATED WITH DIABETES PROTEIN 51 D
RBOH	Respiratory burst oxidase homolog
RLK	Receptor-like kinase
RLP	Receptor-like proteins
RNS	Reactive nitrogen species
ROI	Reactive oxygen intermediate
ROS	Reactive oxygen species
RT-PCR	Reverse transcript polymerase chain reaction
SA	Salicylic acid
SAI1	Salicylic acid insensitive 1
SAMT1	Salicylic acid methyl transferase 1
SAR	Systemic acquired resistance
SDS	Sodium dodecyl sulphate
Ser	Serine
SFA1	Yeast GSNOR
SID2	Salicylic acid induction deficient 2
SNO	*S*-nitrosothiol
SSN2	SUPPRESSOR OF SNI1 2
TGA	TGA-element binding bZIP transcription factor
TIR	Toll-interleukin 1 receptor
TLR	Toll-like receptors
TRX	Thioredoxin
TRXR	Thioredoxin Reductase
TTSS	Type-III secretion system
UAS	Upstream activating sequence
URA	Uracil
WRKY	Transcription factors containing a conserved WRKY domain
YAP1	bZIP transcription factor required for oxidative and nitrosative stress tolerance
YHB1	Flavohemoglobin (nitric oxide oxidoreductase)
YPD(A)	Yeast Peptone Dextrose (Agar)

CHAPTER 1

1. Introduction

1.1 Food Security

Domestication of plant species as crops marks a defining point in the history of humans. The conversion from transient hunter-gatherer to more static farming and pastoralism undoubtedly led to the establishment of densely-populated modern metropoli. For millennia the global population grew steadily with crude farming technologies sufficient to provide sustenance. However, the advent of the industrial and agricultural revolution, fuelled by advances in science, technology and engineering, led to an increase in the global productivity and subsequently net output of many consumable items including food. Combined with a generally improved socio-economic status, improving public-health management and healthcare this has led to a global population boom without placing significant strain on resources. That is until now. The Food and Agriculture Organization of the United Nations (FAO) identifies that between 1951 and 2005 the global population more than doubled from a population of ~3 billion to just over 6 billion. This is, and continues to be a global trend with the global population currently standing at ~7 billion and projected to rise to ~9.3 billion by 2050 (FAO, 2009).

A combination of many factors that include (but not limited to); the rapid progress and expansion of developing nations, changes in dietary habits, crop and animal disease, a reduction in arable land, climate change mean this rise, at present, is not sustainable. To illustrate this point, during the early 20th century, corn production in the US stood at approximately 1.6 tonnes/ha but through a combination of modern farming technologies and irrigation techniques, the use of genetically modified (GM) crops and fertilizer, this yield had increased to 9.5 tonnes/ha by 2009 (Edgerton, 2009). However, given the growing population and environmental pressures, this productivity is now not sufficient and food security is emerging as a major concern. To meet the global requirement for

not only food, but also livestock feed and fuel it is estimated that global production of cereal crops such as corn and wheat would need to increase by 15% before 2017 (Edgerton, 2009). However, suitable available land is limited and those regions with fertile soils with high yield potential have already been extensively cultivated. It is clear that in the near future extraordinary unchartered strain will be placed on the carrying capacity of the earth.

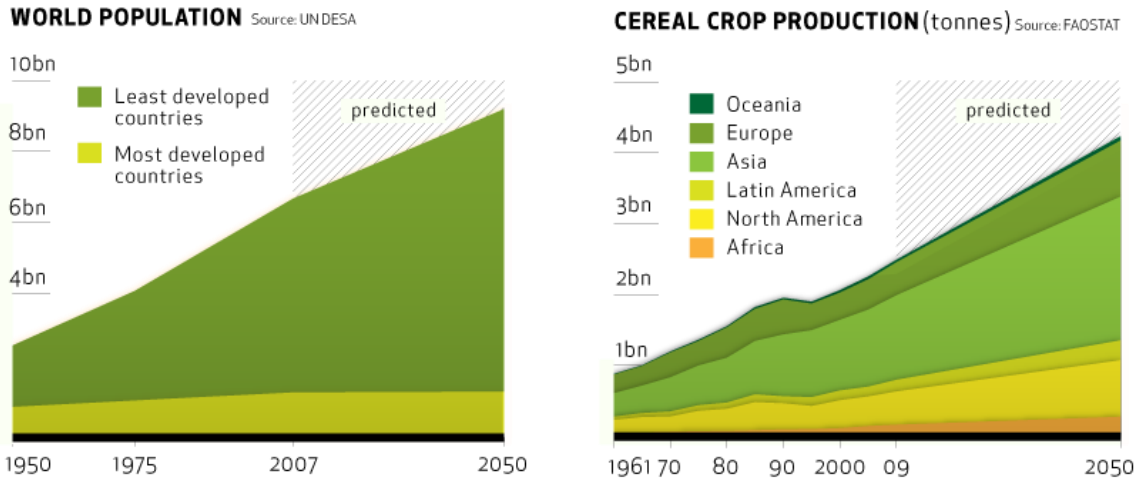

Figure 1-1 Graphical representation of the projected increase in global population by 2050 (left panel) coupled with the combined requirement for all geographical regions to contribute to a 70% increase in food production (right panel). Source: UN DESA and FAOSTAT. Graph obtained from http://www.farmingfirst.org/green-economy/?open=2#cropproduction

Losses in crop yield resulting from fungal and bacterial pathogens, and viruses amass to 12-15% of total crops produced each year (Shah, 1997; Oerke and Dehne, 2004). If this loss could be prevented, it would go some way to alleviate the pressure of increased production. In developing nations where chemical pesticides are not widely available, the current solutions to this problem include both selective breeding and/or transgene technology. For example, New Rice for Africa (NERICA) is a hybrid rice cultivar developed by the Africa Rice Center that aimed to cross and combine advantageous traits of African rice *Oryza glaberrima*, such as drought tolerance along with natural resistance to rice yellow mottle virus and blast disease (*Magnaporthe grisea*) with the high yield potential from an Asian variety *Oryza sativa*. Although still in development,

NERICA has been field tested in large regions of West Africa and data thus far indicates that this hybridised rice strain has the potential to provide many farming communities with a sustainable source of food (Gridley et al., 2002; WARDA/FAO/SAA., 2008). Plant breeding could be considered a game of "genetic roulette" as the correct combination of particular traits from parent plants must be present in progeny without causing adverse effects. This often means laborious screens to select particular characteristics. Meanwhile, transgene technology might be considered a much more direct and precise biotechnology strategy. However, like plant breeding, transgenic crops are often created without fully appreciating the underlying science. To date a wide variety of crop species, each with novel pathogen resistance traits are/have been developed and are undergoing field trials (Toenniessen et al., 2003). Perhaps best characterized is the transgene *Xa21*, that was originally identified in wild rice species *Oryza longistaminata* and provides resistance to bacterial blight, *Xanthomonas oryzae* pv. *oryzae* (*Xoo*). When transferred to domesticated rice species *O. sativa* in 1990, *Xa21* was found to confer broad-spectrum resistance to many races of this pathogen (Ikeda et al., 1990, Khush et al., 1990). However, it was not until 1995, that *Xa21* was fully characterised and found to encode a transmembrane, receptor-like kinase protein with pathogen-recognition capabilities (Song et al., 1995; Wang et al., 1996). In the following years the XA21 signalling cascade was extensively characterised and in 2008, it was described that WRKY transcription factors function downstream of XA21 activation to induce defence genes (Peng et al., 2008; Peng et al., 2010). Hence it has taken 18-20 years from originally generating the transgenic rice line to understanding the molecular mechanisms underpinning pathogen resistance. Designing crops in this manner is fundamentally not cost or time effective. Is it not more prudent to first understand the scientific mechanism underpinning a specific trait and then design an important agricultural or economic crop that displays that particular attribute? Elementary comprehension of the plant immune system should provide scope to achieve this goal.

1.2 The Plant Immune System

1.2.1 Pathogen Recognition, PTI and ETI – The Concept

Plants, in their natural environment are continually exposed to a variety of micro organisms, many of which are pathogens. Plants do not have specialised immune cells that have undergone extensive clonal selection to generate a vast repertoire of potential ligands, or an adaptive immune response whereby immune cells mount specific defence strategies. Instead plants rely on preformed physical barriers such as a waxy cuticle and lignified cell walls along with the ability to produce secondary metabolites such as phytoanticipins that collectively repel many potential pathogens (Nurnberger and Lipka., 2005; Ingle et al., 2006).

Those pathogens that breach constitutive defences activate an innate immune response. Plants recognise the presence of microbes via transmembrane receptor-like kinases (RLK) and/or transmembrane receptor-like proteins (RLP) collectively known as pattern recognition receptors (PRRs) that are triggered by so-called pathogen associated molecular patterns (PAMPs) (Fritz-Laylin et al, 2005). The *Arabidopsis* gene family that encode PRRs has undergone a dramatic expansion with the genome thought to encode ~600 RLK and ~57 RLP, many of which are responsive to pathogen stress and involved in defence signalling (Wang et al., 2008; Lehti-Shiu et al., 2009). By contrast, the human genome encodes just ten Toll-like receptors (equivalent to plant PRRs) (Barreiro et al., 2009). PAMPs typically form indispensable conserved structural components of a pathogen and recognition of such ligands, in plants, leads to PAMP-triggered immunity (PTI). One such example is flg22, a 22 amino acid structure present in bacterial flagella that is recognised by the PRR, FLS2 (flagellin sensing 2). Upon activation, FLS2 rapidly heteromerizes with LRR-receptor like kinase BAK1 (BRI1 associated receptor kinase 1) with subsequent phosphorylation of both FLS2 and BAK1 necessary to transduce the defence signal (Chinchilla et al., 2007; Schulze et al., 2010). FLS2-BAK1 signalling activates a MAP kinase cascade (consisting of MAPKKK - MKK4/MKK5 - MPK3/MPK6) that results in the induced expression of transcription

factors such as WRKY22 and WRKY29, and provides increased resistance to bacterial infection (Asai et al., 2002). Unfortunately, for the vast majority of PRRs, the intermediate signalling steps that establish PTI are poorly defined but often this immune response is characterised by rapid Ca^{2+} and ion fluxes, activation of numerous MAP kinases, the production of reactive-oxygen species (ROS) along with reprogramming of the defence transcriptome (Zipfel, 2008).

Successful gram-negative bacterial phytopathogens have evolved a collection of virulence factors (termed effectors) that can be injected into a plant cell via apparatus collectively termed the type III secretion system that function to disable select components of PTI (Jones and Dangl, 2006). Similarly, pathogenic fungi and oomycetes are able to deliver effectors into the plant cell using the haustoria and/or extrahaustorial matrix (Birch et al., 2008). A recent study indicates the presence of a consensus signal RXLR motif, common to a collection of oomycete effectors that mediates uptake of such proteins by the plant cell (Whisson et al., 2007). Effector translocation appears to require binding of the RXLR domain to phosphatidyl inositol phosphate (PIP) located on the plant cell membrane, but how such effectors enter the cytosol remains unknown (Kale et al., 2010).

Analysis of the plant-pathogen interactome in *Arabidopsis* has identified effectors that indirectly modulate plant immunity by targeting highly-connected proteins that function at the centre of complex networks essential for plant metabolic processes (Mukhtar et al., 2011). In order to counter this advantage, the *Arabidopsis* genome is equipped with a vast library of pathogen-specific resistance (*R)* genes, many of which encode a class of proteins that possess a nucleotide binding site–leucine rich repeat (NBS-LRR) domain. These R proteins are able to directly or indirectly detect microbial virulence factors and initiate defence signalling designated effector-triggered immunity (ETI), that typically culminates in localised cell death at the site of infection termed the hypersensitive response (HR) (Jones and Dangl, 2006). Sequence analysis of the *Arabidopsis* genome reveals ~150 potential genes that are thought to encode the NB-LRR class of R proteins (Dangl and Jones, 2001). R proteins are subcategorised based

on the structural arrangement of their N-terminus, with 60% belonging to Toll/Interleukin-1 Receptor (TIR) domain (TIR-NB-LRR) subclass and the remaining 40% belonging to the coiled-coil (CC) (CC-NB-LRR) subclass. Interestingly, this feature appears to specify their signal transduction properties. Although the intermediary stages are not clear, TIR-NB-LRR dependent signalling requires ENHANCED DISEASE SUSCEPTIBILITY 1 (EDS1) and PHYTOALEXIN-DEFICIENT4 (PAD4), while the glycophosphatidyl-inositol anchored plasma membrane protein NON-RACE-SPECIFIC DISEASE RESISTANCE 1 (NDR1) is essential for signalling by many CC-NB-LRR proteins (Aarts et al., 1998; Coppinger et al., 2004; Wiermer et al., 2005; Day et al., 2006).

1.2.2 Signalling Networks in Plant Immunity

The invasion strategies employed by various classes of plant pathogen differ, but generally these organisms are classified as being either necrotrophic or biotrophic (including hemibiotrophic) pathogens. Dependent on the life history of the pathogen encountered, the plant is able to specifically initiate signalling pathways that produce a specific assortment of anti-microbial compounds that defend against further pathogen colonisation. Specifically, the signalling molecule salicylic acid (SA) mediates the transcriptional transition to favour defence against biotrophic pathogens, while jasmonic acid (JA) performs the same function to restrict cellular damage by necrotophic pathogens and chewing insects. Emerging evidence couples ethylene (ET) to a key modulatory position within this system (Pieterse et al., 2009). Microarray analysis of a number of *Arabidopsis* mutants defective in SA, JA and ET was able to cluster groups of co-regulated genes and reveal the complex nature of this system (Tsuda et al., 2009). Significantly, each signalling cascade does not function independently, but instead forms part of a network that can operate antagonistically or synergistically to allow a cell to fine-tune responses specific to a type of pathogenic organism (Mur et al., 2006).

1.2.3 Systemic Acquired Resistance

Priming is a conditioning phenomenon that increases the action potential of a cell enabling quicker and more robust initiation of defensive transcriptional reprogramming compared to non-primed cells in response to inducing stimuli. In *Arabidopsis,* pathogen detection often results in the initiation of the hypersensitive response (HR), an apoptotic reaction at the site of infection. In addition, plants are capable of initiating a systemic immune response, termed systemic acquired resistance (SAR), that provides robust, long-term, broad-spectrum resistance to subsequent infection by a variety of potential pathogens (Ross, 1961).

Just how SAR is established is not clear. Plant hormones have emerged as key modulators of SAR with SA, in particular, fundamental to orchestrating SAR dynamics. It was initially assumed that SAR was regulated exclusively by SA, however recent work indicates it is likely that cohorts of independently-regulated, temporal transcription pulses contribute to this immune status (Moore et al., 2011). For example, it has been demonstrated that with JA along with transcripts associated with of JA biosynthesis (including *VSP2*, *CORI1*, *CORI3* and *MYC2*) accumulate transiently in distal tissue following pathogen challenge. This early systemic reprogramming precedes SA accumulation and is critical for the establishment of SAR (Truman., et al 2007). Crucially the transition from early JA accumulation to subsequent engagement of SA-dependent responses and SAR appears to be mediated, in part, by auxin transport and signalling. Perturbing auxin influx transporters AUX1 and AXR4 alters both JA and SA transitional signalling dynamics and compromises SAR (Truman., et al 2010). This indicates that distinct sequential hormonal phases, each performing a unique regulatory role, are potentially an essential requirement for the establishment of SAR.

This heightened defensive state is associated with the increased expression of a large number of pathogenesis-related genes (*PR* genes) in both local and distal tissue (Ward et al., 1991; Uknes et al., 1992). This model suggests the presence of an active mobile signal that is able to mobilise defence capabilities in distal tissue. In tobacco, methyl

salicylate (meSA) appears to be a critical mobile signal with the ability to induce *PR* gene expression in distal tissue. Grafting experiments demonstrated that SA methyl transferase (SAMT) is able to convert SA produced at the primary site of infection to biologically inactive methyl salicylate (MeSA). The vascular system then transports MeSA to distal tissue where it is converted back to SA by salicylic acid–binding protein 2 (SABP2), an enzyme with efficient methyl salicylate (MeSA) esterase activity, culminating in defence gene expression (Park et al., 2007). However, contradictory results in *Arabidopsis* question the validity of this observation. Firstly it was shown that pathogen-induced accumulation of MeSA did not correlate with SAR (Attaran et al., 2009). However it has since been demonstrated that functional inactivation of the gene responsible for synthesizing MeSA in *Arabidopsis*, namely BSMT1 (benzoic acid/SA carboxyl methyltransferase 1) disables SAR, while leaving PTI and ETI unaffected (Liu et al., 2010).

In addition, it has been shown that azelaic acid primes plants to accumulate SA and promotes local resistance and SAR. AZELAIC ACID INDUCED 1 (AZI1) encodes a secretary protein that is induced by azelaic acid, and appears to modulate or directly translocate a potential SAR signal from the site of infection to distal tissue (Jung et al., 2009). The exact structural nature of the long-distance SAR signal is not clear but some lines of evidence indicate a potential role for a lipid-derived molecule. Plants defective in DEFECTIVE IN INDUCED RESISTANCE 1 (DIR1), a lipid-transfer protein, exhibit fully functional local resistance but they are however, unable to establish SAR (Maldonado et al., 2002). Similarly mutations that affect glycerolipid metabolism (SUPPRESSOR OF FATTY ACID DESATURASE DEFICIENCY 1 (SFD1)) and chloroplast galactolipid metabolism (FATTY ACID DESATURASE 7 (FAD7), MONOGALACTOSYLDIACYLGLYCEROL SYNTHASE 1 (MGD1) and SUPPRESSOR OF FATTY ACID DESATURASE DEFICIENCY 2 (SFD2)) also abolish SAR while leaving local resistance intact (Nandi et al., 2004; Chaturvedi et al., 2008, Vlot et al., 2008). These observations have led to the suggestion that multiple signals function to produce, translocate and perceive the SAR signal, with the integrated

action of MeSA, DIR1 and SFD1 all necessary to establish functional SAR (Liu et al., 2011).

1.2.4 Salicylic Acid - An Indispensable Defence Hormone

Numerous studies indicate that SA is an essential signalling molecule required during plant immune responses. Early work in tobacco noted that following infection with tobacco mosaic virus (TMV), SA accumulated at both the site of infection and in distal tissue, and this increase correlated with defence gene expression (Malamy et al., 1990). More convincing evidence emerged when the transgenic *Arabidopsis* plant expressing *nahG*, a bacterial gene encoding the enzyme salicylate hydroxylase able to convert SA into catechol, was studied in detail. Most importantly, upon pathogen challenge this plant was unable to accumulate endogenous SA and consequently did not induce transcripts for defence genes nor was it able to establish SAR (Delaney et al., 1994; Gaffney et al., 2003; Lawton et al., 2005). Significantly, exogenous treatment of 2,6-dichloro-isonicotinic acid (INA), an SA analogue, was able to restore these immune capabilities (Vernooij et al., 1995). Moreover, when bacterial *entC* (encoding isochorismate synthase) and *pmsB* (encoding pyruvate lyase), two SA synthesis genes were overexpressed in tobacco, these plants exhibited robust defence gene expression and broad disease resistance (Verberne et al., 2000). Following this early work, vast genetic screens were conducted in order to piece together the SA-dependent defence signalling network. Numerous plants that are defective in SA biosynthesis or signalling have been identified and this data integrated into an evolving model (Vlot et al., 2009).

1.2.5 SA Induction Pathway

Gene expression profiles during PTI and ETI mirror very closely with the main difference being the greater magnitude of defence genes induction during ETI (Tao et al., 2003; Dodds and Rathjen., 2010). Recent work demonstrates that SA signalling is essential during PTI and ETI, and that both defence capabilities are able to promote SAR establishment (Mishina and Zeier., 2007; Tsuda et al., 2008). It is therefore

reasonable to predict that elements of PTI and ETI share common signal transduction pathways. This is indeed the case with genetic dissection identifying a significant overlap in the regulatory proteins that function to promote SA accumulation. Specifically, both PTI and the TIR-NB-LRR subclass of R protein (thus ETI) converge on EDS1 and PAD4, both proteins shown to be necessary for SA-dependent responses (Fig. 1-2) (Zhou et al., 1998; Falk et al., 1999; Jirage et al., 1999). EDS1 appears to act as an immune receptor and is thought to perform both nuclear and cytoplasmic regulatory roles. Activation of defence signalling leads to an increase in the EDS1 nuclear pool and this correlates with transcriptional reprogramming, including the induction of members of the SA transduction pathway (PAD4), the SA biosynthesis pathway (ICS1 and CBP60g) and SA-dependent defence marker gene (*PR-1*) (García et al, 2010). EDS1 has been shown to form spatially distinct heterodimers with co-regulators PAD4 and SENESCENCE ASSOCIATED GENE 101 (SAG101) and this association is thought to perpetuate the defence cascade and potentiate SA biosynthesis (Feys et al, 2001; Feys et al, 2005).

Functioning downstream is ENHANCED DISEASE SUSCEPTIBILITY 5 (EDS5), a protein with homology to members of the MATE (multidrug and toxin extrusion) transporter family, which localises to the chloroplast and promotes SA accumulation. An *eds5* mutant is defective in *PR* gene expression and fails to establish SAR. Transcripts for *EDS5* are induced in an EDS1 and PAD4-dependent manner, and based on structural properties of the protein it is thought EDS5 is involved in the transport of constituent components required for SA biosynthesis (Nawrath and Metraux., 1999; Nawrath et al., 2002; Ishihara et al., 2008).

Unfortunately the stages between the CC-NB-LRR type of R protein activation and SA production are not clear but recognition of pathogen-mediated modifications to RPM1-INTERACTING PROTEIN 4 (RIN4) by NDR1 appears to promote plant immunity (Fig. 1-2) (Mackey et al., 2002; Mackey et al., 2003; Day et al., 2006).

Following pathogen challenge the majority of SA is derived from a metabolic processing step involving isochorismate synthase (ICS), a key enzyme that converts chorismate into isochorismate. Functional SA is then derived from isochorismate by isochorismate pyruvate lyase (IPL) (Vlot et al., 2009). The *Arabidopsis* genome encodes two *ICS* genes (*ICS1* and *ICS2*) with the protein product targeting to the chloroplast (Strawn et al., 2007; Garcion et al., 2008). Both ICS1 and ICS2 are able to synthesize SA, however it is ICS1 that performs the predominant function with regards to the production of SA in response to biotrophic pathogens (Wildermuth et al., 2001; Garcion et al., 2008). Interestingly, the presence of residual SA in an *ics1ics2* double mutant suggests an ability to produce SA independent of ICS processing (Garcion et al., 2008). This is likely to be performed by a second enzymatic pathway in which PHENYLALANINE AMMONIA LYASE (PAL) catalyses the transformation of L-phenylalanine into a metabolic derivative that can be converted to SA (Vlot et al., 2009).

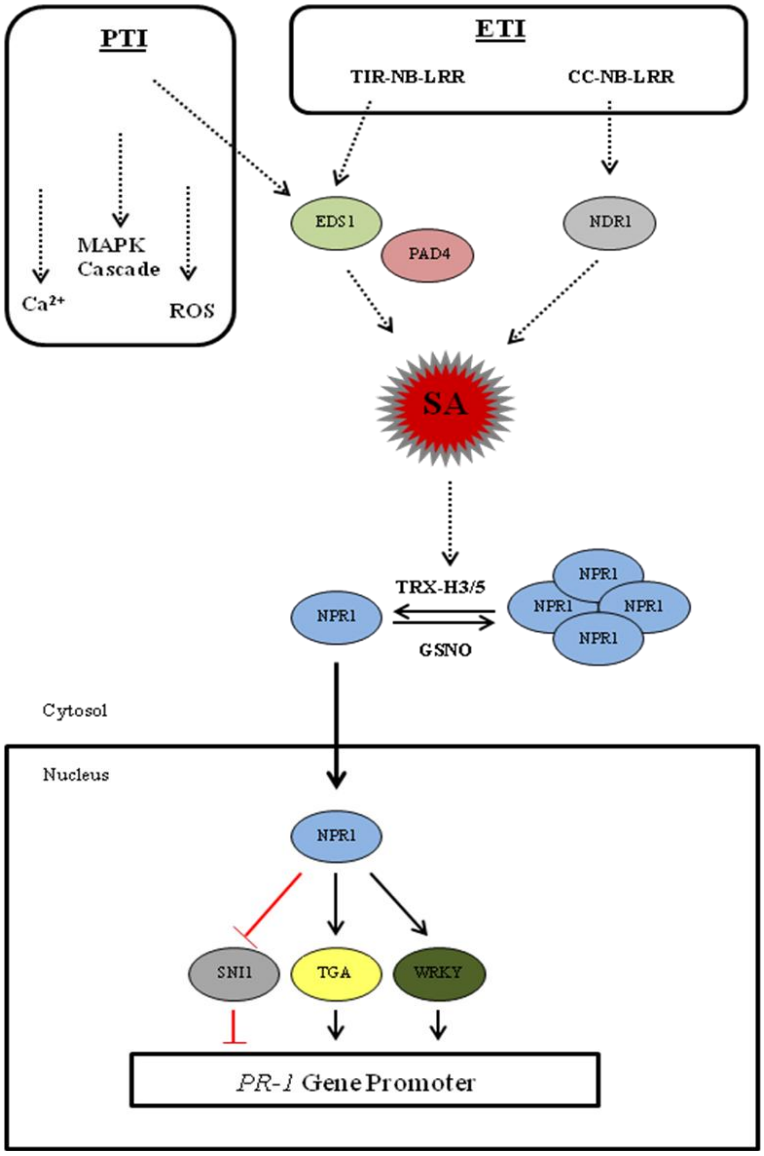

Figure 1-2. Simplified diagram of PTI and ETI defence signalling. PTI and R protein (TIR-NB-LRR subclass) signal through EDS1, while the R protein (CC-NB-LRR subclass) signal through NDR1. This functions to promote the accumulation of salicylic acid, a defence hormone that induces intracellular redox changes. Such redox changes promote NPR1 oligomer disassociation, with NPR1 monomers able to migrate to nuclei, where this protein is able to dynamically alter defence gene transcription (such as *PR-1*) through interaction/association with transcription activators/repressors. Diagram adapted from Vlot et al., 2009.

1.2.6 NPR1 – An Essential Transducer of the SA Signal

NPR1 was identified during several genetic screens in *Arabidopsis* as being an essential positive regulator of SA-dependent immune responses. Extensive characterisation

revealed *npr1* plants are defective in both PTI and ETI, and are unable to initiate a SAR capability (Cao et al., 1994; Glazebrook et al., 1996; Kohler et al., 2002). Significantly, *npr1* plants are able to accumulate endogenous SA following pathogen challenge and/or exogenous treatment with SA analogues (2,6-dichloroisonicotinic acid [INA] and benzothiadiazole S-methyl ester [BTH]) but fail to induce *PR* gene expression (Delaney et al., 1995; Lawton et al., 1996; Shah et al., 1997). This has led to the consensus that NPR1 functions as a transducer of the SA signal (Fig. 1-2). NPR1 was cloned in 1997 and is structurally composed of two characteristic protein-protein interaction domains; the ankyrin repeat domain (ARD) and a *Broad-Complex*, *Tramtrack*, *Bric-a-brac*/Poxvirus, Zinc finger (BTB/POZ) domain as well as a bipartite nuclear localisation signal (NLS) and many conserved cysteine amino acid residues (Cao et al., 1997; Ryals et al., 1997; Mou et al., 2003). Interestingly, NPR1 lacks a canonical DNA-binding domain but has been found to interact with a subclass of basic region/leucine zipper (bZIP) containing TGA transcription factors in both plant cells and yeast two-hybrid screening (Zhang et al., 1999; Després et al., 2000; Zhou et al., 2000; Subramaniam et al., 2001).

1.2.7 TGA Transcription Factors

Gene annotation studies in *Arabidopsis* reveal the presence of between 75 and 81 coding sequences with a characteristic bZIP domain (Riechmann., et al. 2000; Jakoby et al., 2002). The bZIP domain is composed of a region of ~16 amino acids housing the nuclear localization signal adjacent to a N-x7-R/K motif able to dock DNA, and an amphipathic helix structure composed of leucine residue repeats or other bulky hydrophobic amino acids structurally placed in the C-terminus to facilitate hydrophobic interactions between helices. This results in a coiled-coil structure able to bind DNA (known as the zipper). These transcription factors bind DNA that contains the ACGT core motif such as the A-box (TACGTA), C-box (GACGTC) and G-box (CACGTG) motif. Dependent on the electrostatic properties of the polar residues positioned either side of the hydrophobic interaction surface of the helices, bZIP domain containing

proteins are able to selectively form stable homo- and heterodimers (Jakoby et al., 2002).

Based on the primary structure of the basic region and leucine zipper, this gene family can be subdivided into ten distinct groups (Jakoby et al., 2002). Within the context of plant-pathogen interaction, two of these groups are of particular importance. Firstly, a single member of group C designated bZIP10 is known to translocate from the cytoplasm to the nucleus, where it is able to promote pathogen-induced HR and PTI (Kaminaka et al., 2006). Secondly, seven members of group D, designated TGA1-TGA7 are known to be essential for NPR1-dependent defence responses. On the basis of amino acid sequence similarities, these seven members can be further subdivided into three subclasses.

Subclass I contains TGA1 and TGA4, two redox sensitive proteins both containing conserved cysteine residues that facilitate intra-molecular disulfide bridge formation, that under resting conditions, restrict interaction with NPR1. However, initiation of SA-dependent signalling induces cellular redox modifications that reduce TGA1/4 and allow association with NPR1, a process that is thought to promote defence gene transcription (Després et al., 2003). Furthermore it has been reported that once the disulfide bridge is reduced, the exposed cysteine residues are subject to *S*-nitrosylation and *S*-glutathionylation. These modifications are proposed to "protect" TGA1/4 from further oxidative modifications and increase the transcriptional properties of these proteins (Lindermayr et al., 2010). The exact role(s) of TGA1/4 are not clear as they appear to be positive regulators of disease resistance but their function correlates with *PR* gene repression (Kesarwani et al., 2007; Lindermayr et al., 2010).

Subclass II consists of TGA2, TGA5 and TGA6, three functionally-redundant positive regulators of SA-mediated responses and SAR. While the *tga6-1tga2-1tga5-1* triple knockout mutation completely abolishes pathogen-induced *PR* gene expression and SAR, basal *PR-1* expression is elevated, suggesting both positive and negative roles for these transcription factors. The exact properties of each individual transcription factors

have generated much debate. For instance, TGA2 has been shown to function as both a transcriptional activator and repressor of *PR-1* gene expression, with specificity dependent on the presence of TGA5 and TGA6 (Fan and Dong, 2002; Zhang et al., 2003; Kang and Klessig, 2005; Kesarwani et al., 2007). Recent work identified the presence of a repression domain in the N-terminus of TGA2. This domain interacts with the NPR1 BTB/POZ domain, a process that promotes the assembly of an enhanceosome with the capacity to transactivate and function as a transcriptional activator (Rochon et al., 2006; Boyle et al., 2009). NPR1 was shown to enhance the binding affinity of TGA2 to the *as-1* element located in the *PR-1* promoter *in vitro* (Després et al 2000), while independent work indicates that SA promotes NPR1-dependent recruitment of TGA2 to this motif *in vivo* (Johnson et al., 2003). While overexpression of TGA5 does not affect *PR* gene expression, it does however enhance resistance to a highly virulent oomycete pathogen (Kim and Delaney, 2002). Moreover, activation-tagging of TGA6 to overexpress this gene resulted in increased *PR-1* expression, highly indicative for a role as a transcriptional activator (Kesarwani et al., 2007).

Besides modulating *PR* gene expression, TGA2/TGA5/TGA6 are essential for cross-talk modulation and activation of secondary response genes such as WRKY transcription factors (Wang et al., 2006a; Ndamukong et al., 2007). In addition, the *tga6-1tga2-1tga5-1* mutant is more susceptible to the detrimental effects associated with over accumulation of SA, such as arrested growth at the cotyledon stage and bleaching of seedling plants, suggesting these proteins potentially form part of a feedback mechanism to attenuate the SA signal (Cao et al., 1997; Zhang et al., 2003). More recently it has been shown that in the absence of SA, this collection of TGA transcription factors also function as positive regulators of JA and ET- dependent gene transcription (Zander et al., 2010).

Subclass III consists of TGA3 and TGA7, two proteins with apparent markedly different functions. TGA3 is known to be the strongest interactor with NPR1 in yeast two-hybrid experiments and is recruited to the *PR-1* promoter in a NPR1-dependent manner (Zhou et al., 2000; Johnson et al., 2003). Characterisation of a *tga3* knockout

reveals this protein is a potent activator of *PR* gene expression upon SA induction, with this mutant displaying <50% expression of *PR-1* compared to wild-type plants (Kesarwani et al., 2007). Although TGA7 is largely uncharacterised, this protein does appear to interact with NPR1 in yeast two-hybrid work and this association promotes *in vitro* recruitment to the *as-1* element (Shearer et al., 2007). Additionally, although a *tga7* single mutant has increased susceptibility to pathogens, a direct role for TGA7 in *PR* gene activation is unclear (Kesarwani et al., 2007; Song et al., 2011). This can be explained by recent work demonstrating that TGA7 physically interacts with the DNA damage repair protein SSN2 (SUPPRESSOR OF SNI1 2) *in planta* (Song et al., 2011) (more details in next section).

1.2.8 *PR* Gene Expression

Induction of SA-dependent signalling and activation of SAR is invariably associated with the expression of *PR* genes, and therefore these genes serve as a useful indicator when studying plant-pathogen interactions (Ward et al., 1991; Uknes et al., 1992). *PR* genes encode proteins with anti-microbial properties, and it is the combined action of many PR proteins that are thought to promote disease resistance (Van Loon and Van Strien, 1999; Durrant and Dong, 2004). Typically *PR* genes are associated with late onset in defence activation and are therefore categorised as secondary response genes (Moore et al., 2011). In recent times, the *Arabidopsis PR-1* promoter has emerged as a platform in which to study the dynamic processes of defence gene activation and/or fine-tuning. As discussed, TGA transcription factors bind DNA that contains the ACGTCA core motif and analysis of the *PR-1* promoter reveals two SA-responsive motifs designated linker-scan (*LS) 5* and *LS7* (collectively referred to as *activating sequence 1* (*as-1*)) (Lebel et al., 1998). The structural arrangement of the *as-1* element appears to embed regulation specificity as modifying the configuration in the promoter alters activation and repression properties (Pape et al., 2010a).

NPR1 is known to promote *PR-1* gene expression whilst in the nucleus with recent work providing insight into the mechanism that underpins this process. Under resting

conditions, those monomeric NPR1 protein units not secured in the oligomer, which enter the nucleus, are targeted for degradation by the proteasome. This is thought to act as a safeguard to prevent untimely activation of defence genes and SAR (Spoel et al., 2009). Initiation of pathogen-induced cellular redox changes promotes the net translocation of monomeric NPR1 to the nucleus (Mou et al., 2003). NPR1 then interacts with DNA-binding transcription factors, and recruits members of the basal transcription machinery to initiate gene transcription. NPR1 is phosphorylated at residue Ser11/Ser15, possibly by a kinase associated with the transcription machinery, which increases its affinity to a Cullin3-based ubiquitin ligase (CUL3). This promotes rapid degradation of NPR1 by the proteasome, clearing the promoter for unphosphorylated NPR1 to reengage and activate transcription (Fig. 1-3). This process facilitates rapid and efficient activation of defence genes, and significantly reveals that NPR1 is an essential **transcriptional cofactor**. Interestingly, NPR1 and CUL3A do not interact in a yeast two-hybrid system, yet NPR1 can be pulled down using an antibody against CUL3A, suggesting the presence of an unknown adaptor protein that links these proteins (Spoel et al., 2009).

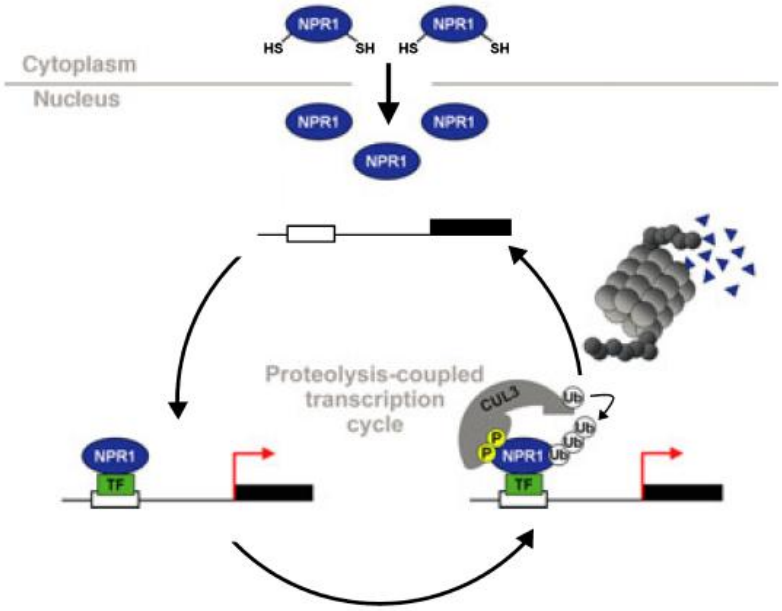

Figure 1-3 Transcriptionally active monomeric NPR1 located in the nucleus interacts and complexes with transcription factors (TFs) at target promoters. Upon activation of gene transcription, NPR1 is phosphorylated (P) increasing its affinity to a Cullin 3 (CUL3) ligase. NPR1 is polyubiquitinylated (Ub) and subsequently targeted by the proteasome. Unphosphorylated NPR1 is then free to reengage and activate transcription. This proteolysis-coupled transcription cycle maintains efficient gene transcription as long as NPR1 transcription cofactor function is active. Diagram adapted from Spoel et al., 2009.

This creates a simple model in which nuclear NPR1 can direct TGA transcription factors to activate gene expression by binding cognate DNA located in the *PR-1* promoter. However, several key studies indicate that events and mechanisms associated with defence gene transcription are much more complicated. Firstly, *SUPPRESSOR OF npr1-1 INDUCIBLE 1* (*SNI1*) was found to specifically repress many SA inducible, NPR1-dependent genes, including *PR-1* (Li et al., 1999). The *SNI1* gene encodes a protein with armadillo repeats suggesting SNI1 may modulate transcription by forming a scaffold to associate with proteins thereby inducing chromatin modifications and restricting the accessibility of DNA (Mosher et al., 2006). More recently it has been shown that following pathogen challenge, SA recruits SSN2 and RAD51D **(**RAS ASSOCIATED WITH DIABETES PROTEIN 51 D) to the *PR-1* promoter and this leads to the eviction of the transcription repressor SNI1 (Durrant et al., 2007; Wang et al., 2010; Song et al., 2011). RAD51D is thought to complex with BRCA2A (BREAST

CANCER SUSCEPTIBILITY PROTEIN 2A), with both proteins shown to be essential for plant immunity. Moreover, NPR1 is thought to co-ordinate the timing of SSN2 recruitment with TGA7 playing an important role in this process. Significantly this indicates that proteins involved in DNA repair are able to modulate defence gene transcription (Wang et al., 2010; Song et al., 2011).

Analysis of the *PR-1* promoter reveals the presence of several W-boxes, the motif selectively bound by WRKY transcription factors (Lebel et al., 1998; Pandey and Somssich, 2009). Although no WRKY proteins have yet been found to bind this promoter, they are certainly implicated in its regulation. Sited adjacent to the *as-1* element is a W-box at position LS4, which appears to repress gene expression. In addition, there are three WRKY binding sites located downstream of LS7 that appear to be regulated by SNI1 and NPR1, and function to promote transcription (Pape et al., 2010b).

1.2.9 NPR1-Mediated Transcription Dynamics

NPR1 appears to exclusively modulate the transcriptional reprogramming associated with SA-dependent immune responses. For example, following treatment with the functional SA analog, BTH (benzothiadiazole S-methylester), wild-type and *npr1* mutant plants display differential expression in 99% (2,248/2,280) of SA-inducible genes, highlighting the central role NPR1 plays in orchestrating transcriptional events (Wang et al., 2006a). While many of these genes are direct primary targets of NPR1-dependent transcription factors, it is likely the vast majority are secondarily activated as part of a "knock-on" transcriptional cascade that was itself initiated by NPR1.

Using large scale global expression profiling and bioinformatic tools, two studies by the same research group have identified many NPR1- responsive genes. Amongst these are defence genes such as *PR-1, PR-5,* chitinase and peroxidase. However, rather unexpectedly NPR1 was also found to directly regulate endoplasmic reticulum (ER) protein channel regulators (Sec61 translocon complex), ER-resident chaperones (such

as BiP2) as well as many co-chaperones involved in protein folding and modification such as calnexins (CNXs), calreticulins (CRTs) and protein disulfide isomerases (PDIs) (Wang et al., 2005). Mutations in these secretory pathway genes resulted in a reduction in the ability of the plant to transport PR-1 protein following elicitation with BTH and increased susceptibility to pathogens. Thus it would appear that NPR1 plays a crucial role in preparing the cell to be able to efficiently and effectively secrete defence-related proteins (Wang et al., 2005).

A second study identified that eight WRKY (WRKY18, 38, 53, 54, 58, 59, 66, and 70) transcription factor genes are directly regulated in an NPR1-TGA 2/5/6 dependent manner. This work established that individually, WRKY18, -53, -54, and -70 all act as positive regulators of SA-mediated resistance while WRKY58 appears to attenuate the defence response in un-induced plants. Significantly, comparison of wild-type and *wrky18* mutant transcription profiles following BTH treatment indicated that the expression and amplitude of 19.8% of NPR1-responsive genes are regulated by WRKY18, suggesting this transcription factor, in particular, mediates a large portion of NPR1-dependent transcriptional responses and may even modulate the transition to SAR (Wang et al., 2006a).

Moreover, independent work indicates that NPR1 is able to mediate hormone cross-talk via an undefined mechanism in the cytosol and it remains to be determined if the NPR1 oligomer or perhaps a cytoplasmic pool of monomeric NPR1 performs this function (Spoel et al., 2003). WRKY62 has been described as a transcriptional target of cytosolic NPR1 but considering WRK62 localises exclusively to the nucleus, any association must be indirect (Mao et al., 2007). Transcripts for WRKY62 accumulate following treatment with either MeJA or SA, but synergistic induction is observed following combined treatment with these two hormones. Induction of WRKY62 by MeJA is abolished in transgenic plants expressing *NahG*, suggesting a SA threshold is necessary to induce expression. Intriguingly, WRKY62 function is correlated with the repression of *LOX2* and *VSP2* (Mao et al., 2007) and *PR-1* (Kim et al., 2008) indicating this protein antagonises both SA and JA responses. One explanation could be that WRKY62

functions to fine-tune JA and SA dependent gene expression, possibly with specificity provided by WRKY38 and/or NPR1. Transcripts for Histone Deacetylase 19 (HDA19) are induced by SA in an NPR1-dependent manner and this protein has been shown to interact with both WRKY38 and WRKY62. Overexpression of HDA19 leads to increased *PR-1* gene expression and enhanced disease resistance, while the *hda19* mutant has compromised resistance. Similarly, disruption of individual WRKY factors increased PTI resistance, with a synergistic effect observed in the double *wrky38wrky62* mutant. This observation led to the presumption that WRKY38 and/or WRKY62 or their transcription targets repress *PR-1* expression, and this action is inhibited by HDA19 (Kim et al., 2008). This further emphasises the complex dynamics of NPR1 function, and the ability of this protein to fine tune transcriptional responses by regulating the activity of both positive and negative regulators of plant immunity.

1.2.10 Cellular Redox Regulates Defence Signalling and HR

1.2.10.1 The Hypersensitive Response

Redox (reduction-oxidation) can be defined as a chemical reaction in which the oxidation state of an atom is changed. Photosynthesis is an essential aerobic metabolic process in which plants use light energy to fix CO_2. Environmental stresses, such as reduced available light, temperature and CO_2 abundance often results in the plant modifying stomatal conductance and this leads to a rapid reduction in the ratio of internal CO_2/O_2. This invariably promotes the photoreduction of oxygen to hydrogen peroxide (H_2O_2) and superoxide anion (O_2^-), with potentially harmful quantities of these reactive oxygen species (ROS) being accumulated as a result (Asada, 2006; Mateo et al., 2006). Fortunately, plants are equipped with an array of cellular antioxidants that act as redox buffers and function to counter any risk ROS may pose. Examples include glutathione and ascorbate and/or scavenging enzymes such as glutathione peroxidases (GPX) and glutathione-S-transferases (GST) which use glutathione as an electron donor (Wojtaszek, 1997).

While plants are well-equipped to regulate redox associated with abiotic stress, they are also able to exploit redox signalling to manage various cellular processes in plant immunity. This includes the formation of an oxidative burst that contributes to hypersensitive cell death. For example, it is well established that to execute efficient HR, an essential conditional prerequisite is a balance in the cellular amount of nitric oxide (NO) and ROS (Delledonne et al., 1998; Delledonne et al., 2001). Upon pathogen recognition, ROS accumulates from an oxidative burst that is generated in the apoplast by plasma membrane-bound NADPH oxidases and/or pH-dependent cell wall peroxidases (Apostol et al., 1989; Wojtaszek., 1997). The *Arabidopsis* genome encodes 10 NADPH oxidase genes, designated *RBOHA* to *RBOHJ* (respiratory burst oxidase homolog), with two seemingly being of significance during pathogen-induced HR. Functional analysis reveals that RBOHD is a major source of ROS, while RBOHF functions to control HR (Torres et al., 2002). Interestingly, SA appears to function as a pro-death signal, but this activity is curbed by RBOHD/RBOHF (Torres et al., 2005). It has been suggested that RBOHD functions to trigger death in cells damaged by pathogen infection but simultaneously inhibits death in adjacent cells by suppressing salicylic acid and ethylene signalling, thereby limiting large-scale cellular damage (Torres et al., 2005; Pogány et al., 2009). NO is produced within the same spatial window as ROS and these molecules function synergistically to modulate HR (Delledonne et al., 1998). Interestingly, *Arabidopsis* plants defective in *S*-nitrosoglutathione reductase (GSNOR) function are known to accumulate high levels of both *S*-nitrosoglutathione (GSNO) and protein-SNO, and this correlates with reduced ROS-mediated cell death (Feechan et al., 2005; Chen et al., 2009). Recent work provides insight into the molecular mechanism that underpins this process. Specifically, a conserved cysteine thiol (Cys890) located in the C-terminus of RBOHD is modified by NO to generate a protein *S*-nitrosothiol (SNO). This functions to regulate NADPH oxidase activity and thus ROS production, which limits cell death (Yun et al., 2011). It is speculated that during the early stages of infection, SA, RBOHD and GSNOR all function dynamically to balance NO and ROS production, and thus act as positive regulators of cell death. However, in order to prevent unnecessary tissue damage upon

successful initiation of cell death, *S*-nitrosylation of AtRBOHD at Cys890 functions as a molecular switch to dampen ROS production (Yun et al., 2011).

1.2.10.2 Defence Signalling

Redox signalling may also actively regulate the defence transcriptome. For instance, microarray data reveals that following elicitation with H_2O_2, up to 175 genes are differentially expressed in *Arabidopsis*. Analysis of the 5'UTR of those genes reveals a high abundance of the *as-1* element binding site (Desikan et al., 2001). Interestingly, in tobacco many defence-related genes that contain the *as-1* elements were shown to be responsive to SA, but significantly the addition of the antioxidants dimethylthiourea (DMTU) and 3-t-butyl-4-hydroxy-anizole (BHA) block this SA-dependent gene transcription (Garreton et al., 2002). This provides a direct link between SA signalling, redox-signalling and defence gene activation. More recently it has been demonstrated that SA levels correlate with total cellular glutathione levels as well as the GSH/GSSG ratio. For instance, *Arabidopsis* mutants which constitutively accumulate SA display increased glutathione biosynthesis whilst in transgenic plants expressing *NahG,* the glutathione pool becomes imbalanced with a higher proportion of this peptide being found in the oxidised (GSSG) form (Mateo et al., 2006).

Significantly, such cellular redox perturbations appear to be perceived by reactive cysteine residues in NPR1. In *Arabidopsis*, *NPR1* is constitutively expressed in the cell and this protein has been shown to be *S*-nitrosylated at cysteine-156 (Cys156), a redox-based posttranscriptional modification that facilitates disulphide bond formation and subsequent oligomer assembly. Under resting conditions, this high molecular weight complex is situated predominantly in the cytosol (Mou et al., 2003). Upon pathogen challenge, SA-dependent redox changes coupled with the reduction of two cysteine residues (Cys82 and Cys216) catalysed by THIOREDOXIN-h3 and THIOREDOXIN-h5 leads to monomer release. Therefore NPR1 is regulated via the opposing action of GSNO and TRX3/5 (Fig. 1-4). Transcriptionally active, monomeric NPR1 has the capacity for nuclear migration and an enriched nuclear pool correlates with increased

PR-1 gene expression and enhanced resistance to biotrophic pathogens (Cao et al., 1997; Cao et al., 1998; Kinkema et al., 2000; Mou et al., 2003; Tada et al., 2008). Thus post-transcriptional modifications to redox-sensitive transcription factors are translated into an operational response. Glutathione seems to be of major importance as *in vitro* NPR1 oligomer – monomer equilibrium correlates with ambient changes to this peptide. Specifically, a low GSH/GGSG ratio promotes oligomer formation while a high GSH/GSSG ratio promotes monomer release (Mou et al., 2003).

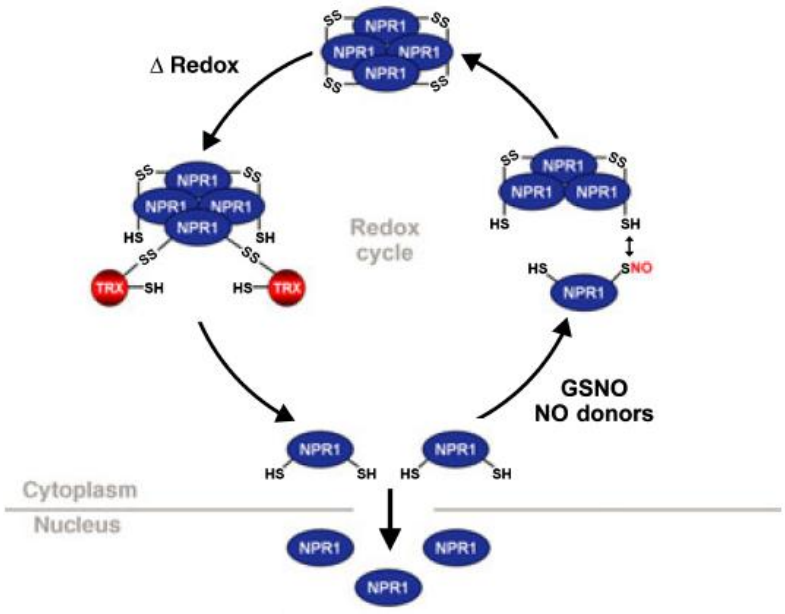

Figure 1-4. Under resting conditions, NPR1 is *S*-nitrosylated by *S*-nitrosoglutathione (GSNO), and this process is maintained in dynamic equilibrium to promote formation of the NPR1 oligomer. Upon pathogen recognition, ambient changes to cellular redox coupled with thioredoxin (TRX)-mediated reduction promotes monomer release. Diagram adapted from Spoel et al., 2009.

1.2.10.3 Plant Hormones and Redox Regulation

Plant hormones appear to regulate glutathione levels in order to modulate SA-JA cross talk. It was recently reported that during multitrophic (simultaneous challenge with pathogenic bacteria and a chewing insect) biological interactions, JA- responsive genes

including *PDF1.2* and *VSP2* are highly sensitive to SA- dependent suppression. Kinetic studies using SA and MeJA as chemical elicitors indicated that this antagonistic effect occurred within a finite time frame and was linked to transient modifications in cellular redox. It was noted that SA-dependent suppression of JA-responsive genes correlated with increased glutathione levels, while conversely, inhibition of glutathione synthesis through the application of the inhibitor L-buthionine-sulfoximine, nullified this suppressive effect (Koornneef et al., 2008). The mechanism underpinning this phenomenon is not clear but it is linked to transcriptional modifications. Several WRKY transcription factors (WRKY33, 38, 41, 62 and 70) are credited with the ability to influence SA-JA cross-talk, but placing this network in context is difficult as functional redundancy and self perpetuation via autoregulation has hindered progress in assigning function to individual WRKY proteins (Li et al., 2006; Zheng et al., 2006; Kim et al., 2008; Higashi et al., 2008).

Moreover, GRX480 is induced in a NPR1- TGA2/5/6-dependent manner in response to SA and has been shown to be a potent regulator of SA-JA cross-talk. GRX480 was first identified in a yeast two-hybrid screen and subsequently shown to interact with TGA2 *in planta*. Overexpression of GRX480 correlates with significantly reduced *PDF1.2* transcripts ordinarily induced by exogenous application of MeJA and this suppression occurs in a NPR1-independent, TGA2/5/6-dependent manner (Ndamukong et al., 2007). GRXs are catalytically active proteins able to reduce structural disulfide bonds that exist in proteins, and this work further strengthens the link between redox modifications, hormone cross-talk and plant immunity.

1.2.10.4 A Conserved Mechanism in both Eukaryotes and Prokaryotes

Interestingly, perception of intracellular redox changes by intrinsic cysteine residues appears to be a ubiquitous signalling mechanism present in both eukaryotes and prokaryotes as a way to sense and respond to oxidative stress. For instance, in response to ROS, the *Saccharomyces cerevisiae* AP-1 transcription factor designated YAP1, is known to induce a large assortment (~100) of anti-oxidant genes such as thioredoxin,

glutathione and glutathione reductase which function to mitigate danger posed by toxic accumulation of ROS (Gasch et al., 2000; Kuge and Jones, 1994). In addition, YAP1 also regulates many genes in response to reactive nitrogen species (RNS)-induced stress although the full role this transcription factor plays in perception and signal transduction is not clear (Horan et al., 2006; Lushchak et al., 2009). Structurally, YAP1 is composed of two cysteine-rich domains each located in the amino and carboxy-termini (termed n-CRD and c-CRD) (Delaunay et al., 2000; Wood et al., 2004). Importantly, under resting conditions this protein is excluded from the nucleus by the combined action of a nuclear export signal (NES) contained within the c-CRD and a protein-protein association with the nuclear export receptor CRM1 (Kuge et al., 1997; Kuge et al., 1998; Yan et al., 1998; Wood et al., 2004). YAP1 does not sense ROS directly, instead this function is performed by a glutathione peroxidase-like protein GPX3 which promotes disulfide bond formation between the n-CRD and c-CRD of YAP1, inhibiting interaction with CRM1 and masking the NES (Coleman et al., 1999; Delaunay et al., 2002; Wood et al; 2004). It is speculated that in response to H_2O_2, the active site cysteine (Cys36) of GPX3 is oxidised to form a sulfenic acid modification that can react with YAP1 at Cys598 to form an intra- or intermolecular disulfide bridge (Fig. 1-5). This promotes disulfide formation between Cys303 and Cys598 in YAP1, which activates and promotes translocation of this protein to the nuclei, where it is able to dynamically modify anti-oxidant gene expression (Delaunay et al., 2002).

In *Escherichia coli*, a single reactive cysteine residue contained in the transcription factor OxyR is able to directly sense the presence of H_2O_2. In this case Cys199 reacts with H_2O_2 to form a sulfenic acid (Fig. 1-5), which results in the formation of a disulfide bond between Cys199 and Cys208. This modification activates the transcriptional properties of this protein and results in the activation of target antioxidant genes (Zheng et al., 1998; Aslund et al., 1999; Tao, 1999; Lee et al., 2004).

1.2.11 *S*-nitrosylation in Plant Defence Signalling - The Redox Switch

Nitric oxide (NO) is a lipophilic, diatomic gas with no electrical charge and an unpaired electron. This unique chemistry facilitates covalent attachment of NO to the sulfhydryl group side chain of receptive cysteine or homocysteine thiols present in protein structures, to form an *S*-nitrosothiol (SNO) (Fig. 1-5) (Wang et al., 2006b). Protein *S*-nitrosylation was first described as being a physiologically-relevant, redox-based modification able to mediate cellular processes in a landmark paper published in 1992 (Stamler et al., 1992). Since this discovery, and with advances in analytical techniques, both *S*-nitrosylation and protein denitrosylation – the removal of NO from a cysteine thiol side chain – have emerged as being of central importance in diverse cellular regulatory, metabolic and signalling processes, including underpinning many aspects of both animal and plant immunity (Jaffrey and Snyder, 2001; Marshall and Stamler, 2001; Erwin et al., 2005; Feechan et al., 2006; Into et al., 2008). SNOs form with great specificity but there is great controversy as to whether an acid–base SNO motif (with flanking acidic (Asp, Glu) and basic (Arg, His, Lys) residues), that predicts an affinity to form such modifications, exists (Pérez-Mato et al., 1999; Greco et al., 2006; Hao et al., 2006; Marino and Gladyshev., 2010). Additional important parameters include thiol electrostatic and allosteric properties such as pK_a and solvent accessibility, as well as local conditions such as redox, pH and the availability of metal ions such as Ca^{2+} or Mg^{2+} (Hess et al., 2005). Understanding the mechanisms by which SNO equilibrium is maintained and how subsequent signalling dynamics are induced and modulated is of great biological interest. During recent years a number of candidates have emerged with two major enzyme processes in particular – the GSNOR/GSNO/GSH and the thioredoxin (Trx)/Trx reductase (TrxR) – subject to a great amount of research (reviewed extensively in Benhar et al., 2009).

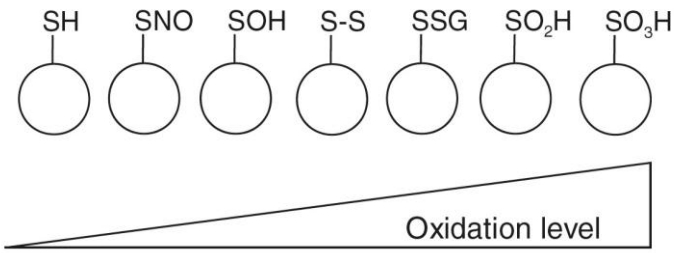

Figure 1-5. Overview of cysteine thiol (SH) redox-based modifications that include: S-nitrosothiol (SNO), sulphenic acid (SOH), disulphide (S–S), *S*-glutathionylation (SSG), sulphinic acid (SO_2H) and sulphonic acid formation (SO_3H). Diagram from Spadaro et al., 2010.

1.2.11.1 GSNO/GSNOR

The product of an association of NO with GSH, *S*-nitrosoglutathione (GSNO) is a low molecular weight SNO able to donate an NO moiety to receptive proteins through a process of transnitrosylation (Hess et al., 2005). GSNO and protein-SNOs are thought to be kept in dynamic equilibrium by the action of GSNOR (Liu et al., 2001; Feechan et al., 2005). GSNOR (known also as GSH-dependent formaldehyde dehydrogenase and class III alcohol dehydrogenase) is able to specifically metabolise GSNO, in a NADH-dependent reaction to GSNHOH (an N-hydroxysulphenamide), thus indirectly modulating protein SNO formation (Figs. 1-6 and 1-7). Functional mutagenesis of the gene encoding GSNOR in *E. coli, S. cerevisiae* and mouse results in increased levels of SNO modified protein and GSNO, thus demonstrating the vital role this enzyme has in maintaining SNO homeostasis (Lui et al., 2001). Analysis of the *Arabidopsis* genome identified a putative *GSNOR*, and when this gene was expressed in *E.coli* it was found to have GSNOR activity (Sakamoto et al., 2002). This was later identified as being of central importance in plant immunity. As expected, a loss-of-function *Arabidopsis* mutant (designated a*tgsnor1-3*) was found to contain an elevated concentration of protein-SNO compared to wildtype plants, that following pathogen infection, became further abundant. Most significantly, this mutation disabled PTI and ETI, dramatically reduced the cellular amount of SA and delayed/reduced expression of *PR-1* (Feechan et al., 2005). Highly indicative of a role in defence responses, the *AtGSNOR1* gene is responsive to hormone treatment, being induced by SA but repressed by JA (Diaz et al.,

2003; Feechan et al., 2005). The molecular mechanisms that underpin this response are beginning to emerge with several protein-SNO targets now documented. Using a proteomic approach, more than 100 proteins were identified as being potential targets of *S*-nitrosylation, many of which are stress-related proteins (Lindermayr et al., 2005). Moreover, a number of independent genetic studies have identified proteins that regulate plant disease resistance. Perhaps most significant, NPR1 has been shown to be selectively *S*-nitrosylated at Cys156 by GSNO, a modification that promotes oligomer formation (Tada et al., 2008). In addition *S*-nitrosylation of *Arabidopsis* salicylic acid-binding protein 3 (AtSABP3) at Cys280, reduces the binding affinity this protein has for SA, as well as reducing inherent carbonic anhydrase (CA) activity, both features that decrease pathogen resistance (Wang et al., 2009).

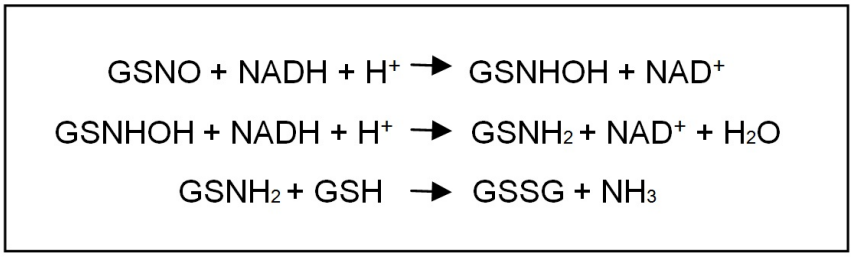

Figure 1-6. The product of *E. coli* GSNOR as described by Liu et al., 2001 with ammonia (NH_3) and glutathione disulphide (GSSG) identified as the main products of GSNOR enzyme activity.

1.2.11.2 TRX/TRXR

Thioredoxins (TRXs) are small (12–14 kDa) proteins found ubiquitously in nature and implicated as important modulators of protein redox modification. The active site of TRX is characterised by the dithiol motif of Trp-Cys-Gly-Pro-Cys, and it is this arrangement that provides this protein with their oxidoreductase properties. Specifically, once the TRX engages a target protein, the N-terminal Cys which is a solvent exposed, highly reactive thiolate, functions as a potent nucleophile to attack the target disulfide. Consequently, a covalent thiol-thiol disulfide intermediate between TRX and protein is formed, which is subsequently reduced by the C-terminal thiolate, resulting in the transfer of the disulfide from the protein to the active site of TRX in a

dithiol–disulphide exchange (Gelhaye et al., 2004; Lillig and Holmgren., 2007; Benhar et al., 2010). This disulfide formed in TRX is subsequently reduced by the flavin containing selenoenzyme TRX reductase (TRXR) in a NADPH-dependent reaction, thus creating a highly efficient recyclable oxidoreduction system in cells (Fig.1-7) (Mustacich and Powis, 2000).

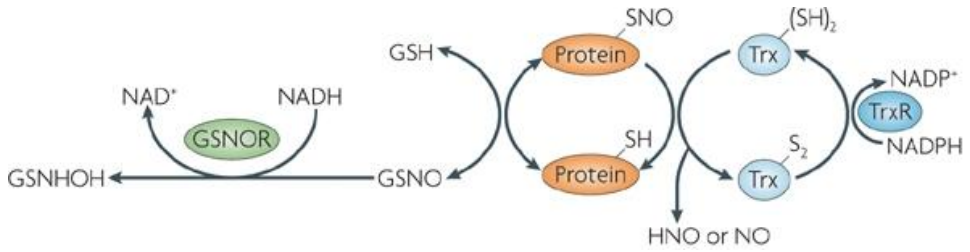

Figure 1-7. The role of *S*-nitrosogluathione reductase (GSNOR) and Thioredoxin (TRX) in regulating protein-SNO status. Diagram from Benher et al., 2009.

Several studies using mammalian cells indicate that TRXs function as protein denitrosylases essential to modulate several cellular processes (Stoyanovsky et al., 2005; Sengupta et al., 2007; Benhar et al., 2008; Sengupta et al., 2009). Using an elaborate, proteomic approach aimed at finding denitrosylase substrates of mammalian thioredoxin 1 (TRX1), a total of 46 potential targets were identified, many with diverse cellular functions such as signal transduction, metabolism and redox homeostasis (Benhar et al., 2010). In *Arabidopsis*, TRX proteins are documented to have denitrosylase activity *in vitro* but the full ramifications of this property *in vivo* are not fully established (Spoel and Loake, 2011). Interestingly, two cytosolic thioredoxins designated TRXh3 and TRXh5 have been shown to be essential positive regulators of plant immunity. Mutations in either *TRXh3* or *TRXh5* potently reduce *PR-1* gene expression associated with exogenous application of SA. In addition these TRXs along with the *Arabidopsis* TRXR (designated NTRA) are required for the establishment of SAR (Tada et al., 2008). Both TRX proteins accumulate in vascular tissues and while *TRXh3* appears to be constitutively expressed, induction of *TRXh5* occurs within 4hrs following pathogen challenge (Reichheld et al., 2002; Laloi et al., 2004). Both TRXh3

and TRXh5 were found to interact with NPR1 *in vitro*, but significantly the SA-induced expression of TRXh5 was shown to correlate with NPR1 monomer release, suggesting TRXh5, in particular, catalyzes NPR1 oligomer reduction (Tada et al., 2008).

1.3 Synthetic Biology

1.3.1 An Overview

Synthetic biology is a nascent field that aims to integrate established engineering principles into the highly dynamic field of biological science. The traditional method utilised by biologists can lead to efficiency and reproducibility issues should this work become the focus of additional theoretical application. Synthetic biology aims to tackle these inconsistencies by providing a standard framework from which scientists should work (Fig 1-8). This discipline undoubtedly has a significant overlap with already established fields such as biotechnology and systems biology, but it is important to distinguish these subjects apart. Synthetic biology, in its own right, provides a logical, systematic, engineering approach to biology (Endy, 2005). The ultimate goal of synthetic biology is to rationally (re) design biological systems with integrated precision to effectively produce a 'bio-machine'. By breaking living systems down into a list of minimal components, synthetic biology has the potential to not only provide insight into already established systems but can also determine how life itself works by systematically re-assembling biological paradigms (Andrianantoandro et al., 2006; Arkin, 2008; Canton et al., 2008; Elowitz and Lim, 2010).

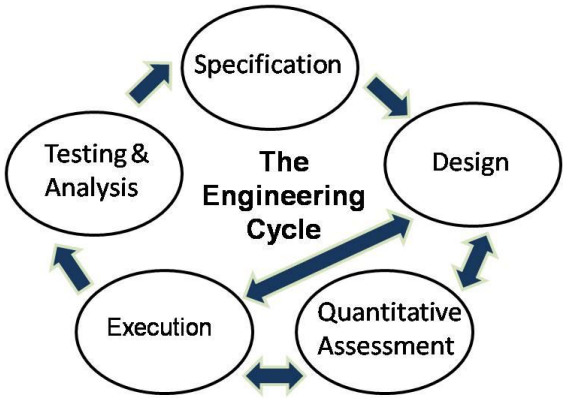

Figure 1-8. Design strategy underpinning many disciplines of engineering, and is directly relevant to the framework employed in synthetic biology.

We are fortunate to live in what could be considered by many to be the early stages of a golden age of synthetic biology. The term synthetic biology was first coined by chemist Stéphane Leduc in 1912, but it is only really in the last decade that this exciting discipline has begun to emerge (de Lorenzo and Danchin, 2008). During recent years there has been an exponential increase in the number of publications relating to synthetic biology and to cope with demand a number of journals have been commissioned dedicated to increasing awareness within this emerging field.

Early work focused on constructing circuits that possess novel properties with the synthetic genetic clock built around transcriptional repressor activity credited with being the first synthetic bio-circuit. By coupling together three repressors and understanding promoters and complimentary ribosome-binding site (RBS) dynamics, protein and mRNA decay rates, together with transcriptional characteristics, it was possible to generate a 'repressilator' that exhibited oscillatory characteristics in *E. coli* (Elowitz and Leibler, 2000). Although this system was inherently noisy, theoretical modelling showed that with tuning, it could be possible to generate a circuit sufficiently robust so that it could resist perturbation by stochastic noise (Barkai and Leibler, 2000). Very soon afterwards work was published demonstrating that by coupling two repressors it was possible to generate a genetic toggle switch able to display robust bistability (Gardner et al., 2000; Kobayashi et al., 2004). By understanding the

biological and theoretical parameters that related to these works, a study followed which showed it was possible to design and assemble an elaborate novel circuit containing feed forward and feedback loops that provided both toggle switch and noise-resistant oscillatory properties to the system (Atkinson et al., 2003). Thus synthetic biology requires that to fully understand the characteristics of a system, there must be an appreciation of quantitative data as well as an understanding of an applicable theoretical numerical model.

These approaches undoubtedly laid the foundations for recent advancements in understanding the oscillatory behaviour of circadian biology. Perception of photoperiodicity is a mechanism used by many eukaryotes as a way to synchronise life strategies, with studies exploring *Arabidopsis* circadian clock biology providing perhaps the greatest insight into these complex regulatory networks (Dodd et al., 2005; Locke., et al 2005; Locke et al., 2006; Salazar et al., 2009; Sorokina et al., 2009). With the recent discovery that components of plant immunity are inextricably coupled to circadian rhythms (Wang et al., 2011), it is possible synthetic biology may offer an approach to unravel the integrated nature of this system.

Breaking a biological circuit down into functional elements makes a complex biological system much more manageable. By utilising these principles, there are numerous biological equivalents of oscillators, logic gates and sensors (Aleksic et al., 2007; Silva-Rocha and de Lorenzo, 2008; Tigges et al., 2009; Khalil and Collins, 2010). By understanding the properties of individual proteins and how their function translates into a wider system, biological circuits can be pieced together to create existing or completely novel circuits. For example, using a heterologous genetic circuit design, it is possible to construct a cell-cell communication network in *S. cerevisiae* using protein machinery from *Arabidopsis*. This team first generated a yeast strain capable of synthesizing the plant hormone cytokinin. Then a second strain was engineered to perceive cytokinin through a phosphorylation event that linked population density to gene expression via a feed-back loop (Chen and Weiss, 2005). More recently, a study exploited the properties of plant phytochrome. This protein is able to perceive both red

(650nm) and far-red (750nm) light, and depending on these lighting conditions, undertake a conformational change that regulates protein function. In the presence of red light, the *Arabidopsis* phytochrome B (PhyB) is known to bind phytochrome interaction factor 3 (PIF3). By attaching PhyB::mCherry to the plasma membrane using the plasma membrane targeting CAAX (C = cysteine, A = aliphatic, X = any amino acid) motif, and linking PIF3 to the DH-PH domains of RhoGEFs Tiam and intersectin (ITSN), which regulate actin cytoskeleton formation, it was possible to stimulate and direct lamellipodia growth in mouse embryo fibroblasts simply by manipulating a red light signal (Levskaya et al., 2009).

1.3.2 Metabolic Engineering

Over a relatively small amount of time, synthetic biology has evolved into a highly intercalated speciality with the scope and scale of this discipline having far reaching implications that make this modern science a very powerful tool. Consequently, the focus of synthetic biology has shifted slightly towards engineering micro-organisms for real-life applications such as the production of therapeutics (Purnick and Weiss, 2009). Perhaps most notable is the manipulation of the mevalonate pathway in *S. cerevisiae* to produce artemisinic acid, a precursor of the anti-malarial drug artemisinin (Martin et al., 2003; Ro et al., 2006). Malaria is of great medical importance affecting millions of people and accounting for thousands of deaths each year, many of which are children. Drug therapy is a proven method to combat *Plasmodium* spp, the causative organism of malaria but multi-drug-resistance against many current market therapies is endemic (Fidock, 2010). Artemisinin is a sesquiterpene lactone with an endoperoxide bridge derived from the herb *Artemisia annua* that has been shown to be highly effective against *Plasmodium* spp (Enserink, 2005). Yet, both direct isolation of artemisinin from plants and/or the semi- synthesis route are considered not to be cost effective. However, by manipulating the mevalonate pathway along with various components essential to derive artemisinic acid, a genetically modified yeast strain could be manipulated to produce up to 100 mg/L of artemisinic acid (Ro et al., 2006). Significantly, with industrial optimisation to increase yield efficiency, the market price of artemisinin has

fallen from $1,100/Kg to ~$200/Kg (Van Noorden, 2010). This irrefutably demonstrates that applied synthetic biology has wide ranging implications and the potential to improve the lives of millions of people. More recently, work has begun to manipulate the methylerythritol-phosphate (MEP) pathway in *E. coli* to produce taxadiene, a precursor of the potent anticancer drug paclitaxel (taxol) (Ajikumar et al., 2010). This, together with data obtained from transcriptome profiling following induction of the native paclitaxel pathway present in *Taxus* spp. presents a great opportunity to produce this drug in a cost effective manner (Lee et al., 2010).

1.3.3 Genomic Engineering

With technology advancing at a rapid pace, the tools available to a synthetic biologist have expanded considerably. Concurrently, there has been a reduction in the costs to manufacture and assemble synthetic DNA. These factors make *de novo* genome synthesis an attractive option. As scientific understanding increases it is highly likely that synthetic biologists will start designing their own biological organism capable of performing a specific task, rather than taking the trouble to modify pathways/circuits already created by evolution. To fundamentally understand how an organism operates ultimately provides a means to manipulate its function (Carr and Church, 2009). Recent pioneering work suggests it is possible for a synthetic biologist to design and assemble an entire genome. In 2008, it was reported that the 582,970bp *Mycoplasma genitalium* genome was artificially synthesised in a five-stage assembly utilising a method of *in vitro* recombination to arrange DNA. The genomic design was slightly modified from wild-type *M. genitalium* to neutralise genes involved in pathogenicity, and several watermarks were added in order to provide a means to identify the synthetic DNA (Gibson et al., 2008). This technology was then employed to design and assemble the much larger 1,077,947bp *M. mycoides* genome. Significantly, this synthetic genome was then transplanted into a modified *M. capricolum* recipient cell to create a modified synthetic cell with cellular function managed exclusively by the synthetic DNA of *M. mycoides* (Gibson et al., 2010). Despite the fact the synthetic *M. mycoides* genome was almost identical to the wild-type version and *M. capricolum* is a very closely related

species of *M. mycoides,* this is undoubtedly a remarkably achievement and paves the way to a new era in genomic engineering. It is worth noting that a major obstacle encountered in this work was DNA mutation, with a single nucleotide substitution in an essential gene necessary for chromosomal replication (*dnaA*) rendering the synthetic genome ineffective (Gibson et al., 2010). Thus, we are reminded that in order to achieve this goal, every facet of cellular function must be understood and accounted for. If achieved, the scope to produce important chemical and pharmaceutical products is vast.

1.3.4 Synthetic Biology – Engineering Plant Immunity

1.3.4.1 Background

Many important food crops such as rice, wheat and maize are grown in monocultures as concentrating a single crop species to a specific area facilitates effective management. However, this creates an ecological niche which can be exploited by plant pathogens, and consequently large quantities of pesticides are required to prevent extensive yield loss. Attempts have been made to exploit the plant immune system with transgenic rice expressing the gene *Xa21* a good example of how this technology can provide broad-spectrum resistance to bacterial blight (Ikeda et al., 1990; Khush et al., 1990). However, this only provides a narrow defence, as plants, in their natural environment are continually bombarded by a variety of pathogens. This makes engineering durable crops with broad resistance to a diverse assortment of pathogenic bacteria, fungus, oomycetes and/or chewing insects incredibly difficult, not least because many of the pathways that regulate specific plant defences are mutually antagonistic. Therefore, if the process of SAR manifestation can be understood and harnessed then the capability to engineer economically important plant species that are able to naturally resist a broad-spectrum of pathogens is a distinct possibility.

1.3.4.2 NPR1-dependent Immune Regulation - A Highly Conserved Mechanism

In *Arabidopsis*, NPR1 is the main transducer of the SA signal and is vital for SAR initiation. Interestingly this signalling system may be conserved across plant species. Significantly, it was found that overexpressing *Arabidopsis NPR1* in rice increased resistance to bacterial blight pathogen *Xanthomonas oryzae* pv. o*ryzae*. In order to determine a potential genetic mechanism, a yeast two-hybrid screen and *in vitro* pull-down experiment was performed. Interestingly these experiments determined that *AtNPR1* interacted with a subclass of rice TGA factors (rTGA2.1, rTGA2.2, rTGA2.3), and rTGA2.1, in particular, was shown to be able to selectively bind *in vitro* with high affinity to the *as-1* sequence housed in the *Arabidopsis PR-1* promoter (Chern et al., 2001). The same group later identified a rice NPR1 homolog designated NH1, that when overexpressed led to constitutive defence gene activation, including *PR-1* (Chern et al., 2005). Similarly, when *Arabidopsis NPR1* is overexpressed in tomato, this correlates with an increased resistance to both fungal and bacterial diseases (Lin et al., 2004). With NPR1 homologues being present in many important plant species such as tobacco, tomato, apple, orange and rice, there is a high likelihood NPR1-mediated resistance is a conserved signal transduction pathway present in both monocot and dicot plants (Durrant and Dong, 2004). Thus, if the dynamic function of NPR1 can be understood then this would potentially provide scope to engineer inducible immune resistance in a variety of plant species.

1.3.4.3 Increased Robustness of Biomass

Biofuel derived from biomass represents a renewable and potentially carbon neutral method to meet global energy requirements. Typically, simple sugars derived from plant cell wall polysaccharides in a process known as saccharification are converted into ethanol and/or other biofuels. However the efficiency of this process is inhibited by a high concentration of the phenolic polymer lignin present in plant material (Weng et al., 2008; Martínez et al., 2009). In order to avoid costly and time-consuming pre-treatments that degrade lignin, work is ongoing to determine if lignin content can be

reduced/removed at the source. If achieved, this approach would be beneficial to both the biofuel and paper pulp industry (Ragauskas et al., 2006). One such study, in which six lignin biosynthetic enzymes were independently downregulated in transgenic *Medicago sativa* (alfalfa) plants, found that reduced lignin content required less pre-treatment and yielded significantly higher quantities of sugars (Chen and Dixon, 2007). Moreover, a study using switchgrass (*Panicum virgatum* L.) defective in *COMT1* (caffeate O-methyltransferase), an essential gene required for lignin biosynthesis, was found to contain reduced levels of lignin and this decrease improved bioethanol yield by up to 38% (Fu et al., 2011). This suggests that potentially any economically important biomass species could be engineered to contain less lignin and thus biofuel production efficiency could be significantly increased. However, in doing this we must be cautious not to inadvertently increase the susceptibility of that modified plant to pathogens. Lignin is a major component of plant cells, providing structural rigidity as well as strength to vascular tissues in order to maintain turgor pressure. A study in which lignin biosynthesis is deliberately altered, suggests plants are highly adaptable and can tolerate modification to lignin content and structure (Boerjan et al., 2003). However, it is well established that during plant defence responses, lignin is deposited in plant cell walls and this process is thought to reinforce the physical barrier to prevent further pathogen ingress (Moershbacher et al., 1990). Consequently it is this phenomenon that may provide the greatest challenge to lignin-modified biomass. Studies in *Arabidopsis* plants defective in *COMT1* were found to be more susceptible to several agronomically important plant pathogens, including necrotrophic fungi *Botrytis cinerea* and *Alternaria brassicicola*, as well as bacterial infection from *Xanthomonas campestris* pathovar *campestris* (*Xcc*) and *Pseudomonas syringae pv. tomato* (*Pst*) (Quentin et al., 2009). Moreover, it has been found that treating wheat with inhibitors of enzymes involved in lignin biosynthesis increases the susceptibility of the plant to the stem rust fungus, *Puccinia graminis* (Moershbacher et al., 1990). This indicates that in order to prevent yield loss to pathogen, any potential lignin-modified biomass must be adequately managed. Undoubtedly this would require extensive use of pesticides, which invariably increases the carbon cost of such fuel. However if these biomass plants, many of which are also food crops, could be engineered to be ‘super-immune’, then this

problem could be circumvented. If we have elementary understanding of the mechanisms by which plants initiate and mount defence reprogramming, this provides scope to allow us to design crops and biomass with particular traits.

1.4 Research Aims and Objectives

If the molecular mechanisms that govern plant local immunity and SAR can be understood then this provides scope to engineer economically-important plant species that are able to resist a broad-spectrum of pathogens. NPR1 orchestrates a highly complex immune network and uncovering the dynamic nature of this protein is of central importance. The traditional method employed by molecular biologists involving large-scale genetic screens is a laborious process and a new approach might be informative. This project aims to set these foundations. A major goal of synthetic biology is to develop a deeper understanding of biological design principles, by building circuits and studying their behaviour in cells. Using a synthetic biology approach this project aims to develop a yeast tool that can be used to manipulate and subsequently understand NPR1 function within the context of plant immune circuits.

This will be achieved by accomplishing the following goals:

- Redox signalling has emerged as a key functional mechanism to control many important regulatory proteins involved in plant immunity. This work aims to create a yeast strain which is redox-tunable so that NPR1 oligomer-to-monomer dynamics can be selectively manipulated.

- Integration of circumstantial evidence from numerous studies in plants has created a basic immunity model. Key constituent proteins from the plant immune system will be rebuilt as a synthetic circuit in yeast.

- A mathematical simulation representative of NPR1-dependent gene activation will be developed.

CHAPTER 2

2. Materials and Methods

Unless otherwise stated, all chemicals were purchased from Sigma-Aldrich® (UK); all oligonucleotides from Invitrogen™ (Paisley, UK and Beijing, China) and the vast majority of yeast SD medium components were from ForMedium™ (Hunstanton, UK).

2.1 Yeast Management

2.1.1 Transformation of yeast

Yeast cells were transformed using an adapted method described by Gietz and Woods, (2002). The cells were grown overnight at 30°C with shaking at 225rpm in 30ml Yeast Peptone Dextrose (YPD) medium (2% difco peptone, 1% yeast extract, 2% glucose, 0.004% adenine hemisulfate (and 2% agar for plates only)). The cells were then diluted to an OD600nm value of ~0.1 in a 40ml volume of YPD medium and grown for a further 3-5 hours at 30°C at 225rpm to a cell density OD600nm value of 0.3-0.4. The cells were centrifuged at 500g for 5 minutes at room temperature, the supernatant removed, and the cells washed again with 40ml sterile ddH_2O. The sample was centrifuged once again at 500g for 5 minutes at room temperature, the supernatant removed, with the cells finally being re-suspended in 1ml ddH_2O. From this, 100µl of the cells were transferred into a sterile 2ml microcentrifuge tube, centrifuged at 20900g for 15 seconds and the supernatant removed. The resultant cell pellet was re-suspended in 360µl of transformation mix (40% PEG 3350, 100mM LiAc, 100mg boiled SS-carrier DNA, 1–4 µg linearized plasmid DNA and ddH_2O) by vortexing vigorously for 10 seconds. The sample was placed at 42°C and cells heat shocked for 40 minutes followed by cooling on ice for 2 minutes. The sample was then centrifuged at 20900g for 15 seconds and the transformation mix carefully aspirated. The yeast cells were re-suspended in 300µl ddH_2O, and the entire quantity plated on selective dropout SD medium (6.7g/L yeast nitrogen base without amino acids, appropriate dropout mixture, carbon source (2% glucose/galactose/raffinose) and 2% agar (for plates only)) and

incubated (on inverted plates) at 30°C for 2-4 days, until individual colonies were visible.

Table 2-1 Yeast strains utilised during this study

Yeast Strain	Mating Type a/α	Genotype (Selection)	Genotype (Gene Disruption)	Source
BY4741	*MAT***a**	his3Δ1; leu2Δ0; met15Δ0; ura3Δ0	N/A	EUROSCARF (acc. no. Y00000)
BY4741	*MAT***a**	his3Δ1; leu2Δ0; met15Δ0; ura3Δ0	*sfa1*	EUROSCARF (acc. no. Y03866)
BY4741	*MAT***a**	his3Δ1; leu2Δ0; met15Δ0; ura3Δ0	*sfa1 yap1 yhb1*	This study

2.1.2 Gene Specific Disruption

The general methodology is described at Voth et al., (2001). In order to disrupt a specific gene, the HO-specific cDNA fragments contained in the vector HOL-hisG-URA3-hisG-Poly-HOR can be substituted with fragments designed with homology to any gene. Using primer sets indicated at table 2-2, target fragment 'Left' was generated by PCR amplification to produce cDNA flanked with the restriction enzyme sites SalI and Xhol, while fragment 'Right' was designed to produce cDNA flanked with the restriction enzyme sites EcoRI and Xbal. These fragments were then sequentially ligated into the HOL-hisG-URA3-hisG-Poly-HOR vector to create YAP1L-hisG-URA3-hisG-Poly-YAP1R and YHB1L-hisG-URA3-hisG-Poly-YHB1R. These vectors contain the *hisG-URA3-hisG* cassette that facilitates detection by uracil prototrophy. Plating successful transformants on complete SD medium (without amino acid selection) supplemented with 150μg/μl 5-Fluorootic acid (5-FOA) (ForMedium™), recombination between the hisG tandem repeats returns the cell to uracil auxotrophy and means the URA3 marker can be recycled.

Yeast cells were transformed using the method described at 2.1.1 with the plasmid being linearized with the enzyme SpeI. To confirm successful targeted integration gDNA was extracted (described at 2.5.1) and PCR analysis performed using one primer specific to the construct (URA3) and the other designed to anneal specifically to

a DNA sequence located in an adjacent gene (see table 2-2). Disruption was confirmed by subsequent RT-PCR analysis using gene-specific primers with *Actin1* acting as a control (see 2.3.2 and table 2-5).

Table 2-2 Oligonucleotides used to disrupt targeted yeast genes

Target Gene	Position (L/R)	Primer Name	Primer sequence 5'- 3'	Size (bp)
YAP1	Left	YAP1 LF XhoI	ATCTCGAGCGGAAACGGCAGTAAACGACG	401
		YAP1 LR SalI	ATGTCGACCAAGTCAACCAGGGGCTCAGGA	
YAP1	Right	YAP1 RF EcoRI	ATGAATTCAATCTGGCTTTCCCAGACGACAA	540
		YAP1 RR XbaI	CGTCTAGAATGCTTATTCAAAGCTAATTGAACGTC	
YHB1	Left	YHB LF XhoI	GCCTCGAGAAATAGTTGATAAATTTGATTAATTTC	960
		YHB LR SalI	CGGTCGACTAAAAAGAATACGTTATATCGGC	
YHB1	Right	YHB RF EcoRI	GCGAATTCGGATTAGTCTCTGAATATTTACACAAGG	480
		YHB RR XbaI	GCTCTAGATGACATCTTTGGACCAAATGGTT	
-	-	URA3-F	CCCGGTGTGGGTTTAGATGACAAGG	-
-	-	YML006C-R	GGTTCTGCAGGTACGGATAAATCTCAGC	-
-	-	YGR235C-R	GGGAATGCAATCAAAAATTGGACTGG	-

2.1.3 Extraction of Yeast Genomic DNA

Yeast genomic DNA was extracted using an adapted procedure described in Ausubel et al., (1995). Briefly, cells were grown overnight to stationary phase in a 10ml liquid culture of YPD medium. The culture was centrifuged at 1700g for 90 seconds at room temperature and the cells were resuspended in 10ml ddH_2O and again centrifuged at 1700g for 90 seconds. The supernatent was removed and the cells re-suspended in 1ml ddH_2O, before being transferred to a 2ml microcentrifuge tube, which was subsequently centrifuged at 17900g for 15 seconds. The supernatant was poured off and 0.3g (200µl volume) 425-600µm glass beads, acid washed (Sigma) added, followed by 200µl breaking buffer (2% (v/v) Triton X-100, 1% (w/v) SDS, 100mM NaCl, 10mM Tris-HCl, pH 8, 1mM EDTA) and 200µl phenol/chloroform/isoamyl alcohol. The sample was vortexed at full power for 3 minutes. 200µl TE buffer was then added and the sample vortexed briefly before being centrifuged at 17900g for 5 minutes. The aqueous layer was transferred to a fresh 1.5ml microcentrifuge tube and 1ml of 100% ethanol added. The sample was mixed by inversion before being centrifuged at 17900g for 3

minutes. The supernatant was removed and 0.4ml TE buffer added to the pellet. 30µl of 1mg/ml RNase A was then added and the sample was mixed by inversion before being incubated for 5 minutes at 37˚C. 10µl of 4M ammonium acetate and 1ml of 100% ethanol were then added. The sample was then mixed and centrifuged at 17900g for 3 minutes. The supernatant was then removed and the pellet allowed to partially dry at room temperature. The genomic DNA was then re-suspended in 50-100µl TE buffer and allowed to dissolve at room temperature for ~30 minutes.

Table 2-3 Plasmids Utilised During This Study

Plasmid Name	Target Loci	MCS Insert	Reference
pRS303	HIS3/ YOR202W	pMEL1:LUC-SKL:CYC Term	Sikorski R S, Hieter P. (1989)
pRS303	HIS3/ YOR202W	pMEL1:MCHERRY:CYC Term	Sikorski R S, Hieter P. (1989)
pRS303	HIS3/ YOR202W	pGAL1: FLAG-GSNOR1:CYC Term	Sikorski R S, Hieter P. (1989)
pRS305	LEU2/ YCL018W	pGAL1:AtGSNOR1:CYC Term	Sikorski R S, Hieter P. (1989)
pRS306	URA3/ YEL021W	pGPD1:TGA2:EYFP:CYC Term	Sikorski R S, Hieter P. (1989)
HOL-hisG-URA3-hisG-Poly-HOR	HO/ YDL227C	pGPD1:TGA2:EYFP:CYC Term	Voth et al., (2001).
HOL-hisG-URA3-hisG-Poly-HOR	HO/ YDL227C	pGPD1:TGA3:EYFP:CYC Term	Voth et al., (2001).
ADE2L-hisG-URA3-hisG-Poly-ADE2R	ADE2/ YOR128C	pGPD1:NPR1:ECFP:CYC Term	Fox et al., (2007)
pIS385	LYS2/ YBR115C	pMET25:NTRA:CYC Term & pMET25:TRXH5:CYC Term	Sadowski et al., (2007).
pIS385	LYS2/ YBR115C	pMET25:FLAG-TRXH5:CYC Term	Sadowski et al., (2007).
YAP1L-hisG-URA3-hisG-Poly-YAP1R	YAP1/ YML007W	N/A	This Study
YHB1L-hisG-URA3-hisG-Poly-YHB1R	YHB1/ YGR234W	N/A	This Study
HOL-hisG-URA3-hisG-Poly-HOR	HO/ YDL227C	roGFP2	Hanson, et al., (2004)

2.2 Bacterial Management

2.2.1 Preparation of KCM competent cells

The XL1-blue laboratory strain of *E. coli* was grown in 500 ml of LB (1% tryptone, 1% NaCl, 0.5% yeast extract and 2% (for plates only)) to an OD600nm value of 0.3-0.4. The culture was chilled on ice for 2 minutes, before being centrifuged (in sterile pre-chilled centrifuge bottles) at 8000g for 10 minutes at 4°C. The cell pellet was re-suspended in 1/10 volume of ice cold sterile TSS (LB with 10% PEG 3350, 5% DMSO,

20mM $MgSO_4$, pH= 6.5). 100µl of the cell suspension was then aliquoted into pre-chilled sterile 1.5ml microcentrifuge tubes, immediately frozen in liquid nitrogen and stored at -70°C until use.

2.2.2 Transformation of bacteria

A 100µl aliquot of cells was placed on ice and allowed to thaw. A total volume of 100µl consisting of 5X KCM (0.5M KCl, 0.15M $CaCl_2$, 0.25M $MgCl_2$), plasmid DNA and sterile ddH_2O was then added to the cells, the sample mixed and incubated on ice for 20 minutes. The cells were then heat shocked for 5 minutes at 37°C. The cells were then chilled on ice for 1-2 minutes before 800µl of pre-warmed LB medium was added. The sample was incubated at 37°C for 40-60 minutes in a shaking incubator at 250 rpm. 300ul of the transformation was added to selective LB medium plates and the sample was incubated at 37°C (on inverted plates) until colonies were visible.

2.2.3 Plasmid Extraction

Plasmid was extracted using either the QIAprep® Miniprep (Qiagen) or GeneJET™ Plasmid Miniprep Kit (Fermentas) in accordance with the manufacturer's instructions.

Table 2-4 Oligonucleotides to generate cDNA for Plasmid Constructs

Primer Name	cDNA	Primer sequence (5'- 3')
GPD-PacI F	GPD1 Promoter	**F**: GCTTAATTAAAGTTTATCATTATCAATACTCGCCATTTC
GPD-EcoRI F		**F**: GCGAATTCATCCGTCGAAACTAAGTTCTG
GPD- PmeI R		**R**: TAGTTTAAACATCCGTCGAAACTAAGTTCTGGT
GAL1-Xbal - F	GAL1 Promoter	**F**: GCTCTAGAATCCGGGGTTTTTTCTCCTTG
GAL1- SalI - R		**R**: ATGTCGACCTAGTACGGATTAGAAGCCGC
wtMELProm58-F	MEL1 Promoter	**F**:ATCTCGAGCATCTATGACGTAAGTAAAATAGTGACGTAGAGTGAAAGCCA ATGCGTCC
mtMELProm58-F		**F**:ATCTCGAGCATCTATAGAATAAGTAAAATAGTAGAATAGAGTGAAAGCCA ATGCGTCC
MEL1P BglII-F		**F**: GCAGATCTCGTCGTTGCTTTTATTACCG
MEL1P SacI-R		**R**: GCGAGCTCTCTTTTTTACTTTAATATTATGTATACTG
MEL1P XhoI-R		**R**: GCCTCGAGAAGAAGAAAGGAAGACATG
MET25 BamHI-F	MET25 Promoter	**F**:ATGGATCCGCCTACGTTCCCAAGCTTAG
MET25- Xbal - F		**F**: GCTCTAGAGTATGGATGGGGGTAATAGAATTG
MET25 - SalI - R		**R**: ATGTCGACCGGATGCAAGGGTT
FDH-XbaI-F	GSNOR	**F**: GATCTAGAATGGCGACTCAAGGTCAGGTT
FDH-XhoI-R		**R**: TGCTCGAGTTATTTGCTGGTATCGAGGAC
NPR1-EcoRI-F	NPR1	**F**: TAGAATTCATGGACACCACCATTGATGG
NPR1-SalI-R		**R**: TAGTCGACCCGACGACGATGAGAGA
TGA2- PmeI –F	TGA2	**F**: GCGTTTAAACATGGCTGATACCAGTCCGAG
TGA2- KpnI –R		**R**: TAGGTACCCTCTCTGGGTCGAGCAAGC
TGA3-F PmeI	TGA3	**F**: GCGTTTAAACATGGAGATGATGAGCTCTTC
TGA3-R KpnI		**R**: TAGGTACCAGTGTGTTCTCGTGGACGAGCT
TRXh5 Xbal-F	TRXh5	**F**:GCTCTAGAATGGCCGGTGAAGGAGA
TRXh5 Xhol-R		**R**; GCCTCGAGTCAAGCAGAAGCTACAAGAC
NTRA Xbal-F	NTRA	**F**: GCTCTAGAATGGAAACTCACAAAACCAAGGT
NTRA XhoI –R		**R**:GCCTCGAGTCAATCACTCTTACCCTCCTG
LUC44 BglII-F	LUC-SLK	**F**: GCAGATCTATGGAAGACGCCAAAAACAT
LUC442 Xhol-R		**R**: ATCTCGAGTTAAAGCTTCTTTCCGCCCTTCTTGG
EYFP-KpnI-F	EYFP	**F**: ATGGTACCATGGTGAGCAAGGGCGAGGAGCTGTTCACCGGG
EYFP-BglII-R		**R**:ATAGATCTTTACTTGTACAGCTCGTCCATGCC
ECFP Sal F	ECFP	**F**: TAGTCGACATGGTGAGCAAGGGCGAG
ECFP PmeI/NotI R		**R**: ATGCGGCCGCGTTTAAACTTACTTGTACAGCT
mCherry- BglII F	mCherry1	**F**:CGAGATCTATGGTGAGCAAGGGCGAG
mCherry- PmeI R		**F**:GCGTTTAAACTTACTTGTACAGCTCGTCCATG
EYFP-KpnI-F	roGFP2	**F**: ATGGTACCATGGTGAGCAAGGGCGAGGAGCTGTTCACCGGG
EYFP-BglII-R		**R**:ATAGATCTTTACTTGTACAGCTCGTCCATGCC
CYC1Term SacI-F	CYC1 Terminator	**F**:TAGAGCTCCGGCCGCAAATTAAAGC
CYC1Term AscI-F		**F**: TAGGCGCGCCCGGCCGCAAATT
CYC1Term EcoRI-F		**F**: TAGAATTCCGGCCGCAAATTAAAGCCTT
CYC1Term PmeI-R		**R**: GCGTTTAAACCTCGAGTCATGTAATTAGTTATGTCAC
CYC Term NotI-R		**R**:TAGCGGCCGCGCCGGCGTTTAATTT
CYC1Term BglII-R		**R**: GCAGATCTCTCGAGTCATGTAATTAGTTATGTCACG
FLAG TRXh5 Xbal-F	FLAG::TRX	**F**:TCTAGAATGGACTACAAAGACGATGACGACAAAATCACAAGTTTGTACAA AAAAGCAGGCTCCGCGGCCGCCCCCTTCACCATGGCCGGTGAAGGAGAAGT
FLAG GSNOR Xbal-F	FLAG:GSNOR	**F**:TCTAGAATGGACTACAAAGACGATGACGACAAAATCACAAGTTTGTACAA AAAAGCAGGCTCCGCGGCCGCCCCCTTCACCATGGCGACTCAAGGTCAGG

2.3 RT-PCR Methodology

2.3.1 Extraction of total RNA

Total RNA was extracted from yeast cells using the RNeasy® Mini kit (Qiagen) in accordance with the manufacturer's instructions and concentration (ng/µl) was quantified using a Nanodrop ND1000 spectrophotometer (Thermo Scientific).

2.3.2 Reverse Transcription (RT)-PCR

Reverse transcription (RT)-PCR was completed using an Omniscript RT-PCR kit (Qiagen) in accordance with the manufacturer's instructions. For cDNA synthesis, 1µg of total RNA (made up to 5µl with diethylpyrocarbonate (DEPC) treated dd$H_2$0 previously incubated with 0.1% v/v DEPC for 1 hour at 37 °C followed by autoclaving for 20 minutes to inactivate DEPC) was denatured at 65 °C for 5 minutes before 5µl RT reaction mixture (1X reaction buffer, 0.5mM dNTPs, 2.5µM oligo(dt) primer, 4U RNAse inhibitor and 2U of Omniscript RT) was added (total volume 10µl). The sample was incubated for 1 hour at 37°C followed by 65°C for 10 minutes to heat inactivated the reaction. The cDNA was diluted 10-fold in DEPC-treated water and stored at -20ºC. PCR reactions were set-up using Crimson *Taq* DNA Polymerase (NEB) in thin-walled 0.2ml PCR tubes (Axygen Scientific) with gene-specific primer sets indicated in table 2-5. PCR products were separated on 1.8% agarose gels containing 0.5µg/ml ethidium bromide with the 1Kb Plus DNA Ladder (Invitrogen™) used as a reference.

Table 2-5 Details of RT-PCR primers and reaction conditions

Gene	Primer Name	Primer sequence (5'- 3')	RT-PCR Reaction Conditions					cycle no.	Size (bp)
			Initial Denaturation	Denaturation	Annealing	Extension	Final Extension		
SFA1	RT SFA1-F	TGCCTGATGGGACCACAAGATTT	95°C for 30 seconds	95°C for 20 seconds	57°C for 30 seconds	68°C for 40 seconds	68°C for 5 minutes	21	248
	RT SFA1-R	TCCTACAGTCCCGCAGCCAAATA							
YAP1	RT YAP1-F	GAAAATGAACCAGGTATGTGGA	95°C for 30 seconds	95°C for 20 seconds	57°C for 30 seconds	68°C for 40 seconds	68°C for 5 minutes	21	244
	RT YAP1-R	GCACTCATATCGAAACCAAGTCG							
YHB1	RT YHB1-F	TGCCAATCACTCCAGGTCAGTAT	95°C for 30 seconds	95°C for 20 seconds	57°C for 30 seconds	68°C for 40 seconds	68°C for 5 minutes	21	207
	RT YHB1-R	CATCACCAACTTTAGCGTCCTTG							
ACT1	RT ACT1-F	ATTGAGAGTTGCCCCAGAAGAAC	95°C for 30 seconds	95°C for 20 seconds	57°C for 30 seconds	68°C for 40 seconds	68°C for 5 minutes	21	246
	RT ACT1-R	TGGCGTGAGGTAGAGAGAAACC							
GSNOR	RT FDH-F	CGTCGCCAAAATTGATCCTACTGC	95°C for 30 seconds	95°C for 20 seconds	57°C for 30 seconds	68°C for 40 seconds	68°C for 5 minutes	19	293
	RT FDH-R	TCACTTCCTGAATTGGCTTGTCGT							
TRXh5	RT TRXh5-F	CATACCCTCGAAGTTTGGAACGAGA	95°C for 30 seconds	95°C for 20 seconds	57°C for 30 seconds	68°C for 40 seconds	68°C for 5 minutes	19	211
	RT TRXh5-R	TGCCTCAACTTTGAATTCCTGAGC							
GSH1	RT-GSH-F	GCCGCTTCCAGGTCTCTGTTTTT	95°C for 30 seconds	95°C for 20 seconds	57°C for 30 seconds	68°C for 40 seconds	68°C for 5 minutes	21	210
	RT-GSH-R	GGAAGCCAGTTTCGCCTCTTTGT							
GLR1	RT-GLR1- F	TTACGAGAACGTCCCCAGCGTAA	95°C for 30 seconds	95°C for 20 seconds	57°C for 30 seconds	68°C for 40 seconds	68°C for 5 minutes	21	223
	RT-GLR1- R	ACCAACAATGTGCAGACCGACAA							
GPX1	RT GPX1 F	AGTGATTGTGGCCTTTCCCTGTG	95°C for 30 seconds	95°C for 20 seconds	57°C for 30 seconds	68°C for 40 seconds	68°C for 5 minutes	21	244
	RT GPX1 R	CACCTTCCCATTTCGGTCTACCA							
GPX2	RT GPX2 F	AATCAGTTCGGGAAGCAGGAACC	95°C for 30 seconds	9°C for 20 seconds	57°C for 30 seconds	68°C for 40 seconds	68°C for 5 minutes	21	266
	RT GPX2 R	TGGTCCAAGGACGATGGTTTTGT							
GRX1	RT- GRX1-F	GAAAACGAGATCTTCGTCGCATCC	95°C for 30 seconds	95°C for 20 seconds	57°C for 30 seconds	68°C for 40 seconds	68°C for 5 minutes	21	228
	RT- GRX1-R	CAAGTCGTCGTTGCCTCCAATATG							
GRX2	RT-GRX2-F	CCAAAAATGGTATCCCAGGAAACAG	95°C for 30 seconds	95°C for 20 seconds	57°C for 30 seconds	68°C for 40 seconds	68°C for 5 minutes	21	200
	RT-GRX2-R	GCGTCTTGAATCTCTGAGCCATTG							
TRR1	RT-TRR1- F	TTCCCAGGTTTCCCAGATGGTCT	95°C for 30 seconds	95°C for 20 seconds	57°C for 30 seconds	68°C for 40 seconds	68°C for 5 minutes	21	203
	RT-TRR1-R	GAAGCGCCTGTGGCCAAGATTAT							
TRX1	RT-TRX1-F	TGCGGTCCATGTAAAATGATTGC	95°C for 30 seconds	95°C for 20 seconds	57°C for 30 seconds	68°C for 40 seconds	68°C for 5 minutes	21	183
	RT-TRX1-R	GGCACCAACAACCTTTGCAACTT							
TRX2	RT-TRX2- F	CACATGGTGTGGGCCATGTAAAA	95°C for 30 seconds	95°C for 20 seconds	57°C for 30 seconds	68°C for 40 seconds	68°C for 5 minutes	21	211
	RT-TRX2- R	TTGCTTGATAGCAGCTGGGTTGG							
AHP1	RT-AHP1F	GTTGACAACCCGTTCGCTAACCA	95°C for 30 seconds	9°C for 20 seconds	57°C for 30 seconds	68°C for 40 seconds	68°C for 5 minutes	21	218
	RT-AHP1R	TCGGTACCTGGGTTGGTTTCCTT							
PRX1	RT PRX1 F	ATGGGTCACTGAAGACCGTGAGG	95°C for 30 seconds	95°C for 20 seconds	57°C for 30 seconds	68°C for 40 seconds	68°C for 5 minutes	21	229
	RT PRX1 R	TTAGCCTTCGCCTCATCATTGGA							
DOT5	RT DOT5-F	CCTATTTCGACACCGGAAGTGCCTA	95°C for 30 seconds	95°C for 20 seconds	57°C for 30 seconds	68°C for 40 seconds	68°C for 5 minutes	21	233
	RT DOT5-R	GTGCTTGCCCTGGGATACACAAAAA							
TSA1	RT TSA1 F	CGAAGAAGAAGGTGTCGCCTTGA	95°C for 30 seconds	95°C for 20 seconds	57°C for 30 seconds	68°C for 40 seconds	68°C for 5 minutes	21	211
	RT TSA1 R	GTCTTCAACGGTTGGCTTGATGG							
TSA2	RT TSA2-2 F	ACCTTCCCAGAAAAGACGGTGGATT	95°C for 30 seconds	95°C for 20 seconds	57°C for 30 seconds	68°C for 40 seconds	68°C for 5 minutes	21	203
	RT TSA2-2 R	AGCTTCATTGACGTTTCTGCCAACA							
SRX1	RT SRX1 F	CATTCCCACCGCTAGCAAGACAT	95°C for 30 seconds	95°C for 20 seconds	57°C for 30 seconds	68°C for 40 seconds	68°C for 5 minutes	21	258
	RT SRX1 R	ATGTCGAGACTGCTGCCCAGGTA							
ECM38	RT ECM38 F	TATGACCCCGATCACTGGATTGC	95°C for 30 seconds	95°C for 20 seconds	57°C for 30 seconds	68°C for 40 seconds	68°C for 5 minutes	21	219
	RT ECM38 R	CCTTAACGCCGCAAGTAGTGCAG							
PDI1	RT PDI1 F	ATCCGGTAAGATTGACGCCGACT	95°C for 30 seconds	95°C for 20 seconds	57°C for 30 seconds	68°C for 40 seconds	68°C for 5 minutes	21	232
	RT PDI1 R	ACCAAAGTAGGGCAAGGCTTCCA							

2.4 Microscopy

2.4.1 Protein Localisation

Yeast strains transformed (described at 2.1.1) with NPR1 and/or TGA2/TGA3 were imaged using a Leica TCS SP5 laser scanning confocal microscope set to 100x optical zoom. Cells were visualised under phase contrast to determine optimal focus. Protein localisation was determined using an excitation wavelength of 458nm and emission of 477-505nm to visualise ECFP fused to NPR1; while an excitation wavelength of 514nm and emission of 525-590nm was used to visualise EYFP fused to TGA2 or TGA3. Nuclear DNA was stained by adding 0.25 mg/ml ethidium bromide and imaged at excitation 512nm and emission 633nm (Sengupta et al., 2003).

2.4.2 Fluorescence resonance energy transfer (FRET)

All images were captured using a Leica TCS SP5 laser scanning confocal microscope set to 100x optical zoom using the ECFP and EYFP excitation and emission wavelengths described at 2.4.1. Protein interactions in live yeast cells were determined using sensitised emission FRET by capturing the following images; 1) donor only using donor filter set; 2) donor only using FRET filter set; 3) acceptor only using acceptor filter set; 4) acceptor only using FRET filter set; 5) FRET specimen only using FRET filter set. The image was analyzed with Image-Pro Analyzer 7.0 using MetaMorph 7.5 software to calibrate for background signal. This was achieved by determining both the signal threshold of the images obtained for the donor only using FRET settings and the donor only using acceptor settings, with this data used to calculate co-efficient (A). This is repeated with the acceptor images to obtain co-efficient (B). The FRET efficiency (%) was determined by analyzing the average threshold of the FRET specimen using only FRET filter set images calibrated with co-efficient A and B.

2.4.3 Imaging with roGFP2

Yeast strains transformed (described at 2.1.1) with roGFP2 were grown overnight in SD minimal medium (pH7) with 2% raffinose as a carbon source. Cells were imaged using

a Leica TCS SP5 laser scanning confocal microscope in the same medium. Simultaneous images were captured at an excitation maximum of 408 and 488nm, with emission at 525nm. To fully reduce or oxidise roGFP2, 20mM DTT or 25mM H_2O_2 respectively, was added directly to the growth medium and incubated at room temperature for 10 minutes, with regular agitation. Ratiometric imaging was completed using Image-Pro Analyzer 7.0.

2.4.4 Determination of actual intracellular redox potential using roGFP2

Images of yeast cells expressing roGFP2 were captured and imaging completed using Image-Pro Analyzer 7.0 in accordance with Para. 2.4.3. Initially the degree of oxidation (*OxD*r*oGFP2*) was calculated in accordance with the following equation.

$$OxD_{roGFP2} = \frac{R - R_{red}}{(I_{488red}/I_{488ox})(R_{ox} - R) + (R - R_{red})}$$

Components of this equation include; R is the actual 405/488nm ratio, R_{red} is the 405/488nm ratio for fully reduced roGFP2 (+DTT) and R_{ox} is the 405/488nm ratio for fully oxidised roGFP2 (+H_2O_2). The factor $I488_{red}$ /$I488_{ox}$ is the measured fluorescence intensities of fully oxidized and fully reduced roGFP2 when measured at excitation wavelength 488nm (Meyer and Brach, 2009).

The actual redox potential (voltage of an electrochemical cell) is determined according to the Nernst equation:

$$E_{roGFP2} = E'_{0\,roGFP2} - \frac{RT}{zF} \ln \frac{1 - OxD_{roGFP2}}{OxD_{roGFP2}}$$

Components in this equation include: *E*'0roGFP = -0.280mV (in accordance with Hanson et al., 2004), R is the gas constant (8.314472 J K^{-1} mol^{-1}), T is the absolute temperature (298.15 K), z is the number of transferred electrons (2), F is the Faraday constant (9.64853399×10^4 C mol^{-1}), at room temperature (21°C).

2.5 Biochemical Techniques

2.5.1 *In vitro S*-nitrosylation pull-down assay

The biotin switch method was used to detect *S*-nitrosylated NPR1 protein in accordance with Jaffrey and Snyder, (2001). Total cellular protein was obtained by mechanically breaking the yeast cells in RIPA buffer (1% NP40, 0.5% Sodium deoxycholate, 150mM NaCl, 50mM Tris-HCl (pH7.5) and 2mM EDTA) containing a protease inhibitor cocktail (Roche) for fungal and yeast cells (containing 4-(2-Aminoethyl) benzenesulfonyl fluoride hydrochloride (AEBSF), 1,10-Phenanthroline, Pepstatin A and E-64) using 0.3g (200µl volume) 425-600µm glass beads, acid washed (Sigma).

The sample was vortexed (using a VWR Mini Vortexer MV-1) using the 60% strength setting for 3 x 40 seconds, placing on ice between sessions. The sample was then centrifuged for 5 min at 20900g to pellet the beads and insoluble material. To exchange the RIPA extraction buffer with HEN buffer (250mM Hepes-NaOH pH 7.5, 1mM EDTA, 0.1mM Neocuproine) three samples (each containing 100µg protein) were purified using a zeba desalting column (Thermo Scientific) in accordance with the manufacturer's instructions. 2mM GSNO was then added to two of the samples (the third is a negative control) and all were incubated at room temperature for 30 minutes in the dark with gentle agitation every 10 minutes. To remove GNSO the protein was then isolated using a zeba desalting column (Thermo Scientific) in accordance with the manufacturer's instructions. One of the samples previously treated with GSNO was exposed to UV set at 304nm for 5 minutes to denitrosylate protein (as a negative control). To block free –SH groups all samples were then treated with 1 x HEN buffer, 2.5% SDS and 25mM methyl methanethiosulfonate (MMTS) and the sample incubated at 50°C for 30 minutes with gentle vortexing every 5 minutes.The MMTS buffer was removed by precipitating the protein in 2 volumes acetone and incubating in the dark for 20 minutes. The protein was isolated by centrifuging at 4°C for 5 minutes at 6500g and the sample washed using 70% acetone. The protein was re-suspended in 500µl HENS buffer (HEN buffer containing 1% SDS) containing 0.4mM Biotin HPDP and 25mM ascorbate. The sample is then rotated in the dark at room temperature for 1 hour. Protein is then precipitated in 2 volumes acetone and chilled at -20°C for 20 minutes,

before being centrifuged at 4°C for 5 minutes at 13000g. The sample is washed with 70% acetone and re-suspended in 100µl H25ENS (contains 25mM Hepes-NaOH, pH 7.5). 10µl is removed from each sample (used as an immunoprecipitation input control) and 1 x SDS loading buffer (containing 50mM DTT) added. The sample is heated to 70°C for 10 minutes and stored at -20°C until required. To the remaining sample (~90µl) 300µl neutralization buffer (1xH25EN, 100mM NaCl, 0.5% Triton X-100) was added. To isolate protein modified with biotin ~25µl of packed streptavidin agarose beads (Invitrogen™) previously washed with neutralisation buffer were also added. The samples were then placed on a rotating incubator for 12-16 hours at 4°C. To remove protein not bound to streptavidin, the beads were washed 5 times using 1ml wash buffer (1xH25EN, 600mM NaCl, 0.5% Triton X-100), and centrifuged at 200g for 1 minute between washes, removing as much buffer as possible on each occasion. 25µl 1xH25ENS buffer containing 1% beta-mercaptoethanol (ß-ME) was added to the beads and the sample incubated at room temperature for 30 minutes with regular agitation. The sample was then centrifuged at 5000g for 1 minute and the supernatant was transferred into a clean 1.5ml microcentrifuge tube. 1xSDS loading buffer (containing 50mM DTT) was added and the sample to heated 70°C for 10 minutes. Both the streptavidin pull-down and immunoprecipitation input control samples were resolved on an 8% (w/v) SDS polyacrylamide gel and subjected to western blot analysis.

2.5.2 GSNO synthesis

GSNO was prepared in accordance with Hart, (1985) with minor modifications. 625mM reduced L-Glutathione was dissolved in pre-chilled 8ml 625mM HCl. An equimolar amount of sodium nitrite was added to the sample and the mixture stirred in the dark for 40 minutes at 4°C. 2.5 volumes of chilled acetone was then added and the sample stirred for a further 40 minutes. Excess liquid was then removed from the GSNO using Whatman Filter paper, grade 1, 185 mm Ø (circle) with the sample being kept at 4°C in the dark. The GSNO was then washed, initially with 5 x 1ml chilled ddH_2O, then 3 x 10ml chilled acetone and finally 3 x chilled diethyl ether, on each occasion being kept at 4°C in the dark. The GSNO is then dried at room temperature and the purity determined by analysing the sample using a UV spectrometer set at 340 nm, and comparing values to a standard concentration curve.

2.5.3 NPR1 GSNO Oligomerization Assay

Protein was extracted as described at 2.5.1.50µl of the protein sample was aliquoted into a thin-walled 0.2ml PCR tube (Axygen Scientific) containing varying concentrations of GNSO. The sample was incubated at 25°C for 60 minutes using a PCR thermocycler. The sample was divided and 1xSDS loading buffer (with and without 50mM DTT) added before being subjected to western blot analysis described at 2.5.7.

2.5.4 Yeast growth – GSNO and H_2O_2

Yeast cells were grown in 30ml liquid YPD medium for 16 hrs at 30°C with shaking at 225rpm. The cells were then diluted to an OD600nm value of ~0.05 in a 15ml volume of liquid YPD medium, and cultured aerobically with minimal light at 30°C with shaking at 225rpm in YPD medium supplemented with either GSNO or H_2O_2. Cell density was measured at OD600nm after 10 hours and relative growth determined by comparing values to an untreated control.

2.5.5 GSH assay

Glutathione levels were determined using the GSH-Glo™Glutathione Assay (Promega) in accordance with the manufacturer's instructions. Briefly, protein was extracted as described at para 2.5.6. A 50µl aliquot of the protein extract was added to two adjacent chambers in a 96-well plate. To one chamber 1mM DTT was added to determine total (GSH and GSSG) glutathione concentration. 50µl of GSH-Glo™ Reagent (Luciferin-NT and Glutathione S-Transferase added at a 1/50 ratio to GSH-Glo™ Reaction Buffer) was added to each sample and incubated at room temperature in the dark for 30 minutes. 100µl reconstituted Luciferin detection reagent was then added, the sample gently mixed and incubated for a further 15 minutes. Luminescence was determined using a MicroLumat Plus LB 96v (Berthold Technologies) luminometer set at 1 second captures and glutathione levels established by comparing data to a standard curve. A standard curve was determined using the 5mM glutathione stock solution provided in the GSH-Glo™ Glutathione Assay (Promega) in accordance with the manufacturer's

instructions. Briefly, a series of serial dilutions ranging from 1.25mM to 9.75µM were made. A 10µl (in triplicate) measure of the appropriate concentration is placed in a 96-well plate and the RLU determined for each standard glutathione concentration.

2.5.6 Protein extraction to determine NPR1 redox status

The yeast pellet (previously harvested and frozen in liquid nitrogen) was freeze-ground in a pre-chilled pestle and mortar using liquid nitrogen. The resultant yeast "powder" was transferred to a clean mortar chilled on ice and subsequently ground in RIPA extraction buffer (1% NP40, 0.5% sodium deoxycholate, 150mM NaCl, 50mM Tris-HCl (pH7.5) and 2mM EDTA) containing a protease inhibitor cocktail (Roche) for fungal and yeast cells (containing 4-(2-Aminoethyl) benzenesulfonyl fluoride hydrochloride (AEBSF), 1,10-Phenanthroline, Pepstatin A and E-64). The resultant extraction buffer/disrupted cell mix was transferred to a chilled 1.5ml microcentrifuge tube and centrifuge at 4°C for 5 mins at 20900g to pellet the insoluble material. The supernatant was transferred to a clean 1.5ml microcentrifuge tube before being subjected to western blot analysis described at 2.5.7.

2.5.7 Western Blot

SDS-PAGE (sodium dodecyl sulfate polyacrylamide gel electrophoresis) 10-well gels (12% acrylamide) were constructed as specified in Sambrook & Russell (2001) using Mini-PROTEAN 3 electrophoresis equipment (BioRad). Crude protein extracts were heated in 1xSDS loading buffer (50mM Tris-HCl (pH 6.8), 2.5% glycerol, 1% SDS, 0.002% bromophenol blue with optional 50mM DTT) to 70°C for 10 minutes before being separated by SDS-PAGE. Protein was transferred onto a Hybond-P PVDF membrane (Amersham Biosciences) in transblotting buffer (200 mM glycine, 25 mM Tris, 20% Me-OH) at 25V for 12-16 hrs at 4 °C, using a PageRuler™ prestained protein ladder (Fermentas) to monitor and quantify protein separation. The membranes were then briefly rinsed in phosphate buffered saline (PBS) before being blocked in 10 ml blocking buffer (PBS/T (1X PBS, 0.1% Tween-20) and 5% non-fat dried milk) for 1hr at room temperature. The membrane was then washed in PBS/T before being incubated with an appropriate primary antibody in 5ml blocking buffer for 2hrs at room

temperature. The membrane was then washed for 2 x 10 minutes in PBS/T before being incubated with a compatible horseradish peroxidase (HRP)-linked secondary antibody for 2hrs at room temperature. The membrane was then washed 3 x 15 minutes in PBS/T. Antibody HRP immuno-detection was completed using the Amersham ECL™ plus western blotting detection kit (GE Healthcare) with X-ray films (CL-XPosure Film, Thermo Scientific, USA) used to detect the target protein.

2.5.8 GSNOR activity Assay

Yeast cells were grown in a 50ml YPD liquid culture supplemented with 2% raffinose to an OD600nm value of ~0.6. Either 2% galactose (to activate pGAL1) or 2% glucose (to repress pGAL1) was added and the cells grown for a further 4 hours. The sample was centrifuged at 10000g for 5 minutes, the pellet washed with ~30ml ddH_2O and centrifuged once again to harvest yeast cells. Protein was obtained by mechanically breaking the cells in 50 mM Tris-HCl (pH 8.0) and 0.1% (v/v) Tween 20 using 0.3g (200µl volume) 425-600µm glass beads, acid washed (Sigma) and vortex for 4 x 1 minute, placing on ice between sessions. The sample was centrifuged at 20900g for 5 mins to pellet the beads and insoluble material, with the supernatant retained.

2.5.8.1 NADH oxidation assay

GSNOR activity was determined by incubating an equivalent of 400µg of protein (in lysis buffer) with 2mM NADH. To initiate the reaction 2mM GSNO was added and the GSNO-dependent oxidation of NADH to NAD^+ measured at absorbance OD340nm.

2.5.8.2 In gel assay

GSNOR 'in-gel' activity was determined by resolving an equivalent of 500µg crude protein extract by non-denaturing 8% (w/v) polyacrylamide gel. The gel was then equilibrated for 1 minute in 0.1 M sodium phosphate buffer (pH 7.0) before being incubated at 25°C in the dark in a solution consisting of: 0.1 M sodium phosphate buffer (pH 7.0), 0.1 mM NAD^+, 0.1mM nitroblue tetrazolium (NBT), 0.1 mM phenazine methosulfate (PMS), 1 mM reduced glutathione and 1 mM formaldehyde.

The gel was inspected at 30 minute intervals and GSNOR activity is confirmed by the presence of clear bands.

2.6 LUC output assay

The method utilised was been adapted from Leskinen et al., (2003). Briefly, yeast cells were grown at 30°C with 225rpm shaking in SD medium (no amino acid lacking) containing 2% raffinose to an OD600nm density of ~1. Cells were then centrifuged at 5000g for 2 minutes and washed (twice) with 40ml ddH_2O. The pellet was re-suspended in 2ml ddH_2O. Cells are then diluted to OD600nm density of ~0.3 in SD medium (with or without 600µM L-methionine) and either 2% glucose or galactose, and grown at 30°C with 225rpm shaking for a further 8 hours. 100µl aliquots of the cell culture were added into individual chamber of a 96-well plate. To this, 100µl of 1 mM D-luciferin (Biosynth AG) solubulised in 100mM sodium citrate buffer (pH 5.0) is added. The plate is then briefly shaken before luminescence is determined using a MicroLumat Plus LB 96v (Berthold Technologies) luminometer set at 1 second captures.

CHAPTER 3

3. Modifying Cellular Redox

3.1 Introduction

NPR1 is a redox regulated transcription cofactor that performs a vital role in both local plant immunity and SAR. A combination of forward and reverse genetic approaches place TGA transcription factors as essential transducers of responses orchestrated by NPR1 in *Arabidopsis* (Zhang et al., 1999; Zhang et al., 2003; Kesarwani et al., 2007). However, despite extensive profiling the exact role NPR1 and individual TGA transcription factors play in modulating dynamic aspects of plant immunity are not fully understood (see section 1.2.7 for comprehensive details).

A synthetic biology approach provides a means to uncover the true nature of protein function. Synthetic biology aims to build circuits in order to understand system behaviour. By constructing such protein networks in a heterologous model system such as the yeast *Saccharomyces cerevisiae,* a system free from biological complexity exists to delineate protein function and understand system dynamics. For such a circuit to be representative, NPR1 structure and function must be manipulated. NPR1 is *S*-nitrosylated at Cys156 by GSNO and this promotes oligomer formation, while reduction of two cysteine residues (Cys82 and Cys216) catalysed by TRXh5/NTRA promotes monomer release (Tada et al., 2009). An initial experiment was completed to check the conformation of NPR1 when expressed in yeast cell BY4741 and this protein was found to exist predominantly as a monomer (representative data can be found at Fig 4-2). Therefore, the decision was made to increase the oxidising potential of a yeast chassis through genetic modification as such a feature would allow manipulation of NPR1 redox status and facilitate tight circuit regulation.

S. cerevisiae has emerged as a model eukaryotic system, and consequently this organism has been extensively characterised using a large molecular toolbox. Accordingly it has been found that disrupting the genes encoding flavohemoglobin (*YHB1*) or GSNOR (*SFA1*) reduces the cells ability to metabolise NO and GSNO, respectively, and consequently there is a higher abundance of cellular protein-SNO formation (in response to NO donor) in these mutant lines (Lui et al., 2000; Liu et al., 2001; Foster et al., 2009). In addition, it is known that in order to preserve cellular homeostasis, *S. cerevisiae* maintains a highly reducing intracellular redox environment (Hwang et al., 1992; Østergaard et al., 2004). Using the redox probe rxYFP, it was determined that the redox potential of the yeast cytosolic glutathione pool is highly reducing at -289mV (in accordance with Nernst equation) with the GSH concentration equating to 13mM (Østergaard et al., 2004). This contrasts with plants, where glutathione, also conditioned predominantly as GSH, is present at concentrations of ~2-3 mM (Creissen et al., 1999; Noctor et al., 2002).

It is well established that glutathione is able to modulate NPR1 oligomer-monomer dynamics (Mou et al., 2003) and such a vast GSH concentration coupled with an inherently reducing environment is the likely reason NPR1 favours the monomeric form when expressed in yeast. A solution could involve perturbing the glutathione pool, but studies in which biosynthesis of this peptide are either genetically or biochemically inhibited, show doing so is highly deleterious to the cell (Izawa et al., 1995; Madeo et al., 1999; Maris et al., 2000). Similarly, GSH is an essential constituent of GSNO and completely removing GSH from the cell would compromise the formation of this important NO-donating peptide. Yeast cells are able to sense and adapt to redox perturbations and respond with the rapid activation and/or suppression of various gene sets. The molecular mechanism utilised by *S. cerevisiae* to maintain optimal redox conditions is fairly well understood, with YAP1 functioning as an essential transcription factor in response to both ROS and RNS (Gasch et al., 2000; Horan et al., 2006). This protein induces an extensive redox defence that collectively alleviates both oxidative and nitrosative-related stress, with examples including genes encoding glutathione

biosynthesis (*GSH1*) and glutathione oxidoreductase (*GLR1*) (Kuge and Jones, 1994; Wu et al., 1994).

Compilation of these data indicates that functional disruption of the genes *SFA1* and *YHB1* in *S. cerevisiae* will result in a larger cellular abundance of NO and GSNO, while disruption of *YAP1* may indirectly limit the cellular amount of glutathione, as well as reduce recycling of GSSG to GSH. If such disruptions were completed in combination, this should lead to a yeast chassis with a lowered intracellular glutathione redox potential coupled with a higher protein-SNO forming capacity. Consequently, it would be expected that NPR1 would favour oligomer formation.

3.2 Genetic approach used to selectively disrupt yeast genes

There are a number of different methods that allow researchers to selectively disrupt individual open reading frames (ORF) contained within the yeast genome, with PCR-mediated homologous recombination perhaps the most widely used approach. This technique often requires selection by amino acid prototrophy, however should there be a requirement to transform with multiple constructs, then this approach is limited by a finite number of auxotrophic markers. Recycling of selection markers, whereby prototrophy is returned to auxotrophy, has emerged as a powerful tool to study multiple gene function. One of the most specific and highly efficient methods requires selection by uracil conferred by a plasmid construct containing the URA3 (coding for orotine-5′-monophosphate decarboxylase) cassette. Significantly, URA3 is able to convert 5-fluoroorotic acid (5-FOA) to the highly toxic compound 5-fluorouracil, thus creating a counter selection method. Where URA3 is flanked with bacterial hisG tandem repeats, the yeast cells in which the URA3 has naturally "looped-out" during recombination can be accurately selected when grown in the presence of 5-FOA.

A similar approached was adopted during this work using the plasmid HO$_L$-hisG-URA3-hisG-Poly-HO$_R$ kindly provided by Dr. David Stillman, University of Utah (Voth et al., 2001). Using the procedure specified in Fig. 3-1, this vector was modified

to purposely disrupt *YAP1* and *YHB1*. In order to accelerate the process a BY4741 *sfa1* mutant was purchased from EUROSCARF that contained the kanMX marker cassette (provides resistance to G418) at the YDL168w locus. This yeast strain would be used to generate the BY4741 *Δsfa1yap1yhb1* triple mutant (see Table 2-1 for all yeast genetic backgrounds used in this study).

Figure 3-1 Schematic of approach adopted to disrupt select *S. cerevisiae* gene(s)

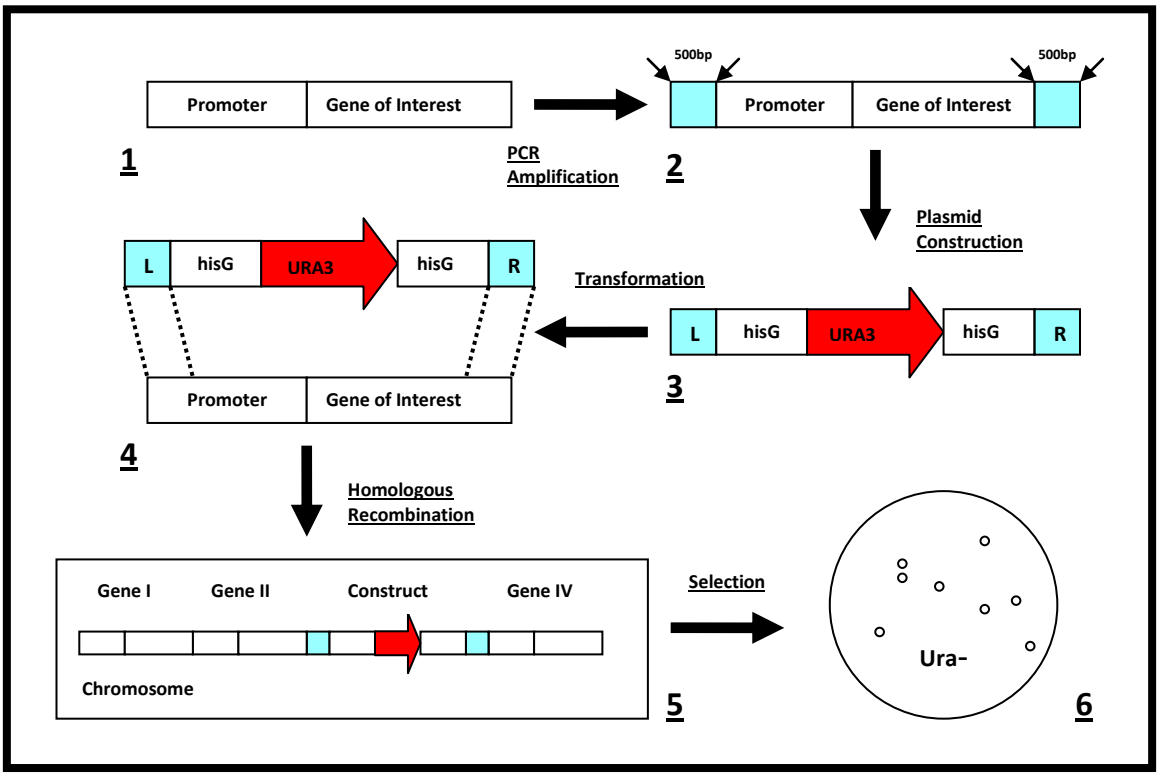

Schematic flow diagram to illustrate the major steps required for PCR-mediated disruption of yeast genes by homologous recombination**.** 1) The specific ORF genomic DNA (promoter and coding sequence) are identified using data available from http://www.yeastgenome.org. 2) Primers are designed that allow amplification of a 500bp-1kb (depending on length of gDNA) PCR fragments at the flanks of the ORF genomic DNA. 3) The homologous L and R fragment are then cloned in the correct orientation into a vector containing the URA3 cassette, which is itself flanked by hisG cassettes. 4) The plasmid is linearized and once transformed into yeast, will target a specific locus. 5) Homologous recombination replaces the gene of interest (both promoter and coding sequence) with the plasmid construct. 6) Plate the transformed yeast cells on SD minimal media and select by uracil prototrophy.

Disruption of *YAP1* in BY4741 *sfa1* was completed first and successful interference was determined by streaking transformants on YPDA agar supplemented with 150µg/µl G418 and 3mM H_2O_2. Genomic DNA was extracted from those colonies unable to grow and PCR analysis confirmed the URA3 cassette was positioned correctly on chromosome XIII at the *YAP1* locus. After returning BY4741 *sfa1yap1* to uracil auxotrophy by 5-FOA selection, *YHB1* disruption was completed and PCR analysis confirmed the URA3 cassette was positioned correctly on chromosome VII at the *YHB1* locus. Generation of BY4741 *sfa1yap1yhb1* (herein *Δsfa1yap1yhb1*) was confirmed by RT-PCR analysis at Fig.3-2. Note that all relevant experiments (growth assay, GSH/GSSG relationship and redox potential) were only completed using BY4741 and *sfa1yap1yhb1*. The aim of this work was to use synthetic biology principles in order to understand NPR1 function within the context of transcriptional regulation. To undertake this, it was necessary to create a yeast chassis defective in cellular redox. In order to characterise the *sfa1yap1yhb1* mutant it was necessary to compare this cell type with the wild-type parent BY4741 strain. As the overall biological relevance of the *SFA1*, *YAP1* and *YHB1* genes were not under investigation, individual mutants were not tested as part of this study.

Figure 3-2 Reverse transcriptase (RT)-PCR analysis confirming gene knockout

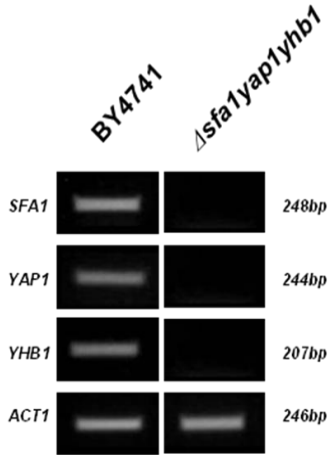

RT-PCR products are shown for GSNOR (*SFA1*), flavohemoglobin (*YHB1*) and *YAP1* with *Actin1* functioning as an internal loading control. Product sizes are: *SFA1* = 248bp, *YAP1* = 244bp, *YHB1* =207bp and *ACT1* = 246bp

3.3 Determination of yeast growth traits

In order to determine if there is any growth defect associated with *Δsfa1yap1yhb1*, cells were grown in rich YPDA media and growth monitored over 12 hours. Both BY4741 and *Δsfa1yap1yhb1* follow a standard growth curve, although *Δsfa1yap1yhb1* is slightly delayed in entering log phase and grows at a slower pace as compared to BY4741 (Fig. 3-3).

Fig. 3-3 Growth comparison of BY4741 and *Δsfa1yap1yhb1* yeast strain

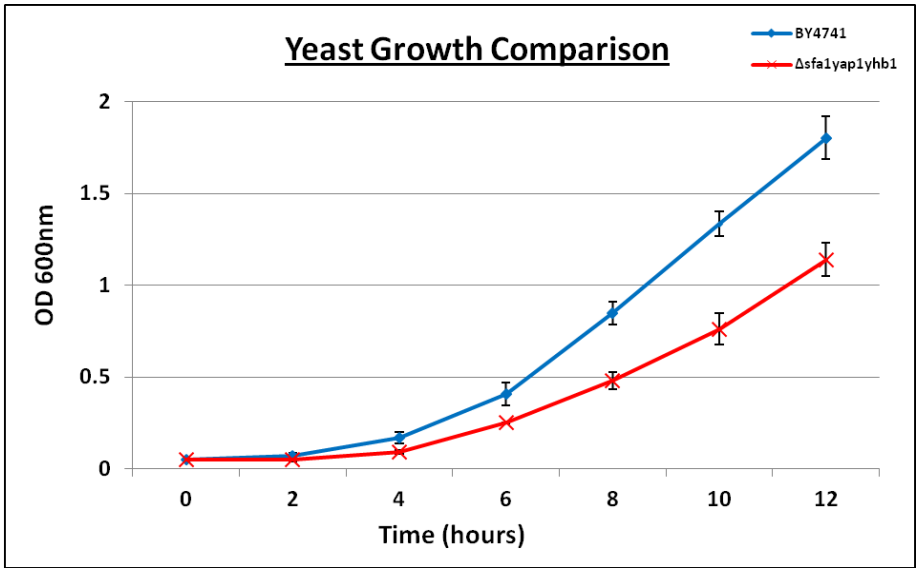

Yeast cells were diluted to OD600nm value 0.05 in YPDA and grown at 30°C for a further 12 hours in aerobic conditions. Samples were collected every 2hrs to monitor growth over time. Data is representative of three independent biological replicates. Error bars indicate SE

3.4 Determination of glutathione levels

Glutathione is an extremely effective antioxidant highly influential in determining the redox potential of a cell. In addition, GSH occupies a central position in the glutaredoxin and glutathione peroxidase systems (Arthur, 2000; Lillig et al., 2008). Activation of SA-dependent plant defences results in a dynamic increase in cellular reduction potential that is linked to a higher cellular concentration of this tri-peptide

(Mateo et al., 2006; Koornneef et al., 2008). The subsequent activation of many defence genes is likely to be the result of NPR1 monomerization (Mou et al., 2003). The intracellular concentration of glutathione in yeast is in the millimolar range with the GSSH/GSH ratio shown to equate to 7% (Østergaard et al., 2004). In order to perturb GSH/GSSG homeostasis, the gene encoding the bZIP transcription factor *YAP1* was functionally disrupted. Glutathione measurements on whole-cell extracts were completed using the GSH-Glo™Glutathione Assay (Promega) whereby a luciferin derivative (Luc-NT) is converted into functional luciferin in the presence of glutathione, catalyzed by glutathione S-transferase (GST). Using the relative light unit (RLU) to directly quantify both GSH and GSSG, in accordance with a standard curve, it was found that under resting conditions BY4741 contained 2.91μM/μg protein total glutathione, of which 2.7μM/μg protein was in the reduced GSH form. Strikingly *Δsfa1yap1yhb1* contains a ~5 fold reduction in total glutathione at 0.55 μM/μg protein as well as a similar fold reduction in reduced GSH at 0.39 μM/μg protein (Fig. 3-4). Consistent with the central role of YAP1 in GSSG-GSH recycling, we found the GSSG/GSH ratio for BY4741 to be 7.7% but this increases to 41% in *Δsfa1yap1yhb1* (Fig. 3-4).

Figure 3-4 Glutathione content of BY4741 and *Δsfa1yap1yhb1*

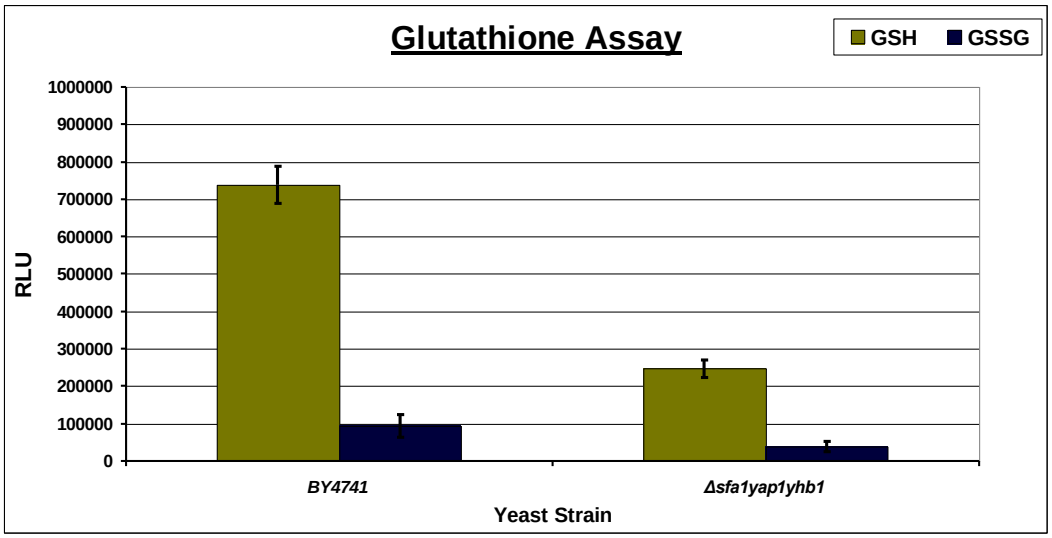

Cellular glutathione content was determined using total crude protein extract from BY4741 and *Δsfa1yap1yhb1*. Samples were analyzed using a GSH-Glo™Glutathione Assay (Promega) with the amount of glutathione provided as a relative light unit (RLU) (a). The yellow bar represents GSH while the dark blue bar represents GSSG. Actual glutathione (Table 3-1) concentration was determined by comparing values to a standard curve at Fig. 3-5. Data obtained is from three independent experiments and error bars represent SEM.

Genotype	**Glutathione content (µM/µg protein)**			
	GSH	**GSSG**	**Total**	**GSSG/GSH (%)**
BY4741	2.7 ± 0.2	0.21 ± 0.01	2.9	7.7
Δsfa1yap1yhb1	0.39 ± 0.02	0.16 ± 0.01	0.55	41

Table 3-1 Numerical quantification of glutathione content. Values represent the mean ± SD of data obtained from three independent cultures

Figure 3-5 Standard curve required to convert glutathione concentration into relative light unit (RLU)

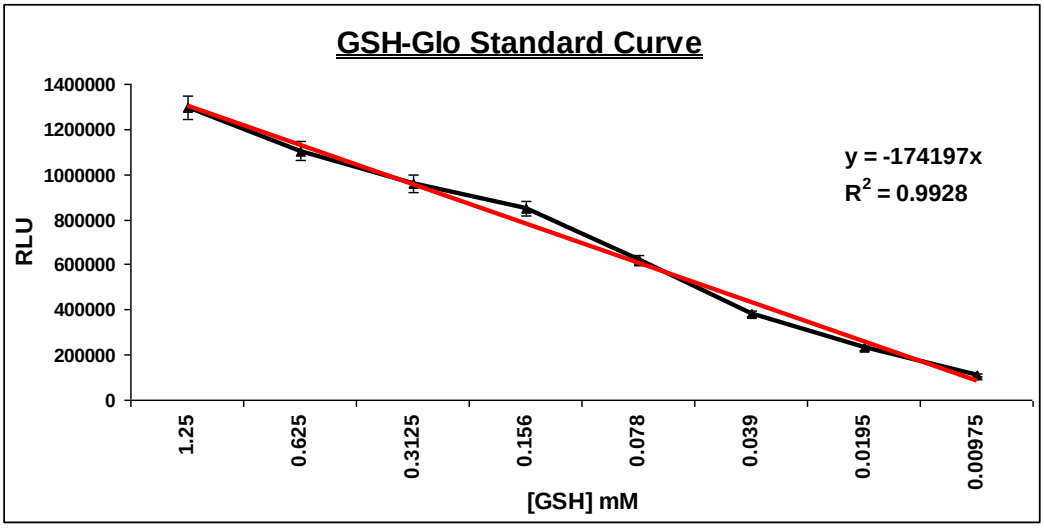

A standard curve was determined using the GSH-Glo™ Glutathione Assay (Promega) in accordance with the manufacturer's instructions. Using the 5mM Glutathione stock solution provided, a series of serial dilutions (in triplicate) were made ranging from 9.75µM to 1.25mM. After adding reconstituted Luciferin Detection Reagent, the appropriate RLU was ascertained using a MicroLumat Plus LB 96v (Berthold Technologies) luminometer set at 1 second captures. Error bars represent SEM.

3.5 Intracellular redox potential – characterisation using roGFP2

Whilst levels of cellular glutathione are able to act as a gauge of cellular redox, actual quantitative determination of the intracellular redox balance can be accurately achieved using the probe reduction-oxidation GFP (roGFP). Creating two cysteine residues (Q204C/S147C) in GFP on adjacent β-strands modifies chromophore conformation through the generation of a disulfide bond (Hanson et al., 2004). Consequently roGFP has two fluorescence excitation maxima at 405 and 488nm that display dynamic reversibility of fluorescence intensities in response to changes in ambient redox conditions. Accordingly, variants of roGFP have been successfully employed to determine the redox potential in a variety of cell types such as HeLa cells, vascular

smooth muscle and *Arabidopsis* cells (Hanson et al., 2004; Jiang et al., 2006; Waypa et al., 2010). To determine possible modifications in redox potential of *Δsfa1yap1yhb1* in comparison to BY4741, the probe roGFP2 (modifications include S65T/S147C/Q204C) was employed (kindly donated by Alberto Munoz, University of Edinburgh). Ratiometric imaging (under resting conditions) of BY4741 yeast strain transformed with roGFP2 reveals the 405/488nm ratio to be 0.75, while the 405/488nm ratio for *Δsfa1yap1yhb1* transformed with roGFP2 is 1.39 (Fig. 3-5). The addition of 20mM DTT to BY4741 cells further reduces roGFP2 as indicated by a 405/488 ratio of 0.64, while the addition of 25mM H_2O_2 rapidly oxidised roGFP2 with the resultant 405/488 ratio shifting to 1.42 (see Appendix A).

Figure 3-6 Ratiometric images of yeast cells expressing roGFP2

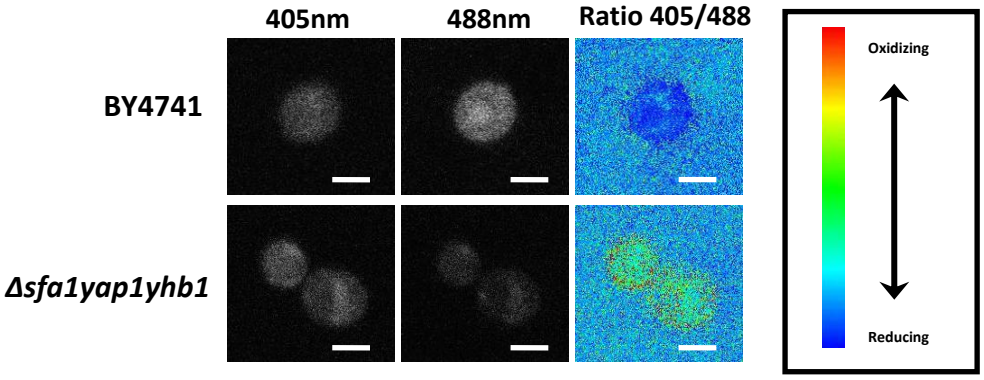

The roGFP2 gene was placed in the MCS of HOL-hisG-URA3-hisG-Poly-HOR under the constitutive GPD1 promoter. Confocal laser scanning microscopy (CLSM) of cells expressing roGFP2 reveals that under resting conditions the intracellular environment of BY4741 is highly reducing, while the intracellular environment of *Δsfa1yap1yhb1* is more oxidising. The probe is ubiquitously expressed throughout the cytoplasm and is highly responsive to exogenous application of H_2O_2 and dithiothreitol (DTT) (Appendix A). White bar indicates 5μm

This data can be utilised to determine the actual intracellular redox potential of both BY4741 and *Δsfa1yap1yhb1*. Initially the degree of oxidation (*OxDroGFP2*) is calculated in accordance with para 2.4.4. Accordingly, the $I488_{red}/I488_{ox}$ parameters were calculated using images analyzed with Image-Pro Analyzer 7.0 and determined as

I_{red} = 89.6 and I_{ox} = 58. Using these inputs reveal that the degree of oxidation (*OxD*ro*GFP2*) for BY4741 is 0.09667, while the same calculation for *Δsfa1yap1yhb1* is 0.9422. Solving the Nernst equation reveals that the actual redox potential of roGFP2 (*Ero*GFP2*) for BY4741 is -308.3mV, while the same calculation for *Δsfa1yap1yhb1* is -244.6mV. This equation solved using software provided at: http://www.calctool.org/CALC/chem/electrochem/nernst.

3.6 Yeast strain *Δsfa1yap1yhb1* is hypersensitive to exogenous treatment with GNSO and H_2O_2

Previous work demonstrated that in response to a relatively high concentration (5mM) of GSNO, a yeast *sfa1* mutant displays severely reduced growth traits that is correlated with a high accumulation of total protein-SNOs (Liu et al., 2001). A possible consideration during this work is that in order to promote NPR1 oligomer formation, it may be necessary to add sufficient quantities of GSNO to the culture media. In order to test such a procedure and determine optimal concentrations of GSNO, the ability of *Δsfa1yap1yhb1* to grow (and thus sensitivity) in the presence of various concentrations of GSNO were determined. In addition, it is well established the yeast *yap1* mutation confers increased sensitivity to H_2O_2 (Kuge et al., 1997) and therefore it was also decided to determine sensitivity of this cell to this particular ROS. Results indicate that the *Δsfa1yap1yhb1* mutant is hypersensitive to even very low concentrations of GSNO, with 1mM sufficient to inhibit 66% of relative growth (as indicated by a reduced OD600 nm value) compared to *Δsfa1yap1yhb1*grown in the absence of GSNO (Fig. 3-7a). In contrast, BY4741 which contains both functional GSNOR and the FHb scavenging mechanism is for the most part, largely resistant to GSNO-induced nitrosative stress, with notable inhibition not observed until the 3 - 4mM GSNO range (Fig. 3-6a). Similarly the *Δsfa1yap1yhb1* strain is extremely sensitive to oxidative stress induced by a low μM concentration of H_2O_2, while growth of BY4741 remains unperturbed until concentrations reach the 400μM H_2O_2 range (Fig. 3-7b).

Figure 3-7 Sensitivity of BY4741 and *Δsfa1yap1yhb1* to GSNO and H_2O_2

a)

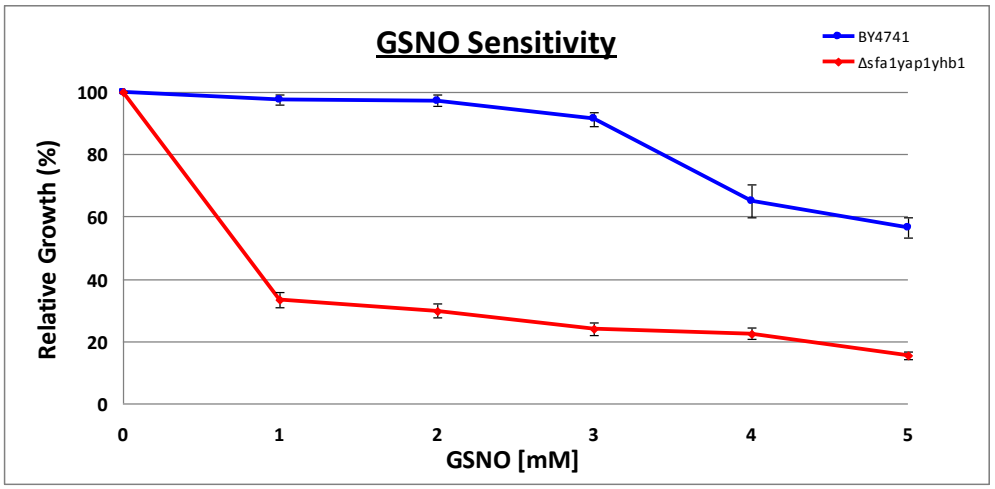

b)

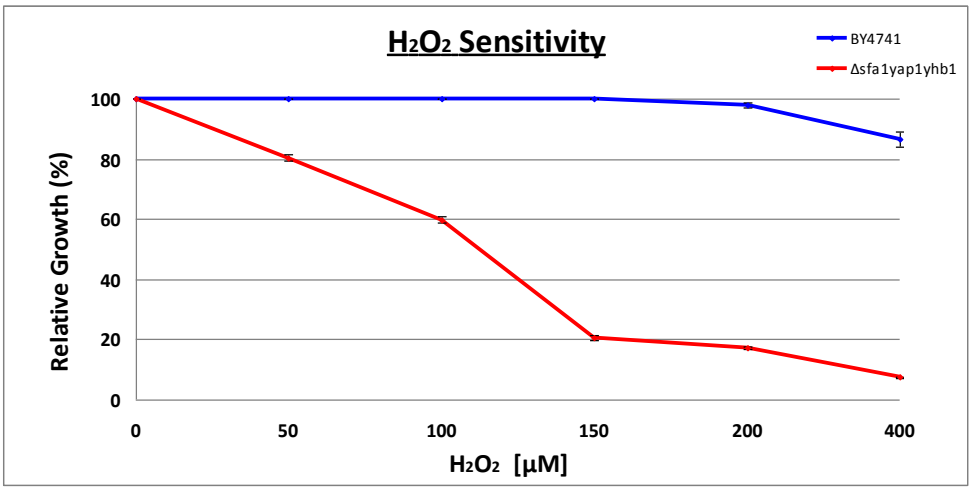

From an initial starting cell density of OD 600nm of 0.05, yeast strain BY4741 and *Δsfa1yap1yhb1* were cultured for 10 hours in the presence of a) GSNO or b) H_2O_2 to measure final cell density. Relative growth was determined by comparing the OD 600nm values of cell cultures at 10 hours with the value of an untreated (concentration 0) control and the amount of cells provided as a percentage. Note the *Δsfa1yap1yhb1* displays reduced overall growth in accordance with Fig.3-3. Data is representative of three independent replicates. Error bars indicated SEM.

3.7 Analysis of mRNA transcript for yeast redox environment modulators

Under normal conditions, *S. cerevisiae* strictly regulates redox in order to maintain efficient cellular function. It was demonstrated that *Δsfa1yap1yhb1* contains a more oxidising redox environment that is linked to a reduced cellular concentration of glutathione (Figs 3-4 and 3-6). This effect is likely the result of collectively disrupting the harmony of many redox environment modulators. Such modifications are likely to be detrimental to cellular homeostasis and therefore it is possible the cell may compensate for such a dramatic perturbation by increasing the action potential of redundant redox regulators that ordinarily under resting conditions would play a less significant role. In order to determine whether such an imbalance exists, transcripts of genes credited as being involved in regulating cellular redox conditions were analyzed under both resting conditions and following GSNO-induced nitrosative stress. These genes can be broadly categorised into four groups.

1). The glutathione redox system comprising**;**

- *GSH1* - Glutathione
- *GLR1* - Glutathione oxidoreductase
- *GPX1* - Glutathione peroxidase
- *GPX2* - Glutathione peroxidase
- *GRX1* - Glutaredoxin
- *GRX2* - Glutaredoxin

2). The thioredoxin system comprising;

- *TRR1* - Thioredoxin reductase
- *TRX1* - Thioredoxin
- *TRX2* - Thioredoxin

3). The thioredoxin peroxidase system comprising;

- *AHP1* - Alkyl Hydroperoxide reductase
- *PRX1* - Peroxiredoxin
- *DOT5* - Nuclear thiol peroxidase
- *TSA1* - Thioredoxin peroxidase
- *TSA2* - Thioredoxin peroxidase
- *SRX1* - Sulfiredoxin

4). Others (those credited with an ability to regulate redox status)

- *ECM38* - γ-glutamyltranspeptidase
- *PDI1* - Protein disulfide isomerase

Gene expression was monitored by sqRT-PCR at t=0 in order to determine basal expression and at 30 minute intervals (up to 90 minutes) following the addition of 3mM GSNO to monitor any response to nitrosative stress. Of the genes analyzed, only three displayed an observable difference in expression profiles for *Δsfa1yap1yhb1* as compared to BY4741. Two members belong to the thioredoxin peroxidase gene cluster (*AHP1* and *TSA1*), whilst the third is a glutathione peroxidase (*GPX2*). Interestingly all three were depressed in *Δsfa1yap1yhb1* under resting conditions (Fig. 3-7). Following the addition of GSNO, mRNAs for *TSA1* and *GPX2* remained fairly constant in both wild type and *Δsfa1yap1yhb1* strains (Fig. 3-7 a, b). However, comparison of *AHP1* indicates that while mRNA abundance remains constant for BY4741, the addition of GSNO to *Δsfa1yap1yhb1* results in an increased level of mRNAs that is comparable to those found in BY4741 (Fig. 3-7c).

Figure 3-8 sqRT-PCR analysis of yeast genes credited with regulating cellular redox

a)

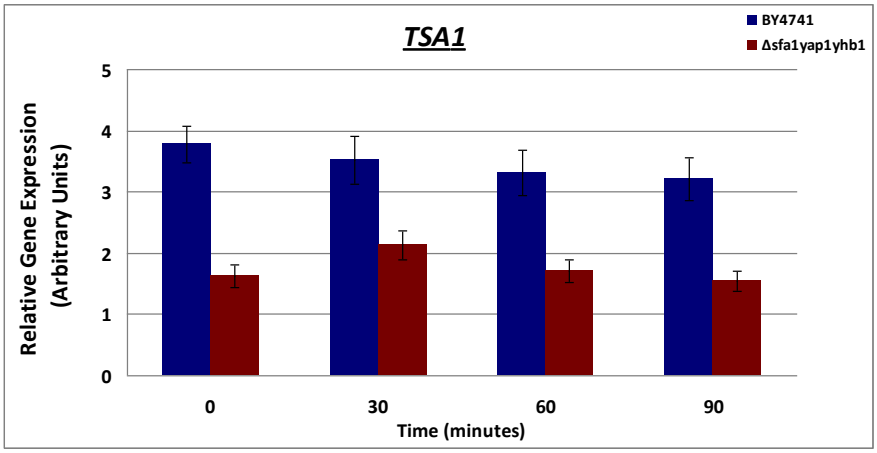

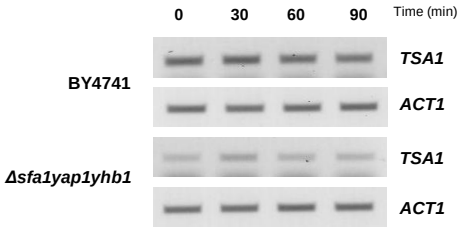

b)

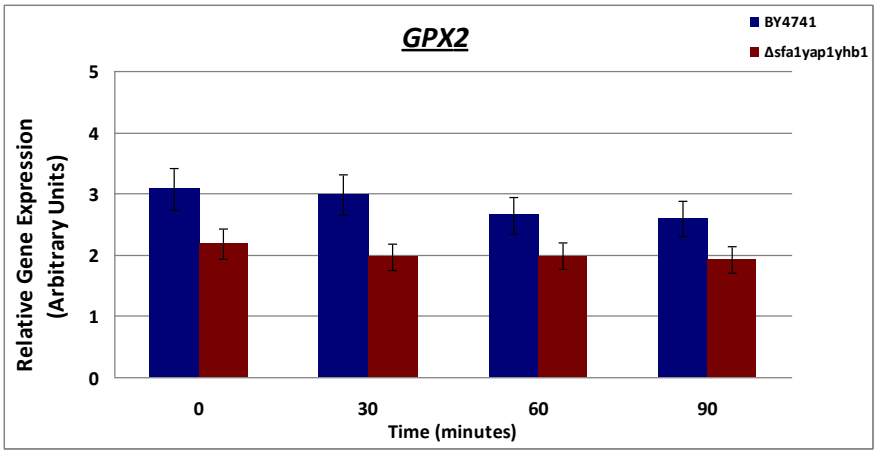

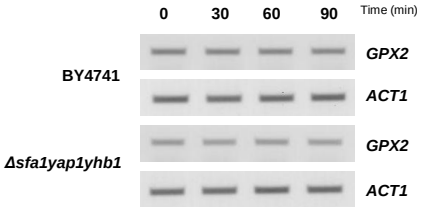

c)

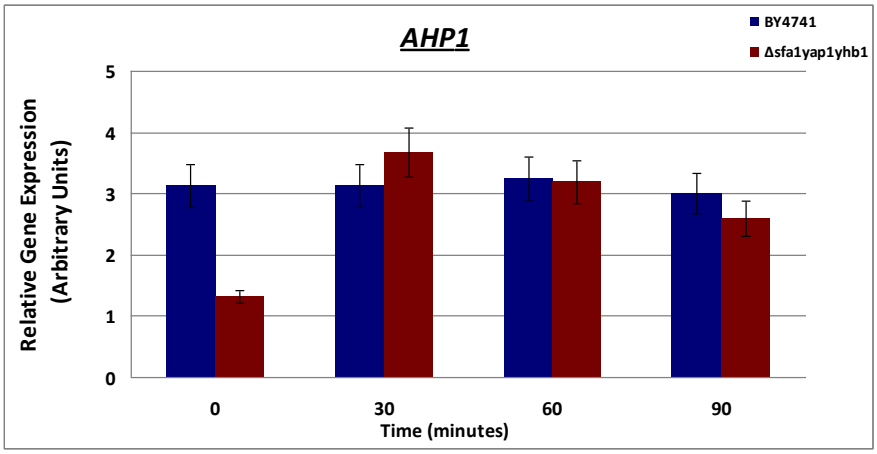

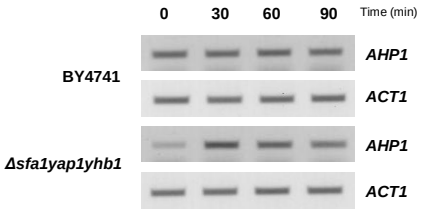

Expression of a). *TSA1*, b). *GPX2* and c). *AHP1* was analyzed by sqRT-PCR, using total RNA extracted from BY4741 and *Δsfa1yap1yhb1*. Samples were resolved on a 1.8% aragose gel and densitometry completed using *Actin1* as an internal control. Data obtained is from two biological replicates. See Table 2-5 for reaction conditions, cycle numbers and product size. The densitometry analysis was completed using ImageJ as described at: http://stanxterm.aecom.yu.edu/wiki/index.php?page=Using_ImageJ .

3.8 Conclusions

This work aims to manipulate the redox status of NPR1 and by doing so this will create an on-off switch that can be used as part of a heterologous protein circuit to understand NPR1 cofactor function. This chapter outlines the rationale and approach used to modify the redox environment of a yeast cell to make it amenable to redox manipulation. *S. cerevisiae* maintains a highly reducing redox potential in order to maintain efficient cellular function and thus it was necessary to disrupt three genes that are known to regulate redox conditions using a method of homologous recombination

(Figs. 3-1 and 3-2). Both *SFA1* and *YHB1* function in *S. cerevisiae* to regulate the cellular content of GSNO and NO, respectively (Liu et al., 2000; Liu et al., 2001; Foster et al., 2009). Furthermore, glutathione is ordinarily the most abundant low molecular weight thiol in cells and functions as an essential redox buffer. This peptide is known to be highly influential in modulating NPR1 oligomer-monomer equilibrium (Mou et al., 2003). The cellular concentration of glutathione in yeast is thought to be 4-6 fold higher than in plants (Creissen et al., 1999; Noctor et al., 2002; Østergaard et al., 2004). It is not possible to disrupt biosynthesis of this peptide as it is a constituent of GSNO, the substrate known to specifically *S*-nitrosylate NPR1 in *Arabidopsis* (Tada et al., 2008). Therefore to limit glutathione biosynthesis the gene encoding transcription factor YAP1 was disrupted. Determination of the actual intracellular redox potential using the molecular probe roGFP2 reveals *Δsfa1yap1yhb1* has a lower cellular reduction potential as compared to BY4741 (Fig. 3-6 and Para 3.5). Analysis of glutathione content reveals the *Δsfa1yap1yhb1* mutant has a ~5 fold reduction in total glutathione levels as compared to BY4741 (Fig 3-4). In combination, these features indicate that cellular conditions of *Δsfa1yap1yhb1* are more oxidising and this may be sufficient to maintain NPR1 in the inactive oligomeric form (confirmation of this in chapter 4).

CHAPTER 4

4. Building, Characterising and Modelling a Synthetic Circuit

4.1 Introduction

In plant immunity, NPR1 is of central importance, orchestrating the action of thousands of primary and secondary response genes required for many aspects of local immune responses and SAR (Wang et al., 2006). *NPR1* is constitutively expressed in the cell, with mRNA for this gene only increasing 2-3 fold following pathogen challenge (Cao et al., 1997). In resting cells NPR1 is subject to a redox-based posttranscriptional modification with *S*-nitrosylation at Cys156 promoting oligomer assemblage (Tada et al., 2008). This scenario means the cell is primed in a "ready-to-go" position should there be a requirement to initiate defence signalling. Such activation requires SA-induced modifications to the ambient intracellular redox environment, coupled with the action of a member of the cytosolic thioredoxin system (TRXh5) which appears to promote NPR1 monomer release (Tada et al., 2008). Active monomeric NPR1 is known to interact with a subclass of bZIP domain containing transcription factors, known as TGA factors, with this association essential for the activation of many defence genes (Zhang et al., 1999; Després et al., 2000; Zhou et al., 2000). Characterisation of this interaction reveals TGA3 has the highest affinity for NPR1 of the individual TGA factors tested (Zhou et al., 2000). Significantly a *tga3* knockout mutant displays <50% expression of the *PR-1* defence gene as compared to wildtype plants, indicating this protein is a potent activator of *PR* gene expression (Kesarwani et al., 2007). The *PR-1* promoter is a model system for studying plant immune activation with recent work indicating the complex nature of gene modulation (Wang et al., 2010; Song et al., 2011).

Extrapolation of this plant immune cascade identifies the requirement for several proteins that function systematically to influence the outcome of defence signalling.

Engineering a heterologous protein circuit that is representative of this defence pathway provides a means to further understand system behaviour. It is clear from the literature that defence activation is redox-regulated and the decision was made to modify the cellular redox potential of a yeast chassis (see chapter 3). Similar to plant cells, NPR1 will be constitutively expressed in yeast using the powerful GPD1 promoter and the expectation is that NPR1 would mainly be present in the oligomeric form and hence the system would be, by default, switched off. Although the general redox environment of the cell would not change, selectively inducing circuit inputs in the form of GSNOR and TRXh5/NTRA would specifically promote reduction of NPR1 to the monomeric form. This should lead to an activation cascade whereby monomeric NPR1 can interact with and direct TGA3 to a cognate DNA binding site. By placing these inputs under an inducible promoter, both with comparable strengths (pGAL1 and pMET25), this creates a circuit with an on-off switch. The upstream activation sequence (UAS) of pMEL1 has been removed and this results in minimal background expression when transformed into yeast (Melcher et al., 2000). By substituting the specific region of the *PR-1* promoter (-666 to -634 from ATG start codon) containing the native *as-1* element as a novel UAS in pMEL1, it is reasoned this will result in an inducible reporter system exclusively dependent on activation by TGA-type transcription factors. The gene *LUCIFERASE* was selected as a reporter due to the robust quantifiable nature of this protein and the accessibility of suitable equipment. It should be noted that at present the parameters required to activate NPR1 in *Arabidopsis* are not known and there were concerns that monomeric NPR1 may not be transcriptionally active when expressed in yeast. Consequently, the GAL4 activation domain (GAL4 AD), which is compatible with pMEL1, was fused to NPR1 to circumnavigate any potential problems this may cause. A diagram of the heterologous protein circuit recreated in yeast is detailed at Fig. 4-1.

Figure 4-1 Design of the synthetic circuit

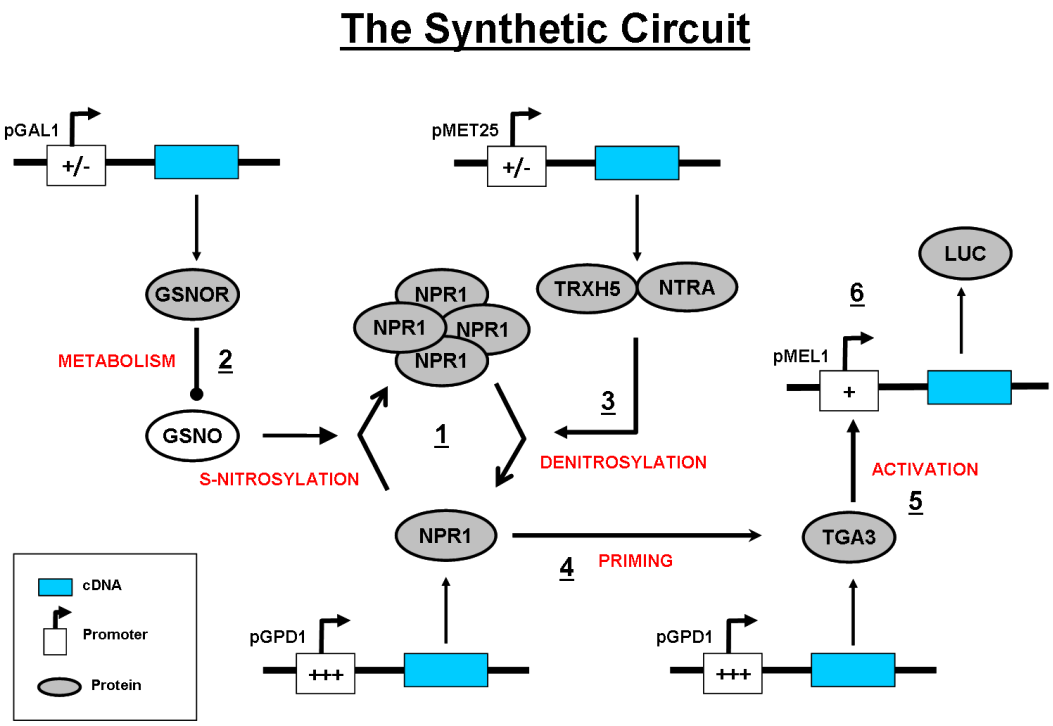

A schematic of the synthetic protein circuit. 1.) NPR1 is constitutively expressed and under resting conditions an endogenous GSNO pool will promote oligomer formation. 2. Selectively activating the expression of GSNOR would increase the rate at which GSNO is metabolised thereby reducing *S*-nitrosylation of NPR1 and indirectly limiting oligomer formation. 3. Activation of TRXh5 together with NTRA would denitrosylate the NPR1 oligomer and promote monomer release. 4. The NPR1 monomer pool will increase leading to an activation cascade whereby NPR1 will interact with constitutively expressed TGA3. 5. This will potentiate TGA3, 6. promote binding to the *as-1* element housed in the inducible pMEL1, activating the expression of the LUC reporter gene.

4.2 *In vivo* identification of NPR1 oligomer-monomer equilibrium

Yeast cell walls are very robust typically comprising up to 30% of the dry mass of the cell, and composed of mannoprotein, chitin and β1,3 glucan (Lipke and Ovalle., 1998). Mechanical disruption of yeast using glass beads is a highly efficient and consequently popular method of obtaining whole protein extracts. However, during this work it was

found that this common approach was not suitable as it often resulted in significant NPR1 oligomer disassociation. Consequently after a degree of optimisation, it was identified that cyrogrinding the yeast pellet in a pestle and mortar using a modified RIPA cell lysis buffer was an effective method of cell lysis and protein solubilisation. Contained within the RIPA buffer is the ionic detergent sodium deoxycholate, but it was found that when used at a low concentration (0.5%) this did not dramatically alter the structure of the NPR1 oligomer.

To compare the conformation of NPR1 between BY4741 and *Δsfa1yap1yhb1* total protein was resolved by non-reducing SDS-PAGE using a western blot probed with αGFP (Roche). The NPR1::GFP fusion protein has been used extensively in *Arabidopsis* research to monitor NPR1 dynamics and this protein chimera does not appear to influence NPR1 stability (Mou et al., 2003). This analysis revealed that in BY4741 yeast cells, NPR1 favours the reduced momomeric conformation, while for the engineered *Δsfa1yap1yhb1* cell line this configuration alters with NPR1 favouring oligomer formation (Fig. 4-2). Although there is residual monomeric NPR1 present in *Δsfa1yap1yhb1*, it is considered an acceptable margin as it is clear the vast majority on NPR1 in present as an oligomer. Interestingly, the monomer exists in two different conformations as indicated by the presence of two bands, but the reason for this is not clear.

Figure 4-2 Identification of NPR1 oligomer-monomer equilibrium

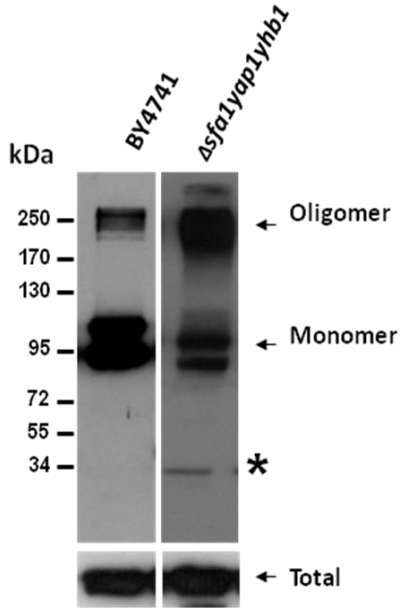

NPR1 exists mainly as a monomer in BY4741 yeast cells. However, this configuration alters in *Δsfa1yap1yhb1* with NPR1 favouring oligomer formation. 50µg total yeast protein was resolved by non-reducing SDS-PAGE and probed with α-GFP immunoglobulin to detect NPR1::ECFP. Both primary αGFP and HRP-linked secondary antibodies were used at dilution ratio of 1/3000. Total protein represents loading control and was determined by adding 50mM DTT to the SDS loading buffer. Asterisk signifies protein occasionally observed at ~30kDa and may represent free GFP.

4.3 NPR1 is *S*-nitrosylated and forms an oligomer in a GSNO-dependent manner

It was shown that NPR1 favours oligomer formation in *Δsfa1yap1yhb1* but the exact mechanism underpinning this status is not clear. In *Arabidopsis*, it is known that *S*-nitrosylation of NPR1 at Cys156 by GSNO promotes oligomer formation, possibly by directly inducing disulfide bridges between NPR1 monomers (Tada et al., 2008). In order to test if GSNO is able to modulate NPR1 oligomer-monomer equilibrium of NPR1 synthesized in yeast, total protein was incubated in the presence of various concentrations of this NO donor. Subsequent analysis by western blot at Fig. 4-3a clearly demonstrates that NPR1 oligomerizes in a GSNO concentration-dependent manner. To confirm this mechanism is likely the result of GSNO-induced *S*-

nitrosylation of NPR1, total protein extract was initially incubated in the presence of 2mM GSNO at room temperature. If NPR1 is modified by *S*-nitrosylation, the SNO motif present can be exchanged with biotin, and accordingly such biotinylated proteins are captured and co-purified using streptavidin agarose beads. Subsequent analysis by western blot using αGFP immunoglobulin to detect the presence of NPR1 confirms this protein is modified by *S*-nitrosylation (Fig. 4-3b). In this case, treatment of the sample with UV at 304nm specifically denitrosylates protein and thus acts as a negative control, while an untreated sample confirms NPR1 cannot be detected without first being modified by GSNO.

Figure 4-3 Identification of GSNO-mediated modifications to NPR1

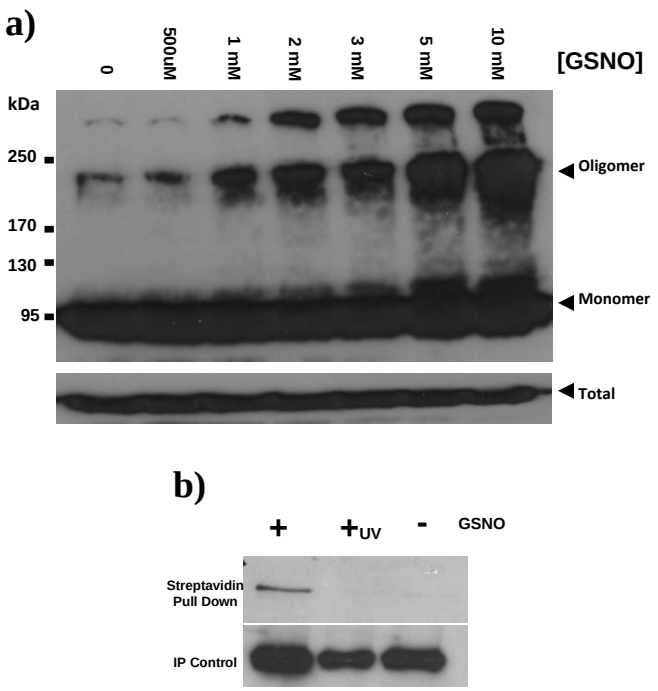

GSNO *S*-nitrosylates NPR1 and promotes oligomer assembly. a) 50µg total yeast protein was incubated in the presence of GSNO for 60 minutes at 25°C and subsequently resolved by non-reducing SDS-PAGE and probed with αGFP immunoglobulin to monitor NPR1 monomer-oligomer dynamics. Total protein represents loading control and was determined by adding 50mM DTT to the SDS loading buffer. (O = oligomer and M- monomer) b) 100µg total yeast protein is treated with 2mM GSNO and proteins subject to *S*-nitrosylation are detected using the biotin switch method. The IP control represents 1/10 of protein subjected to streptavidin pull down and confirms equal loading. Both primary αGFP and HRP-linked secondary antibodies were used at a dilution ratio of 1/3000.

4.4 Adding GSNO to cell cultures induces nitrosative stress and increases cellular reduction potential

Although NPR1 exists predominantly in the oligomeric form in *Δsfa1yap1yhb1* and this is likely the result of GSNO-mediated *S*-nitrosylation, it appears some residual monomer remains. When incorporated into the full circuit, it is possible this monomeric portion will result in detectible background reporter gene expression. If NPR1 could be manipulated so that this protein existed entirely in the oligomeric form, it would prevent such anomalies and provide tight circuit regulation. Previous work demonstrated that incubating a *sfa1yhb1* double mutant with GSNO resulted in a significant increase in total cellular protein-SNOs, as compared to wildtype cells (Forster et al., 2009). To assess if NPR1 could be modulated in *Δsfa1yap1yhb1* under such conditions, cells were incubated with GSNO for 90 minutes and NPR1 oligomer-monomer equilibrium monitored at 15 minute junctures. Although such an assay would likely increase the total cellular abundance of protein-SNOs, it did however result in a noticeable shift from what is predominantly NPR1 oligomer at t=0 to a higher proportion of monomer at t=90 (see Fig. 4-4 for representative image). This result was rather unexpected but indicates a general shift in cellular reduction potential, likely the result of GSNO-induced nitrosative stress. (Note data presented at Fig.4-4 is representative of several independent experiments, each with identical results).

Figure 4-4 GSNO-induced nitrosative stress alters NPR1 oligomer-monomer equilibrium

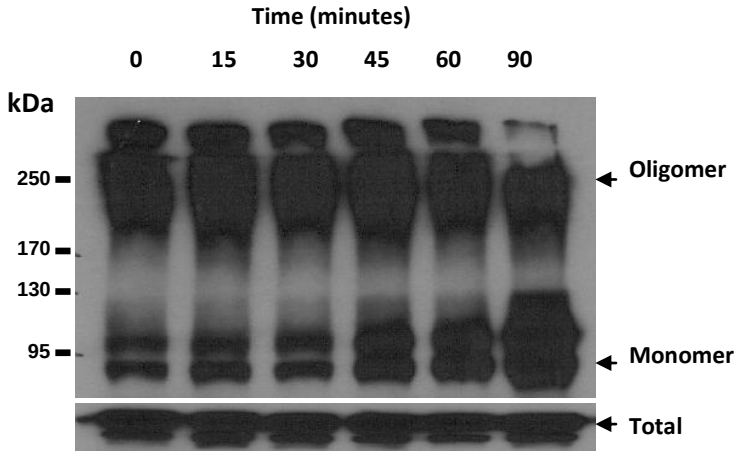

Δsfa1yap1yhb1 cells were incubated with 2mM GSNO and NPR1 oligomer-monomer equilibrium monitored at 15 minute junctures. 50µg total yeast protein was resolved by non-reducing SDS-PAGE and probed with αGFP immunoglobulin. Total protein represents loading control and was determined by adding 50mM DTT to the SDS loading buffer. Both primary αGFP and HRP-linked secondary antibodies were used at a dilution ratio of 1/3000.

As previously discussed, glutathione is a vital cellular buffer that has been shown to modulate NPR1 dynamics (Mou et al., 2003). To determine if an increased cellular concentration of this peptide could account for changes in NPR1 dynamics observed at Fig. 4-4, total cellular glutathione content was assayed following treatment with 2mM GSNO. Samples were collected at t=0 in order to determine basal expression and at t=30 min and t=90 min to determine glutathione (both GSH and GSSG) biosynthesis in response to GSNO. Consistent with data at Fig. 3-4 there is a ~5 fold reduction in basal concentrations of both GSH and GSSG between BY4741 and *Δsfa1yap1yhb1*. With the addition of GSNO, both GSH and GSSG content increase in both cell types at t=30 min. For BY4741, glutathione biosynthesis (GSH and GSSG) continues to increase for 90 minutes with a ~4 four fold increase observed (as compared to t=0), but this contrasts with *Δsfa1yap1yhb1*, where glutathione biosynthesis (GSH and GSSG) peaks at t=30 min (Fig. 4-4b). Interestingly, the GSSG/GSH ratio decreases for both cell types

following the addition of GSNO indicating that GSSG-GSH recycling functions as part of the cellular defence to GSNO-mediated stress. However this process appears to function less efficiently for *⊿sfa1yap1yhb1*. Thus together with data at Fig. 3-7 demonstrating mRNA for cellular redox environment modulators such as *AHP1* are responsive to GSNO-induced nitrosative stress, it is likely an ambient shift in cellular reduction potential (induced by nitrosative stress) with the increased production of glutathione contributes to this perturbation in NPR1 oligomer-monomer equilibrium observed at Fig. 4-4.

Figure 4-5 GSNO-induced nitrosative stress alters cellular glutathione dynamics

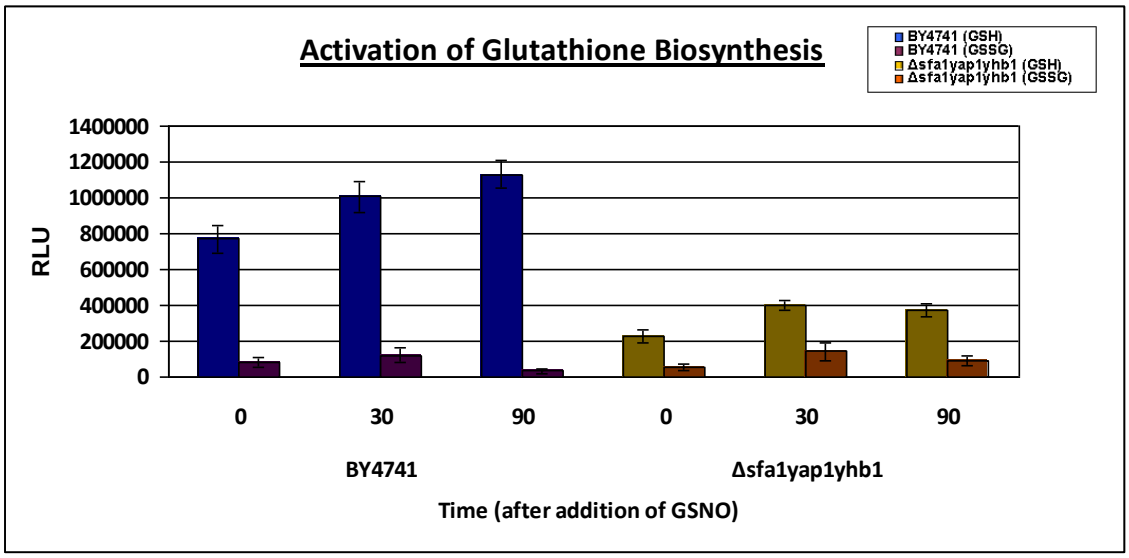

GSNO-induced nitrosative stress promotes glutathione biosynthesis. Cellular glutathione content was determined using total crude protein extract from BY4741 and *Δsfa1yap1yhb1*. Samples were analyzed using a GSH-Glo™Glutathione Assay (Promega) with the amount of glutathione provided as a relative light unit (RLU). Actual glutathione concentration was determined by comparing values to a standard curve (Fig. 3-5) and the numerical value is provided at table 4-1. Data obtained is from three independent experiments and error bars represent SEM.

Genotype	**Time (min)**	**Glutathione content (µM/µg protein)**			
		GSH	**GSSG**	**Total**	**GSSG/GSH (%)**
BY4741	0	2.7 ± 0.2	0.19 ± 0.005	2.9	7.2
BY4741	30	7.8 ± 0.5	0.24 ± 0.01	8.0	3.1
BY4741	90	12.8 ± 0.7	0.14 ± 0.01	12.9	1.1
Δsfa1yap1yhb1	0	0.39 ± 0.01	0.17 ± 0.004	0.56	43.6
Δsfa1yap1yhb1	30	0.71 ± 0.06	0.26 ± 0.02	0.97	36.6
Δsfa1yap1yhb1	90	0.58 ± 0.04	0.21 ± 0.01	0.78	37.4

Table 4-1 Numerical quantification of glutathione content. Values represent the mean ± SD of data obtained from three independent cultures.

4.5 Modifying L-methionine availability does not alter cellular glutathione abundance

It is known that cysteine and methionine are the only sulfur-containing amino acids. In humans, cysteine is derived from methionine using the transsulfuration pathway (McBean., 2011). However this process functions in reverse in *S. cerevisiae*, as this organism possesses an endogenous sulfate assimilation pathway whereby O-acetylhomoserine sulfhydrylase (MET17) can assimilate sulfide into O-acetylhomoserine to catalyze the formation of homocysteine. L-methionine is then derived from homocysteine and 5-methyltetrahydropteroyltri-L-glutamate catalyzed by N5-methyltetrahydropteroyltriglutamate-homocysteine methyltransferase (MET6) (Thomas and Surdin-Kerjan., 1997). Significantly in yeast, GSH is derived from a two stage process; initially glutamylcysteine synthetase (GSH1) converts glutamate and cysteine to γ-glutamylcysteine, with GSH derived when a glycine is attached to γ-glutamylcysteine by GSH synthetase (GSH2) (Ohtake and Yabuuchi, 1991; Grant at al., 1997).

This synthetic circuit relies on the efficient reduction of NPR1 to initiate a transcriptional cascade. To achieve this, protein levels of the inputs, GSNOR and TRXh5/NTRA must be sufficiently high to promote effective monomerisation. It was therefore necessary to select two promoters with established reliability as well as strong comparable induction strengths. The GAL1 promoter is regulated by carbon source, whereas the MET25 promoter is regulated by L-methionine availability. An increased production of glutathione is linked to NPR1 monomerisation in *Δsfa1yap1yhb1* (Fig. 4-5). By controlling L-methionine levels to regulate pMET25 activity, it is feasible this process may alter the transsulfuration pathway and therefore the cellular amount of glutathione. To confirm such a procedure is not directly modulating GSH abundance and thus potentially indirectly controlling NPR1 oligomer-monomer equilibrium, the cellular abundance of glutathione was determined by growing both BY4741 and *Δsfa1yap1yhb1* cells in various growth media required to suppress and/or activate pMET25. This included four separate growth conditions; cells grown in rich YPDA

media; cells grown minimal SD medium (2% raffinose) with or without 600μm L-methionine for 4 hours; or cells grown in minimal SD medium (2% raffinose) lacking L-methionine for 3 hours, followed by the addition of 600μm L-methionine and grown for a further 1 hour. Analysis of glutathione reveals that regardless of the growth conditions the cellular amount of GSH and GSSG does not vary notably for BY4741 and *Δsfa1yap1yhb1*. There is a slight increase in glutathione production when *Δsfa1yap1yhb1* cells are grown in YPDA, but when grown in SD MET-medium, there is little deviation in cellular content. In addition there is a slight increase in the GSSG/GSH ratio when *Δsfa1yap1yhb1* is grown in media lacking L-methionine, resulting from a reduced production of GSH, but generally the basal variation is limited with *Δsfa1yap1yhb1* consistently possessing considerably less glutathione compared to BY4741. It is therefore considered that pMET25 is a suitable promoter that can be exploited within the circuit as altering L-methionine availability does not appear to dramatically alter glutathione biosynthesis.

Figure 4-6 Cellular glutathione content for cells grown in various liquid media

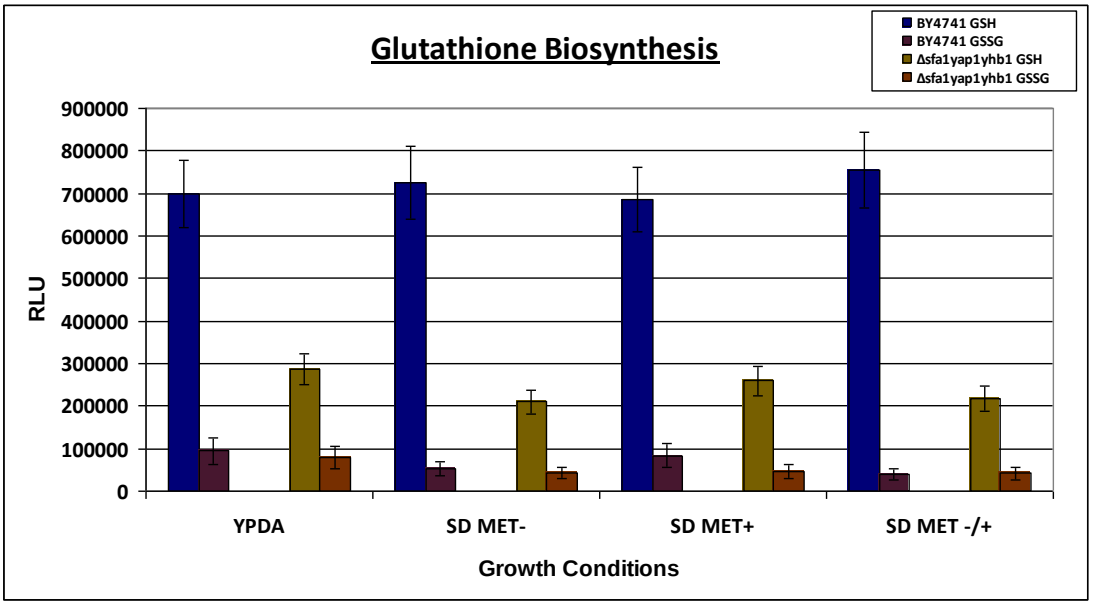

Modifying L-methionine availability does not alter the cellular content of glutathione. Cellular glutathione content was determined using total crude protein extract from BY4741 and *Δsfa1yap1yhb1*. Samples were analyzed using a GSH-Glo™Glutathione Assay (Promega) with the amount of glutathione provided as a relative light unit (RLU). Actual glutathione concentration was determined by comparing values to a standard curve (appendix A) and the numerical value is provided at table 4-2. Data obtained is from three independent experiments and error bars represent SEM.

Genotype	**Growth Media**	**Glutathione content (µM/µg protein)**			
		GSH	**GSSG**	**Total**	**GSSG/GSH (%)**
BY4741	YPDA	2.34 ± 0.2	0.2 ± 0.006	2.54	8.5
BY4741	SD MET-	2.6 ± 0.3	0.17 ± 0.003	2.77	6.5
BY4741	SD MET +	2.26 ± 0.3	0.2 ± 0.002	2.45	8.6
BY4741	SD MET -/+	2.78 ± 0.4	0.16 ± 0.001	2.94	5.8
Δsfa1yap1yhb1	YPDA	0.45 ± 0.01	0.19 ± 0.004	0.64	42.2
Δsfa1yap1yhb1	SD MET-	0.32 ± 0.02	0.17 ± 0.002	0.49	52.2
Δsfa1yap1yhb1	SD MET +	0.37 ± 0.02	0.18 ± 0.002	0.55	48.1
Δsfa1yap1yhb1	SD MET -/+	0.33 ± 0.02	0.18 ± 0.002	0.51	54.5

Table 4-2 Numerical quantification of glutathione content Values represent the mean ± SD of data obtained from three independent cultures.

4.6 Protein Localisation

In order to track protein location as well as detect protein-protein interaction between NPR1 and TGA3 by Förster resonance energy transfer (FRET) analysis in yeast, the genes encoding the flourophores ECFP and EYFP were fused to the C-terminal domains of NPR1 and TGA3, respectively. (It should be noted that ECFP was also fused to the N-terminal of NPR1 in order to test FRET but this lead to significant protein instability). NPR1 contains a bipartite NLS which promotes accumulation of the monomeric form of this protein in *Arabidopsis* cell nuclei (Cao et al., 1997; Ryals et al., 1997; Mou et al., 2003). To confirm that both NPR1 and TGA3 localise in yeast nuclei, the wild type BY4741 cell, where NPR1 is primarily present as a monomer, was imaged by laser scanning confocal microscopy (LSCM). Images at Fig. 4-7 clearly demonstrate that both NPR1 and TGA3 co-localise in the same subcellular compartment. The EYFP control, whereby EYFP is constitutively expressed in BY4741 cells without being fused to TGA3 confirms the nuclear localised TGA3::EYFP is dependent on properties associated with TGA3 (Fig. 4-8). To confirm this location was the nucleus, cellular DNA (and thus the nucleus) was identified by pre staining with ethidium bromide (Fig. 4-7).

It should be noted that a similar fluorescence pattern is observed for *Δsfa1yap1yhb1* cells under resting conditions (data not shown). This is rather surprising considering NPR1 is present predominantly as an oligomer in this cell (Fig. 4-2) with previous data presented in *Arabidopsis* indicating the NPR1 oligomer is excluded from nuclei (Mou et al., 2003). One possible explanation could be the fluorescence properties of the fluorophor used. It is well known that ECFP is not particularly bright and for many experiments this low efficiency can be a hindrance (hence the reason many groups now favour an EGFP-mCherry pairing) (Rizzo et al., 2004; Tramier et al., 2006). Thus it may be possible that CLSM simply cannot detect diffuse cytosolic oligomeric NPR1, and the nuclear localised NPR1 pattern observed in *Δsfa1yap1yhb1* is the detection of the concentrated residual monomeric NPR1 present in these cells (Fig. 4.2). Consistent

with this notion, the EYFP control at Fig. 4-8 demonstrates that the brightness of EYFP diminishes when this probe is expressed ubiquitously throughout the cell.

Figure 4-7 Confocal microscopy demonstrating NPR1 and TGA3 co-localise in yeast nuclei

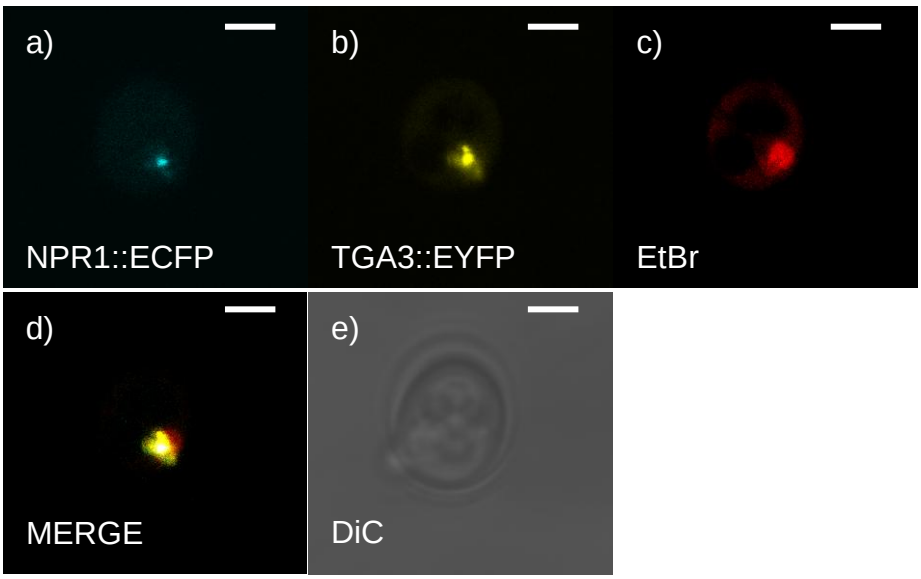

Confocal microscopy reveals that NPR1 and TGA3 co-localise in the same subcellular compartment. BY4741 cells expressing NPR1 and TGA3. a) Excitation at 458nm and emission at 477-505nm to visualise ECFP fused to NPR1. b) Excitation at 514nm and emission at 525-590nm to visualise EYFP fused to TGA3. c) Excitation at 512nm and emission at 633nm to visualise nuclear DNA stained with ethidium bromide. d) Merge of images superimposed on each other. e) Yeast cells visualised under phase contrast. All images captured at 100x optical zoom using a Leica TCS SP5 laser scanning confocal microscope. White bar indicates 5μm.

Figure 4-8 EYFP control

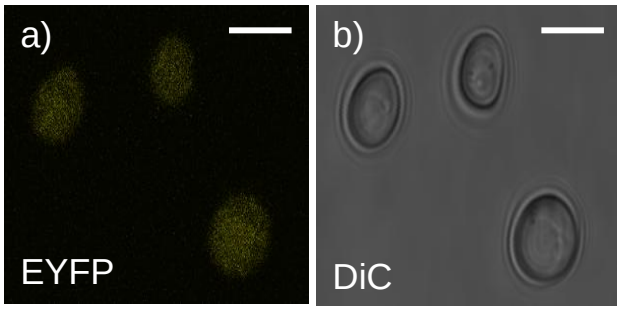

BY4741 cells expressing EYFP. a) Excitation at 514nm and emission at 525-590nm to visualise EYFP. b) Yeast cells visualised under phase contrast. All images captured at 100x optical zoom using a Leica TCS SP5 laser scanning confocal microscope. White bar indicates 10μm.

4.7 NPR1 and TGA3 interact in yeast nuclei

NPR1 and TGA3 have previously been shown to interact in *Arabidopsis* and this association is thought to potentiate the transcriptional function of TGA3 (Zhou et al., 2000; Johnson et al., 2003). To detect such an association in yeast, both BY4741 and *Δsfa1yap1yhb1* cells expressing NPR1::ECFP and TGA3::EYFP were examined by LSCM. By exciting the donor ECFP chromophore and detecting energy transfer to the acceptor EYFP chromophore, it is possible to conclude protein pairs are at an interface less than 10 nm apart, and thus likely to be undergoing protein-protein contact. Protein interactions between NPR1 and TGA3 in live yeast cells were determined using sensitised emission FRET by capturing a series of images (described at Para. 2.4.2). This approach detects the simultaneous decrease in donor emission but increase in acceptor emission. To gain accurate data the background signal is first identified. By analyzing images captured using Image-Pro Analyzer 7.0 and MetaMorph 7.5 software these parameters are identified as: coefficient A = 0.3 and coefficient B = 0.65. This data can then be integrated into the FRET equation (FRET = FRET image - (coefficient A x FRET image using Acceptor filter set) - (coefficient B x FRET image using Donor filter set)) and the FRET efficiency ascertained. Accordingly the average FRET efficiency for BY4741 cells (under resting conditions) was determined to be 37.75% (±

6.2%) (n=15), indicative of a fairly strong interaction between monomeric NPR1 and TGA3, while the average FRET efficiency for *Δsfa1yap1yhb1* cells (under resting conditions) is 19.25% (± 3.6%) (n=15), thus indicating a weaker interaction (Fig. 4-9). This is consistent with the fact there is residual monomeric NPR1 present in these cells, with the FRET efficiency seemingly being proportional to the abundance of NPR1 monomer. Interestingly, images at Fig. 4-9 also demonstrate that TGA3 occupies the entire volume of the nucleus, but NPR1 appears to reside in a subcellular compartment and this is where the protein-protein interaction takes place.

Figure 4-9 FRET data indicates protein-protein interaction between NPR1 and TGA3 in yeast nuclei

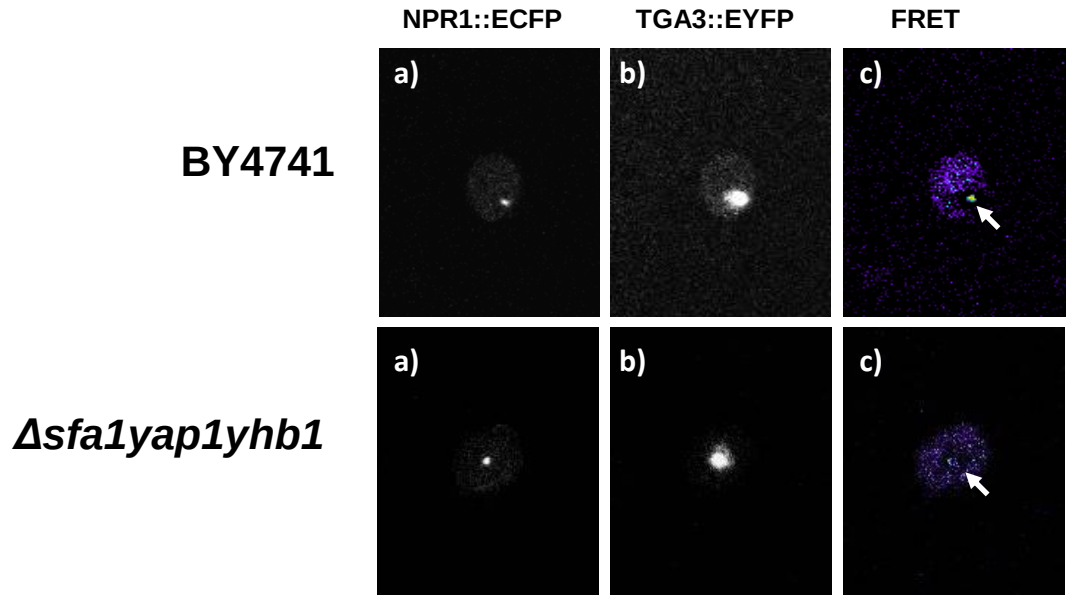

Fluorescence Resonance Energy Transfer (FRET) reveals that NPR1 and TGA3 interact in yeast nuclei (arrow). a).Images of donor were collected. b) Images of accepter were collected, c) and used to determine the FRET efficiency. Image presented in pseudocolour and represents corrected FRET.

4.8 Determination of circuit input parameters

In order to assess the dynamic nature of the protein circuit, it was necessary to determine the kinetic rate at which input proteins (GSNOR and TRXh5/NTRA) accumulate. This would facilitate subsequent experiments to confirm input-dependent reduction of the NPR1 oligomer. The circuit was designed so that two independently regulated promoters, pGAL1 and pMET25, drive the expression of GSNOR and TRXH5/NTRA, respectively. Unfortunately, an antibody directed against GSNOR and TRXh5 was not available, so consequently a FLAG tag was fused to the N-terminus of these proteins. To induce expression of GSNOR, the GAL1 promoter was activated by the addition of 2% galactose to the growth media, while to induce expression of TRXh5, the MET25 promoter was activated by growing cells in media lacking L-methionine. Protein accumulation was determined over 4 hrs and protein stability ascertained by repressing pGAL1 and pMET25 through the addition of 2% glucose and 600μm L-methionine, respectively, to the growth media and monitoring protein levels for a further 4 hours. Protein accumulation was ascertained by western blot using the commercial αFLAG antibody (Invitrogen™). It was determined that both GSNOR and TRXH5 are detectable at 2 hours with protein levels highly enriched at 4 hours (Fig. 4-10a). The proteasome subunit S5a was used as a loading control. A negative control consisted of cells grown for the duration of the assay (8 hours) in media containing 2% raffinose which is neutral for pGAL1 and 600μm L-methionine. Extraction of mRNA from cells and analysis by RT-PCR confirmed transcriptional activation and suppression of pGAL1 and pMET25 at the desired time points (Fig. 4-10b). It appears GSNOR and TRXH5 are highly stable in yeast as protein levels remain constant even after each respective promoter is switched off.

Figure 4-10 Determination of promoter strength and the kinetic rate at which input proteins accumulate

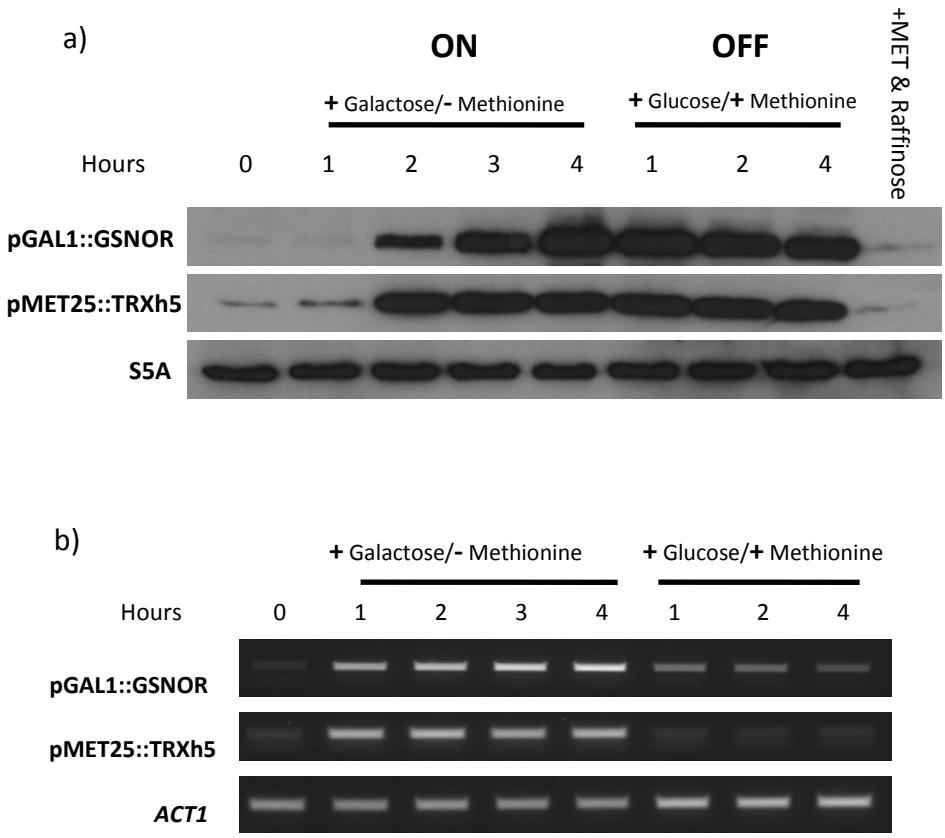

Kinetic determination of circuit input. a) Total yeast protein extracts were subjected to SDS-PAGE and western blot analysis. Primary antibodies was used at a dilution ratio of; αFLAG at 1/3000, αS5A at 1/5000, while the HRP-linked secondary antibody was used at 1/2500. Protein for GSNOR runs at ~42kDa, protein for TRXh5 runs at ~15kDa, protein for S5A runs at ~35kDa. b). Total RNA was subjected to RT-PCR analysis using gene specific primers and *Actin1* as a loading control. See Table 2-5 for reaction conditions and cycle numbers. Product sizes are GSNOR = 293bp, TRXh5 = 211bp and Actin1 = 246bp.

To confirm the GSNO-metabolising capacity of *Arabidopsis* GSNOR protein when expressed in yeast, two approaches were undertaken. The first would confirm enzyme activity by *in situ* staining. By resolving total protein extracts by native PAGE, such activity can be accurately determined. Fig. 4-11a clearly demonstrates that under resting conditions, endogenous GSNOR activity is detectible in BY4741 cells but absent in *Δsfa1yap1yhb1* cells. When *Δsfa1yap1yhb1* is transformed with

pRS305pGAL1:GSNOR and grown in 2% galactose, this transformant displays robust GSNOR activity, yet this feature remains absent when the same transformant is grown in the presence of 2% glucose.

A second approach allows GSNOR activity to be determined by monitoring GSNO-specific oxidation of NADH to NAD^+ (molar absorption coefficient for NADH at 340nm is 6220 $M^{-1}cm^{-1}$) (Dawson, 1985; Liu et al., 2001). A starting concentration of 0.2mM NADH provides a basal OD340nm value of ~1.5. By incubating crude protein extracts with NADH and GSNO it is possible to confirm GSNOR activity by monitoring a decrease in the absorbance at OD340nm. Fig. 4-11b confirms robust GSNOR activity for both BY4741 and *Δsfa1yap1yhb1* pRS305pGAL1:GSNOR grown in 2% galactose, further confirming *Arabidopsis* GSNOR synthesized in yeast is metabolically active. In contrast, oxidation of NADH was not detected when protein from *Δsfa1yap1yhb1* cells or the transformant (containing pRS305pGAL1:GSNOR) grown in the presence of 2% glucose, were incubated with GSNO.

Figure 4-11 Confirmation that *Arabidopsis* GSNOR is metabolically active when expressed in yeast

a)

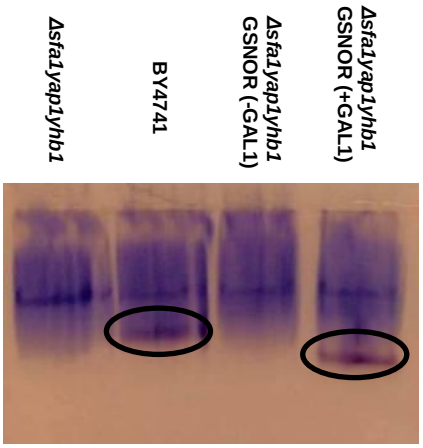

b)

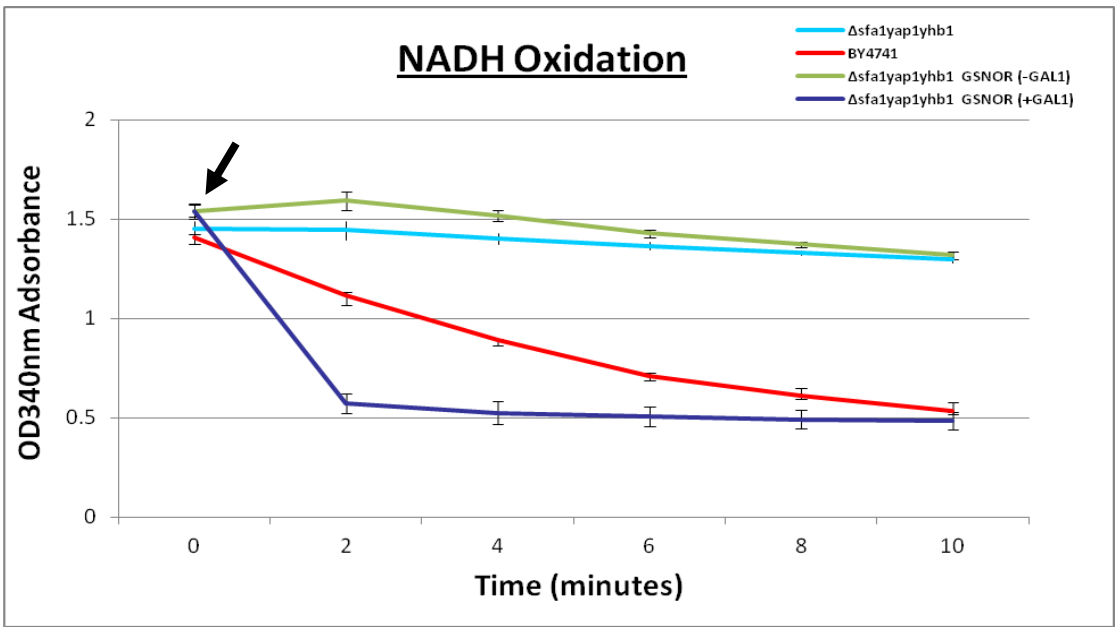

Arabidopsis GSNOR is metabolically active in yeast. a) In-gel activity was determined by resolving 500µg total protein (crude extract) on a non-denaturing polyacrylamide gel and incubating overnight with a reaction mixture to reveal active GSNOR bands (circled) b) 500µg total protein (crude extract) was incubated with 0.2mM NADH in the presence of 1mM GSNO, and NADH consumption (absorbance at 340 nm) was followed over time. Arrow indicates the addition of GSNO to initiate the reaction. Data shown are representative of three similar experiments.

4.9 GSNOR and TRXh5/NTRA function synergistically to reduce the NPR1 oligomer

An essential stipulation of the circuit design requires that the inactive oligomeric NPR1 complex present in *Δsfa1yap1yhb1* can be selectively reduced into an active monomeric form. The experimental analysis at Fig. 4-10a confirmed that once transcription of GSNOR and TRXh5/NTRA is induced, large quantities of protein accumulate at 4 hours. To confirm these inputs are able to operate as NPR1 reductants, NPR1 oligomer-monomer equilibrium was correlated with the functional GSNOR and TRXh5/NTRA individually, and when both inputs are active simultaneously. Yeast strain *Δsfa1yap1yhb1* constitutively expressing NPR1 was grown for 4 hours in minimal SD- MET media with either 2% raffinose or 2% galactose (to activate GSNOR) as a carbon source with 600μM L-methionine added (to repress TRXh5/NTRA) where required. Analysis by western blot at Fig. 4-12 indicates that individual activation of GSNOR has little effect on NPR1 oligomer-monomer equilibrium. However when TRXh5/NTRA is activated a dramatic reduction in the overall cellular abundance of the NPR1 oligomer is observed. Although TRXh5/NTRA is able to reduce the vast majority of the oligomer present in the cell, this protein does appear to function synergistically with GSNOR, as residual oligomer almost completely disappears when both inputs are active simultaneously. This is likely a consequence of GSNOR-dependent metabolism of endogenous GSNO, reducing the frequency at which NPR1 is modified by *S*-nitrosylation, while TRXh5/NTRA will most likely be directly catalyzing disulphide dissociation between NPR1 monomers housed in the oligomer.

Figure 4-12 Circuit inputs are able to promote NPR1 monomerisation

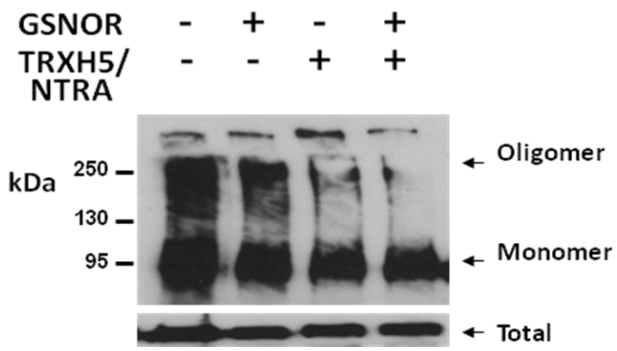

Synergistic function of GSNOR and TRXh5/NTRA in reducing the NPR1 oligomer. 50μg total yeast protein was subjected to SDS-PAGE and immunoblot analysis. Both primary αGFP and HRP-linked secondary antibodies were used at a dilution ratio of 1/3000. Total protein confirms equal loading.

4.10 Determination of circuit output parameters

To determine an input-output relationship and correlate circuit activation to NPR1 monomerisation, induction of the luciferase reporter was determined for various circuit configurations. All contained circuit inputs (GSNOR and TRXh5/NTRA) along with the reporter construct containing either the native (designated *as-1*) or mutagenized (designated *mut_as1*) version of the *Arabidopsis as-1* element present in pMEL1. Cellular content of luciferase was then quantified when either NPR1 or TGA3 were present individually, or in combination using the method described at para 2.9. The yeast strain BY4741, where NPR1 is present predominantly in the monomeric form acted as a control. Data at Fig. 4-13a demonstrates that there is cross-talk between the yeast chassis and the synthetic circuit, as indicated by the background induction present for all configurations apart from when NPR1 and TGA3 are present in combination. Interestingly, this background is suppressed in cells expressing both NPR1 and TGA3, suggesting that TGA3 engages (and thus out competes) the *as-1* element in a NPR1-dependent manner. This implies that the NPR1-TGA3 interaction promotes DNA

binding but this does not activate reporter gene expression. The reason for this is unclear as the GAL4 AD fused to NPR1 should function to recruit transcriptional machinery. The *as-1* element contains two TGA binding motifs and therefore to examine if properties of TGA heterodimers are required to activate gene expression, TGA2 was incorporated into the fully integrated circuit. However no difference in reporter gene activation was noted. In addition, it has previously been reported that salicylic acid is able to directly potentiate the transcriptional properties of NPR1 in yeast (Maier et al., 2011). Consequently, circuit induction was determined in the presence of 0.3mM SA, but again no difference in reporter gene activity was observed.

A similar pattern was observed in *Δsfa1yap1yhb1* cells but overall background expression is reduced and this may indicate a potential reduction in general efficiency of cellular function and performance in this cell type (Fig. 4-13b). Interestingly background expression is also suppressed when NPR1 and TGA3 are co expressed, under both on and off input states, and this feature is likely the result of residual NPR1 monomer present in these cells, interacting with TGA3 and this protein complex then remaining stationary on the DNA.

As the observed background is specific to the native *as-1* binding site, this suggests a *S. cerevisiae* bZIP transcription factor might be responsible. Analysis of the *Saccharomyces* genome database (http://www.yeastgenome.org/) indicates many yeast bZIP factors are involved in nutrient starvation responses. To investigate the possibility this pattern is a consequence of growing cells in minimal SD MET- media, circuit output parameters were ascertained for BY4741 cells grown in media complemented with all amino acids for optimal yeast grown. However, no difference in background expression was observed.

Figure 4-13 determination of output parameter for various circuit configurations

a)

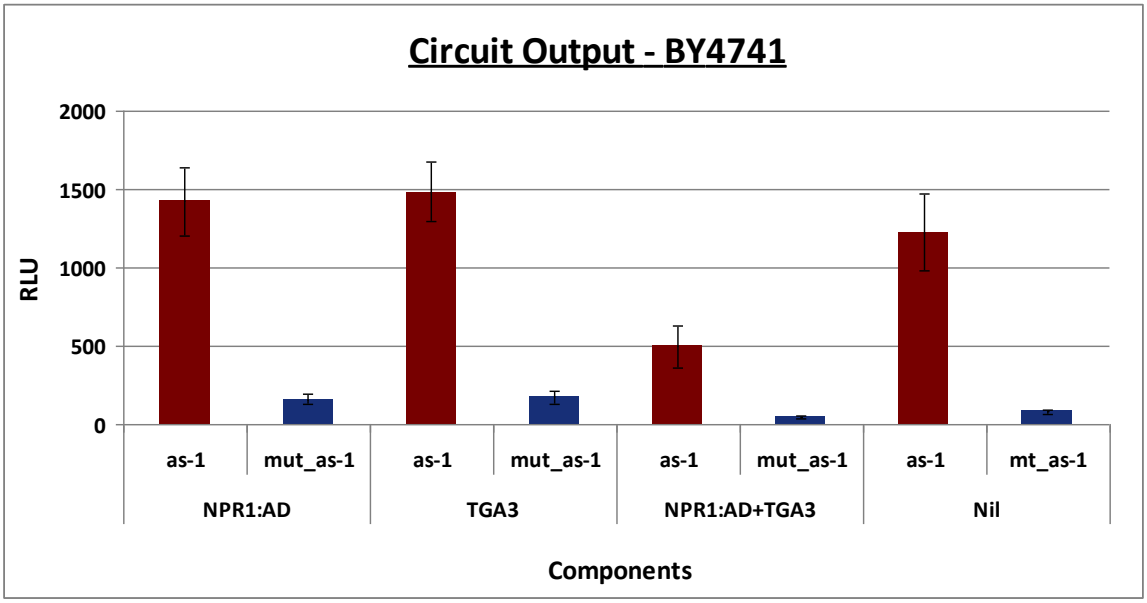

b)

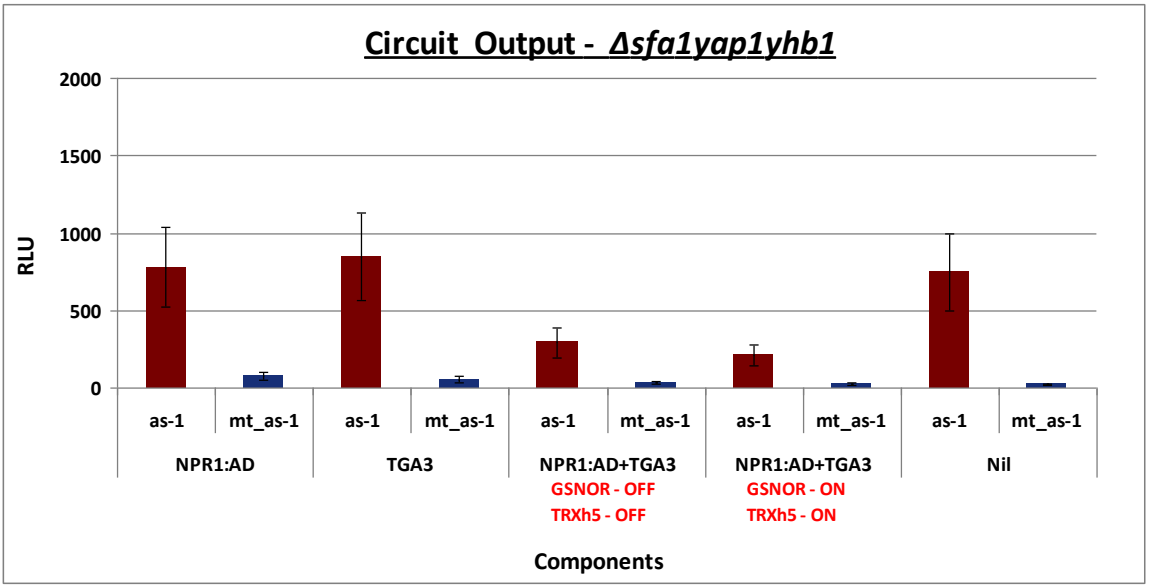

Determination of circuit output parameters for various circuit configurations a). BY4741 b). *Δsfa1yap1yhb1*. Live cells were incubated with D-luciferin in a 96-well plate and luminescence determined. Data obtained is from three independent experiments and error bars represent SEM.

4.11 NPR1 is not a target for proteasomal degradation in *S. cerevisiae*

Destruction of NPR1 by the proteasome is known to play a dual role in regulating plant immunity in *Arabidopsis.* In resting cells, NPR1 monomers not fixed in an oligomer that enter the nucleus are targeted for degradation to prevent untimely activation of defence genes. In addition it is known that upon activation of defence signalling, NPR1 functions as a transcriptional cofactor, possibly engaging components of the basal transcriptional machinery and initiating gene transcription (Spoel et al., 2009). To maintain gene induction and ensure efficient generation of mRNA, "fatigued" NPR1 is phosphorylated, and this modification increases the affinity of this protein to a Cullin3-based ubiquitin ligase (CUL3). Consequently, NPR1 is rapidly degraded by the proteasome, which clears the promoter for an "unused" NPR1 to reengage and activate transcription (Spoel et al., 2009). Gene output therefore should be relative to the amount of NPR1 monomer. Analysis of the *S. cerevisiae* genome reveals a gene encoding *CUL3* (YGR003w) with evolutionary similarities to those encoded by plants (Marín., 2009). It was shown at Fig. 4-2 that a low number of NPR1 monomers remain in *Δsfa1yap1yhb1* which are able to enter nuclei and engage TGA3 (Fig. 4-9). Moreover data at Fig. 4-13 indicate that the NPR1-TGA3 interaction might promote DNA engagement, but this does not appear to activate gene transcription, even when the GAL4 AD is used. To determine if the proteasome-mediated mechanisms that are essential for NPR1 dynamics in *Arabidopsis*, are active in yeast, crude protein extracts were incubated with or without the proteasome inhibitor MG115 (50μM) for 120 minutes at 25°C. Subsequent analysis by western blot at Fig. 4-14 demonstrates that NPR1 is not a target for degredation via a proteasome-mediated mechanism in yeast, thus providing a potential reason why NPR1 monomers persist in *Δsfa1yap1yhb1* under resting conditions. Moreover, it is possible that upon NPR1-TGA3 interaction this protein complex remains stationary at the promoter as no endogenous mechanism is in place to turn-over NPR1 and promote efficient reporter gene transcription.

Figure 4-14 NPR1 protein is highly stable in *S. cerevisiae*

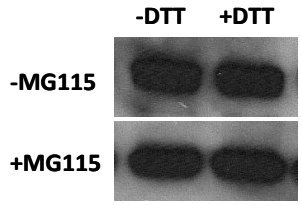

NPR1 is not targeted to the proteasome in yeast. 50µg total yeast protein was incubated with or without MG115 and subjected to SDS-PAGE and immunoblot analysis to determine if NPR1 is targeted for proteasome-mediated destruction. Both primary αGFP and HRP-linked secondary antibodies were used at a dilution ratio of 1/3000. Total protein (+ 50mM DTT) confirms equal quantities of protein after incubation for 120 minutes.

4.12 Mathematical Modelling – Simulation of the NPR1 oligomer-to-monomer switch

The aim of mathematical modelling is to provide a numerical representation of a system. If this system, defined itself by a set of variables is accurate, then this model provides a means to understand acute changes in circuit dynamics resulting from single or multiple perturbations. Accordingly, the synthetic circuit stipulated at Fig. 4-1 was modelled using parameters defined in this study. This approach may be informative and provide a platform to comprehend the complex function of NPR1 in context of plant immune signalling. The model identified at Fig. 4-15 was completed by John Wilson-Kanamori, School of Informatics, University of Edinburgh using Kappa language, a rule-based stochastic modelling tool that provides concise and comprehensible biological simulations. The Kappa code and parameters used to develop this model are included at Appendix B. The model indicates a chronological input-output relationship, whereby the activation of inputs (GSNOR and TRXh5/NTRA) leads to an increase in monomeric NPR1 located in nuclei which correlates with the activation of an output (LUC). The Systems Biology Graphical Notation (SBGN) diagram is included at Appendix C. With further development it may be possible to rationally test feasibility studies of novel theories by introducing single or multiple perturbations to this model.

Figure 4-15 mathematical simulation of the synthetic circuit

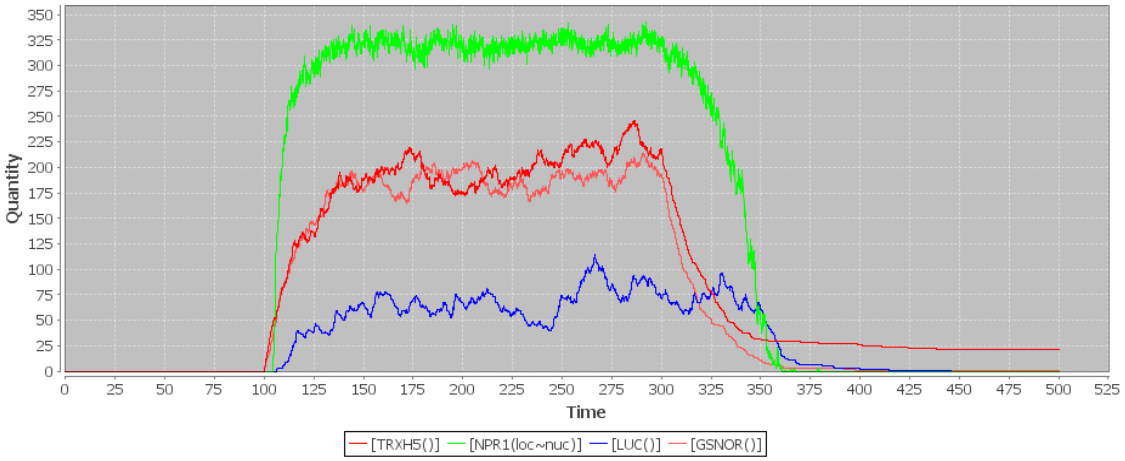

Stochastic simulation of the NPR1 oligomer-to-monomer switch modelled using Kappa. Preliminary graph demonstrating that nuclear-localised monomeric NPR1 and subsequent reporter gene expression is dependent on induction of GSNOR and TRXh5/NTRA. GSNOR and TRXh5/NTRA are switched on at t=100 and off at t=300.

4.13 Conclusion

Using a synthetic biology approach we sought to build a conceptual protein circuit based on theoretical data from plant immunity. Using a heterologous system removes biological complexity and should provide insight into the exact functional properties of NPR1 in relation to interacting TGA transcription factor partners and gene activation. This chapter outlines the approach used to build and subsequently characterise the synthetic circuit. Like most eukaryotes, *S. cerevisiae* maintains a highly reducing intracellular redox environment and thus the *Δsfa1yap1yhb1* triple mutant was generated on the basis that collective disruption of these three genes would increase the GSNO and protein-SNO forming capacity of the yeast cell, as well as limit genetic responses associated with perturbed cellular homeostasis (see chapter 3). We find this perturbation renders the yeast chassis to be sufficiently oxidising to maintain NPR1 predominantly in the oligomeric form (Fig. 4-2) with *in vitro* data indicating this conformation is dependent on GSNO induced *S*-nitrosylation of NPR1 (Fig. 4-3). To

control NPR1 oligomer-monomer equilibrium two circuit inputs, GSNOR and TRXh5/NTRA, were selected. The *Arabidopsis* GSNOR protein is metabolically active in *S. cerevisiae* (Fig. 4-11) and would appear to indirectly modulate NPR1 oligomer formation, by metabolising GSNO, thus limiting *S*-nitrosylation of NPR1 (Fig. 4-12). In addition, the TRXh5/NTRA system appears to have potent denitrosylase properties in *S. cerevisiae* (Fig. 4-12). The NPR1 monomer and TGA3 co-localise in yeast nuclei (Fig. 4-7) and this is where the protein-protein interaction takes place (Fig. 4-9) with this association appearing to induce promoter binding (Fig. 4-13). Similar to the regulatory function in *Arabidopsis*, it is likely NPR1 and TGA3 complex on DNA in *S. cerevisiae*, but this is insufficient to activate transcription of the *LUC* reporter gene. The reason is not clear but could be linked to a defective proteolysis-coupled transcription cycle that ordinarily regulates NPR1 coactivator function in *Arabidopsis* (Spoel et al., 2009) (Fig. 4-14).

CHAPTER 5

5. General Discussion

5.1 Introduction

Plants possess an integrated, multi-layered cellular defence system that functions cooperatively to counteract the action of invading pathogens. In compatible pathogen interactions, plants are capable of initiating a systemic immune response, termed systemic acquired resistance (SAR) that provides robust, long-term, broad-spectrum resistance to subsequent infection. If the molecular mechanisms that govern both local plant immunity and SAR can be understood, then this provides scope to engineer economically-important plant species that are able to resist a broad-spectrum of pathogens.

Plant hormones have emerged as key modulators of plant immunity with salicylic acid in particular being of central importance. The transcription cofactor NPR1 is an essential transducer of the SA signal in *Arabidopsi*s and has been assigned a prominent role in defence gene induction, hormone cross-talk modulation and SAR (Cao et al., 1994; Glazebrook et al., 1996; Kohler et al., 2002; Spoel et al., 2003). This protein is redox regulated, and when active in the monomeric form, is known to interact with an assortment of transcription factors to regulate the expression of over 2200 immune-related genes in *Arabidopsis* (Mou et al., 2003; Wang et al., 2006). Of particular importance are the bZIP domain containing (group D) proteins collectively known as TGA transcription factors (Zhang et al., 1999; Després et al., 2000; Zhou et al., 2000; Subramaniam et al., 2001; Kesarwani et al., 2007). However, despite several concerted attempts, both functional redundancy and stochastic factors limit the effectiveness of standard genetic approaches used in plant research, and thus much of the hierarchical processes surrounding NPR1 function are not fully understood.

Synthetic biology is a nascent field that aims to provide a logical, systematic, engineering approach to biology. By breaking biological systems down into a list of minimal components, synthetic biology can unravel biological paradigms by systematically re-assembling biological systems. Accordingly, abstract protein circuits are a central requirement of this field. Using a synthetic biology approach we aim to set the foundations for the development of a yeast tool that can be used to manipulate and subsequently understand NPR1 function within plant immune circuits. We sought to create a conceptual protein circuit based on theoretical plant immunity using a yeast system that has been engineered to be amenable to redox manipulation.

5.2 Knocking out three redox-related genes dramatically alters the reducing potential of a yeast cell

S. cerevisiae maintains a highly reducing intracellular environment so the *Δsfa1yap1yhb1* mutant was generated on the basis that collective disruption of these three genes would be sufficient to perturb cellular redox homeostasis. Determination of the actual intracellular redox potential using the molecular probe roGFP2 (section 3.5) reveals *Δsfa1yap1yhb1* has a dramatically lowered cellular reduction potential, as compared to BY4741. We find the redox potential of a wild type yeast cell (BY4741 in this instance) under resting conditions to be -308mV. This is more oxidising than previous estimates and may be the consequence of using a different redox probe and/or genetic variant of *S. cerevisiae* (Østergaard et al., 2004). This figure decreases by 64mV to -244mV in *Δsfa1yap1yhb1*. Although *Δsfa1yap1yhb1* confers a distinct growth disadvantage (Fig. 3-3), this is perhaps not as severe as one might expect as modifications to redox status are considered detrimental to cellular homeostasis. Thus, the *Δsfa1yap1yhb1* cell appears highly adaptable to a more oxidising redox environment but there is little tolerance in this margin as inducing ROS or RNS-related stress is highly deleterious to *Δsfa1yap1yhb1* growth (Fig. 3-7).

In *S. cerevisiae,* YAP1 is known to induce a large assortment (~100) of anti-oxidant genes in response to oxidative stress, as well as be involved in the regulation of 23% of

genes altered in response to nitrosative stress (Kuge and Jones, 1994; Gasch et al., 2000; Horan et al., 2006). It is therefore not surprising that investigation of transcripts by sqRT-PCR revealed three redox modulators for which mRNA abundance is decreased in *Δsfa1yap1yhb1* (Fig. 3-8). The *GPX2* gene is known to be induced in a YAP1-dependent manner, and together with glutathione peroxidase homologues, is known to alleviate oxidative stress (Inoue et al., 1999). Interestingly, GPXs have also been shown to decompose GSNO *in vitro*, suggesting this enzyme may possess the capacity to regulate GSNO and protein-SNO formation (Hou et al., 1996). Both TSA1 and AHP1 are peroxiredoxins that have been shown to interact with yeast TRX proteins in a bidimensional electrophoresis assay and Y2H work (Vignols et al., 2005). Although the significance of this interaction is not clear, it could be linked to recent work which demonstrates that TSA1 and AHP1 are able to induce disulfide bond formation in important stress-related transcriptional activators, such as YAP1 and CAD1 (Tachibana et al., 2009; Iwai et al,. 2010). Interestingly, kinetic analysis reveals *AHP1* is induced in response to GSNO in *Δsfa1yap1yhb1* (Fig. 3-8c) but the function of this enzyme in yeast has not been established. In bacteria, subunits of alkyl hydroperoxide reductase protect the cell from nitrosative stress, and a transgenic human epithelial cell line 293, expressing the *Mycobacterium tuberculosis* version of *ahpC* are afforded increased protection from GSNO-induced stress (Chen et al., 1998). Thus, it is conceivable AHP1 performs a similar function in yeast.

The *GSH1* promoter contains a YAP1 binding site (Wu et al., 1994; Sugiyama et al., 2000) and the observed reduction in glutathione concentration in *Δsfa1yap1yhb1* (Fig 3-4 and table 3-1) is likely attributable to the functional disruption of this transcription factor. Alternatively, glutathione production could be regulated by an unknown mechanism involving protein *S*-nitrosylation/denitrosylation, and altering SFA1 and YHB1 function could potentially directly modify biosynthesis of this peptide. Although a difference in *GSH1* and *GLR1* gene expression could not be detected between *Δsfa1yap1yhb1* and BY4741, it is well established that mRNA abundance does not always directly correlate with protein content (Gygi et al., 1999). Ordinarily, glutathione is the most abundant low molecular weight thiol in cells and an essential

component in the glutaredoxin and glutathione peroxidase systems (Grant, 2001; Meyer et al., 2009). Overall, the *Δsfa1yap1yhb1* mutant has a ~5 fold reduction in total glutathione levels along with a GSSG/GSH ratio that increases to 41% (from 7.7% in BY4741) (Fig. 3-4), indicating *Δsfa1yap1yhb1* is unable to efficiently reduce GSSG (to GSH). Taken together, these data indicate that the glutathione-regulated redox environment of *Δsfa1yap1yhb1* is less capable of maintaining reduction potential.

5.3 Ambient changes to cellular redox modulate NPR1 monomer-oligomer equilibrium in yeast

Structural analysis of NPR1 by western blot reveals that in the relatively reducing environment of the cytoplasm of wild type yeast strain BY4741, the transcription cofactor NPR1 invariably favours momomer formation. However, by attenuating cellular redox, NPR1 structure can be manipulated with this protein found predominantly as an oligomer in *Δsfa1yap1yhb1* (Fig. 4-2), although residual monomeric NPR1 does remain being located within nuclei (Figs. 4-7 and 4-9). In *Arabidopsis*, the current paradigm states that in resting cells, oligomeric NPR1 is located in the cytoplasm, and it is not until SA-induced intracellular redox changes promoting reduction of this complex, is a notable accumulation of NPR1 monomer in the cell nucleus (Mou et al., 2003; Spoel et al., 2009). This suggests that to prevent unnecessary large scale protein loss, NPR1, once translated and upon exiting the endoplasmic reticulum, must very rapidly form into an oligomer. To achieve this, GSNO must be resident and local cellular conditions must be sufficiently oxidising. As a safeguard to prevent untimely activation of defence genes, those NPR1 monomers which do "escape" are very rapidly degraded by the proteosome (Spoel et al., 2009). In yeast we find NPR1 to be highly stable (Fig. 4-14) and under resting conditions NPR1 monomers are present in nuclei (Fig. 4-14), indicating that the proteosome-mediated degradation mechanism present in *Arabidopsis* is either not present or not functional in yeast. Were such a system in place then it is expected that monomeric NPR1 found in *Δsfa1yap1yhb1* under basal conditions would be removed by the proteosome.

Cellular redox is a highly dynamic process with many factors functioning in concert to modulate this system. Both protein *S*-nitrosylation and denitrosylation of redox sensitive thiols are regulated principally (but not exclusively) by two enzymatic pathways; the thioredoxin and GSH/GSNO/GSNOR pathways (Benhar et al., 2009). The *S. cerevisiae* genome encodes three thioredoxin genes, of which two are cytoplasmic (*TRX1* and *TRX2*) and a single complementary TRX reductase (*TRR1*), which "powered" by the oxidation of NADPH to $NADP^+$, functions to directly reduce oxidised TRX (Gelhaye et al., 2004). Analysis by sqRT-PCR of *TRX* genes reveals no difference between BY4741 and *Δsfa1yap1yhb1* (Section 3.7). Therefore it is conceivable that the TRX system is largely unperturbed in *Δsfa1yap1yhb1* and as NPR1 exist mainly as an oligomer in this cell, it can be concluded that there is little or no cross-talk between the synthetic circuit and the endogenous thioredoxin system.

In the second system, GSNOR is able to indirectly modulate protein *S*-nitrosothiols by metabolising GSNO. In *Arabidopsis*, *S*-nitrosylation of NPR1 by GSNO is known to promote oligomer formation (Tada et al., 2008), and we have demonstrated in this study that NPR1 generated in yeast is responsive to GSNO *in vitro* (Fig. 4-3). As *Δsfa1yap1yhb1* lacks functional flavohemoglobin, this cell is unable to scavenge free NO. Coupled with the fact this mutant is unable to regulate the endogenous glutathione system (Fig. 3-4), it is likely that GSNO makes up a larger relative proportion of the low molecular weight XNOs present in this cell, as compared to BY4741. Glutathione is a major thiol-disulfide redox buffer that has been shown to modulate NPR1 oligomer-monomer equilibrium (Mou et al., 2003). It is therefore likely that the large reduction in the cellular glutathione content coupled with a reduced cytosolic buffering capacity and an increase in GSNO abundance, are the key determining factors in the shift in NPR1 dynamics observed. Consistent with this notion we find that GSNO-induced stress leads to an increase in glutathione biosynthesis in *Δsfa1yap1yhb1*, and this correlates with NPR1 monomerisation (Figs. 4-4 and 4-5).

It should also be noted that glutaredoxins have the potential ability to regulate protein thiol- disulfide balance but the functional relevance of this system in both *S. cerevisiae*

and *Arabidopsis* is largely undescribed (Grant, 2001; Meyer et al., 2009). Oxidised GRX is reduced by GSH, with GSSG in turn, cycled back to the reduced form by a glutathione oxidoreductase (GLR1) (Meyer et al., 2009). In *S. cerevisiae*, the GRX family has eight members (GRX1-GRX8) and sqRT-PCR analysis of two cytosolic GRX genes (*GRX1* and *GRX2*) reveals little difference in mRNA abundance between BY4741 and *Δsfa1yap1yhb1*. Thus it would appear, like the TRX system, there is little or no cross-talk between the synthetic circuit and the endogenous glutaredoxin system. However, considering there is a dramatic reduction in the overall cellular concentration of glutathione, this system is likely to function less efficiently in *Δsfa1yap1yhb1* as compared to BY4741. Thus it cannot be entirely discounted at this stage that a member(s) of yeast GRXs, or other factors, are able to promote NPR1 monomerisation.

5.4 The TRXh5/NTRA system is able to denitrosylate NPR1 *in vivo*

Thioredoxins (TRXs) possess a highly conserved active site dithiol motif capable of mediating protein denitrosylation. The thioredoxin system requires the action of selenoenzyme Trx reductases (TrxR) to function efficiently (Trotter and Grant, 2005; Lillig and Holmgren, 2007; Benhar et al., 2010). The *S. cerevisiae* thioredoxin system is composed of three TRXs and it appears there is not any cross talk with NPR1 and this endogenous oxidoreductase system (section 5.3). In *Arabidopsis*, the *TRX* gene family has undergone rapid expansion with the cytosolic (*TRXh)* gene family alone having eight members, each being differentially expressed and appearing to have diverse function (Reichheld et al., 2002; Laloi et al., 2004). Two members, *TRXh3* and *TRXh5*, have been shown to be essential positive regulators of plant immunity, with *TRXh5* being highly inducible upon pathogen challenge, indicative of a role in pathogen-activated cellular redox regulation (Tada et al., 2008). In *Arabidopsis*, TRX proteins are documented to have *in vitro* denitrosylase activity with TRXh5 also being able to interact with NPR1 *in vitro*, but the full biological implications of this have not been established (Tada et al., 2008; Spoel and Loake, 2011). Here we provide further evidence that the TRXh5/NTRA system has highly efficient NPR1 reduction function. When expressed in *S. cerevisiae*, accumulation of TRXh5/NTRA correlates with a net

shift from NPR1 oligomer to monomer (Fig. 4-12). Together, both GSNOR and TRXh5/NTRA appear to function synergistically to reduce the NPR1 oligomer and this is likely a consequence of GSNOR-dependent metabolism of endogenous GSNO, reducing the frequency at which NPR1 is modified by *S*-nitrosylation, while TRXh5/NTRA will most likely be directly catalyzing disulphide dissociation between NPR1 monomers housed in the oligomer.

5.5 Identification of potential new regulatory processes surrounding NPR1

NPR1 appears to localise to a subcompartment in the nucleus, with FRET data indicating that the NPR1-TGA3 protein interaction takes place in this location (Figs. 4-7 and 4-9). This site is likely to be the nucleolus and this assumption stems from the observation that in some (<1%) yeast nuclei, ECFP fluorescence representative of NPR1 was located as several bodies occupying a large region of the nucleus (data not shown). This is attributable to an age-related phenomenon in yeast, whereby nucleoli become enlarged or fragmented (Sinclair et al., 1997). Although yeast and plant nuclei are structurally similar it is not known if NPR1 positions in this location in plant nuclei. If so, this could suggest a role for NPR1 in RNA processing, ribosome synthesis or chromatin modification.

From an evolutionary perspective such a feature makes sense. NPR1 is likely to interact with a vast library of transcription factors and other regulatory proteins to modulate the expression of thousands of genes. Transcription factors are highly mobile and thought to scan the entire volume of the nucleus for cognate binding sites in just a few minutes (Hager et al., 2009). Little is known about the mobility of NPR1 in nuclei but based on the volume of the nuclei and the number of protein units, from a logistical perspective, the frequency at which two proteins encounter one another is likely to increase should one (e.g NPR1) remains predominantly static. As NPR1 functions as a transcription cofactor, such a mechanism provides an inherent regulatory advantage in gene activation (such as preventing over accumulation of mRNA) as transcription becomes

proportional to not only NPR1-TGA3 protein abundance but also protein-protein interaction frequency.

5.6 Transcriptional activation at the *PR-1* promoter is highly complex and dependent on factors other than NPR1 and TGA3

NPR1 regulates a diverse array of primary and secondary response defence-related genes in *Arabidopsis* (Wang et al., 2005; Wang et al., 2006a). Induction of SA-dependent signalling is invariably associated with the expression of *PR* genes and therefore accumulation of mRNA for these genes serves as a useful marker of defence activation (Delaney et al., 1995; Lawton et al., 1996; Shah et al., 1997). NPR1 lacks a canonical DNA-binding domain and is known to mediate its regulatory function though interaction with transcriptional factors. Accordingly, both NPR1 and TGA transcription factors are essential activators of *PR-1* (Fan and Dong, 2002; Kesarwani et al., 2007). NPR1 has been shown to interact with seven TGA factors (TGA1-TGA7) in *Arabidopsis* but the exact role of individual TGA proteins in context of *PR-1* expression is not fully understood, since functional redundancy makes it difficult to assign properties to specific members of this group.

In this synthetic circuit we used the NPR1-TGA3 combination as in *Arabidopsis* TGA3 is recruited to the *PR-1* promoter in a NPR1-dependent manner and known to be a potent activator of *PR* gene expression upon SA signalling induction (Zhou et al., 2000; Johnson et al., 2003; Kesarwani et al., 2007). Work presented here demonstrates a strong NPR1-TGA3 interaction in yeast nuclei as determined by a FRET efficiency of 37.75% (Fig. 4-9) in wild type yeast strain BY4741, where NPR1 is present almost exclusively in the momomeric form (Fig. 4-2), with this interaction able to potentiate the DNA-binding properties of TGA3 (Fig. 4-13). In *Arabidopsis*, there is some data suggesting TGA factors remain stationary on DNA in a transcriptionally inactive state in the absence of NPR1 (Rochon et al., 2006; Boyle et al., 2009). This study provides evidence to challenge this proposal. In particular, background reporter gene expression was noted for all circuit configurations, except for when NPR1 and TGA3 were

included in combination, suggesting that the *as-1* element housed in the MEL1 promoter remains vacant until the NPR1-TGA3 interaction facilities DNA binding (Fig. 4-13). As background expression is reduced in this configuration it is likely that TGA3 is engaging and remaining static on DNA.

In *Arabidopsis*, both NPR1 and TGA factors are recruited to, and form a transcriptional complex at the *PR-1* promoter. In this scenario NPR1 functions as a transcription cofactor operating to promote the recruitment of transcription machinery (Spoel et al., 2009). It is likely NPR1 is also recruited to the modified MEL1 promoter used in this synthetic circuit, although this is not sufficient to initiate transcription. The reason for this is unclear as the GAL4 AD fused to NPR1 should induce expression of the reporter gene, with mRNA abundance relative to the amount of monomeric NPR1. One possible explanation is that TGA3 functions as a transcription repressor, however information contained within the literature suggests this is very unlikely. So what is going wrong?

5.6.1 DNA-located NPR1 is not being turned-over

In recent years a number of studies have identified that many transcription (co)factors associate only transiently with their target binding sites (reviewed in Hager et al., 2009). In many cases, this process is regulated by proteasome-mediated turnover of the transcription (co)factor and functions to maintain highly efficient gene activation by ensuring a continual supply of fresh DNA-bound activator (Kodadek et al., 2006). Such a mechanism was recently shown to promote NPR1-dependent gene transcription in *Arabidopsis*. Specifically, NPR1 is phosphorylated at residue Ser11/Ser15 and subsequently poly-ubiquitinated by the Cullin3-based (CUL3) ubiquitin ligase. This promotes rapid degradation of NPR1 by the proteasome, clearing the promoter for unphosphorylated NPR1 to reengage and activate transcription (Spoel et al., 2009). Significantly, pharmacological inhibition of the proteasome or genetic knockdown of CUL3 lowers NPR1 target gene expression, indicating this mechanism is a vital component of transcriptional activation (Spoel et al., 2010). Although *S. cerevisiae* contains an evolutionally-related CUL3, it does not appear to target NPR1, and thus this

protein is highly stable in yeast cells (Fig. 4-14). This appears to result in a NPR1-TGA3 complex unable to activate reporter gene transcription (Fig. 4-13). There are three possible explanations for this: 1) the *Arabidopsis* and *S. cerevisiae* CUL3 ubiquitin ligase are structurally diverse and this protein does not target NPR1 in yeast. 2) NPR1 is not phosphorylated in yeast. 3) a potential adapter protein that couples NPR1 to CUL3 in *Arabidopsis* is not present in yeast. The literature indicates that cullin-containing ubiquitin ligases are evolutionary ancient among eukaryotes (Marín, 2009). Alignment of CUL3 protein sequences from *A. thaliana* (Genbank accession NM_102447.4) and *S. cerevisiae* (Genbank accession NP_011517.1) reveals just ~26% similarity, indicating *S. cerevisiae* CUL3 may not possess the capability to specifically target NPR1. It therefore may be necessary to include AtCUL3 as part of the synthetic circuit. It is thought that NPR1 is phosphorylated by members of the basal transcription machinery it has itself recruited. The GAL4 AD fused to NPR1 should perform this function in yeast, and thus it is likely NPR1 is phosphorylated. This assumption would be confirmed by completing mass spectrometry analysis and/or raising an antibody that specifically recognises modified NPR1. Another explanation is that in *Arabidopsis*, evolution has introduced a plant specific adapter protein that couples NPR1 to CUL3, which is absent in *S. cerevisiae.* Accordingly, NPR1 and *S. cerevisiae* CUL3 are not able to associate and this prevents the proteolysis-coupled cycle that regulates NPR1 (co)activator transcriptional activity in *Arabidopsis.*

5.6.2 Additional regulatory components are required

It has been established that two motifs designated linker-scan (*LS) 5* and *LS7* (collectively referred to as *activating sequence 1* (*as-1*)) in the *PR-1* promoter are *cis*-acting regulatory elements responsive to SA (Lebel et al., 1998). These sites contain the TGA transcription factor core motif TGACG, and with the identification of the NPR1-TGA interaction, it was long assumed this protein interface was/is sufficient for *PR-1* gene expression. However during the course of this Ph.D a number of studies have emerged which indicate transcriptional regulation at the *PR-1* promoter is highly complex. In particular, proteins involved in homologous recombination and DNA repair

are all thought to promote *PR-1* expression, but the exact nature of this process is not clear (Wang et al., 2010; Song et al., 2011). To add further confusion, it has also been reported that NPR1 can activate *PR-1* independent of the TGA binding sites, with a NPR1-WRKY transcription factor interaction the most likely reason (Pape et al., 2010b). Thus it is possible that multiple factors, in addition to NPR1-TGA regulation at *as-1*, are required to activate *PR-1* gene expression. Placing the entire *PR-1* promoter in yeast and aiming to determine an input-output relationship is not practical because the many *cis*-acting elements contained in this region are likely to result in significant background expression. Thus, until the dynamic regulatory processes that take place at the *PR-1* promoter can be dissected, it is not clear what additional components are likely to be required in order to obtain a functional synthetic circuit.

5.7 Conclusions and Future Prospects

Synthetic biology is already a highly established and reliable methodology to understand protein function in the context of system behaviour. We sought to use this discipline to develop a synthetic yeast tool that can be used to understand NPR1-dependent plant immune regulation. Through selective gene disruption we have developed a redox modified yeast strain that can be exploited as a functional chassis. The *Δsfa1yap1yhb1* strain exhibits a highly oxidising intracellular redox environment and thus NPR1 is, by default, assembled in the transcriptionally inactive oligomeric form. By activating GSNOR and TRXh5/NTRA (thus mimicking SA responses in *Arabidopsis*), which both function to promote NPR1 denitrosylation, we have created a redox switch to selectively induce NPR1 monomerisation.

Although many of the regulatory parameters from the synthetic circuit developed in this work are reflective of plant immune circuitry, it was not possible to create a fully functional circuit. The main challenge encountered was activation of the reporter gene. This indicates that an element(s) of plant immune circuitry is missing from the synthetic circuit. The most likely candidate is either a CUL3 ubiquitin ligase able to target NPR1 and/or an unknown adapter protein that couples NPR1 to CUL3 at the promoter, both of

which are essential to promote NPR1-dependent gene transcription in *Arabidopsis* (Spoel et al., 2009). Moreover, as NPR1 monomers are highly stable in *Δsfa1yap1yhb1* under resting conditions (Fig. 4-2) and able to interact with TGA3 (Fig. 4-9), the mechanism in place to degrade NPR1 "escapees" in *Arabidopsis* is either not present or not functional in *S. cerevisiae.* As reporter gene expression should be proportional to monomeric NPR1, this may prove problematic as it would most likely lead to elevated background expression. Presumably, a separate mechanism must be in place to degrade NPR1 "escapees" under resting conditions before this protein can engage transcription. For this to happen, a distinct signal (i.e. other than phosphorylation by members of the basal transcription machinery) or a separate adaptor protein must be present.

Significantly, it may be possible to actually identify these components using this synthetic system. The Cullin3-based ubiquitin ligase is generally known to specifically complex with BTB domain-containing proteins in *Arabidopsis* (Gingerich et al., 2005; Weber et al., 2005). Although NPR1 contains such a domain, there is no direct interaction with CUL3 (Spoel et al., 2009). Thus future work could involve identification of candidate BTB domain-containing proteins encoded by the *Arabidopsis* genome. These candidates could be incorporated into Y2H and/or Co-Immunoprecipitation (Co-Ip) assays to identify an interaction/association with both NPR1 and CUL3. Functional confirmation would be achieved by incorporating such components into the synthetic circuit and observing the removal of NPR1 monomers from *Δsfa1yap1yhb1* (under resting conditions), as well as achieving a robust input-output relationship in terms of reporter gene activation. Such an achievement might represent the next big stride in understanding NPR1 transcriptional regulation. Potential candidates may include the NPR1 paralogs, NPR3 and NPR4, which both contain a characteristic BTB/POZ domain, are important modulators of plant immunity (Zhang et al., 2006) and have been proposed to play an important role in regulating *PR-1* gene expression in *Arabidopsis* (Pape et al., 2010b).

Should an input-output relationship be achieved, then this would allow comprehensive system modelling that will provide a platform for future works. Building a synthetic

circuit and calibrating input device(s), regulatory elements and output(s) through quantitative approaches provides a means to establish predictive paradigms. Such a model may help identify missing elements of plant immune circuitry and/or provide impetus to uncover important defence-related genes concealed in the *Arabidopsis* genome.

In addition, this synthetic circuit could be used to complete high-throughput screens with a view to identifying novel interacting regulatory elements of plant immunity. Although to create the full circuit in *Δsfa1yap1yhb1* seven plasmid constructs were required (two for gene knockout and five for the synthetic circuit) this was designed to specifically leave two commonly used auxotrophic markers intact. As such, this yeast tool could also be used to characterise novel regulatory elements in the context of plant immune circuitry.

CHAPTER 6

6. Bibliography

Aarts, N, Metz M, Holub E, Staskawicz BJ, Daniels MJ, et al. (1998) Different requirements for *EDS1* and *NDR1* by disease resistance genes define at least two *R* gene-mediated signaling pathways in *Arabidopsis*. *Proc. Natl. Acad. Sci. USA* 95:10306–11

Africa Rice Center (WARDA)/FAO/SAA. 2008. NERICA®: the New Rice for Africa – a Compendium. EA Somado, RG Guei and SO Keya (eds.). Cotonou, Benin: Africa Rice Center (WARDA); Rome, Italy: FAO; Tokyo, Japan: Sasakawa Africa Association. 210 pp.

Ajikumar, PK, Xiao WH, Tyo KEJ, Wang Y, Simeon F, Leonard E, Mucha O, Phon TH, Pfeifer B, Stephanopoulos G: (2010) Isoprenoid Pathway Optimization for Taxol Precursor Overproduction in *Escherichia coli*. Science, 330 (6000):70-74.

Aleksic, J., Bizzari F., Cai Y., Davidson B, de Mora K., Ivakhno S., Seshasayee S.L., Nicholson J., Wilson J., Elfick A., French C., Kozma-Bognar L., Ma H. and Millar A. (2007) Development of a novel biosensor for the detection of arsenic in drinking water, IET Synth. Biol. 1, (1–2), pp. 87–90

Andrianantoandro, E, Basu S, Karig D, Weiss R. (2006) Synthetic biology: new engineering rules for an emerging discipline, *Mol Sys Biol* [doi:0.1038/msb4100073]

Apostol, I., Heinstein P.F., Low P.S (1989) Rapid stimulation of an oxidative burst during elicitation of cultured plant cells: role in defense and signal transduction. Plant Physiol 90: 109–116

Arkin, A, (2008) Setting the standard in synthetic biology. *Nat Biotechnol,* 26: 771–774

Arthur, J.R. (2000) The glutathione peroxidases. Cell Mol Life Sci; 57:1825-35.

Asada, K (2006) Production and Scavenging of Reactive Oxygen Species in Chloroplasts and Their Functions Plant Physiology, Vol. 141, pp. 391–396,

Asai, T., Tena, G., Plotnikova, J., Willmann, M. R., Chiu, W.-L., Gomez-Gomez, L., Boller, T., Ausubel, F. M. and Sheen, J. (2002) MAP kinase signalling cascade in *Arabidopsis* innate immunity. Nature 415, 977–983.

Aslund, F., Zheng, M., Beckwith, J., and Storz, G. (1999) Regulation of the OxyR transcription factor by hydrogen peroxide and the cellular thiol-disulfide status. Proc. Natl. Acad. Sci. USA 96, 6161–6165.

Atkinson, M. R., Savageau, M. A., Myers, J. T. and Ninfa, A. J. (2003) Development of genetic circuitry exhibiting toggle switch or oscillatory behavior in *Escherichia coli*. Cell 113, 597–607

Attaran, E., Zeier, T. E., Griebel, T. and Zeier, J. (2009) Methyl salicylate production and jasmonate signaling are not essential for systemic acquired resistance in *Arabidopsis*. The Plant Cell 21, 954–971.

Ausubel, F.M., Brent, R., Kingston, R.E., Moore, D.D., Seidman, J.G., Smith, J.A. and Struhl, K. (1995) Short Protocols in Molecular Biology, John Wiley & Sons, New York.

Barkai, N., and Leibler, S. (2000) Biological rhythms: circadian clocks limited by noise. Nature *403*, 267–268.

Barreiro, L.B, Ben-Ali M, Quach H, Laval G, Patin E, et al. (2009) Evolutionary dynamics of human Toll-like receptors and their different contributions to host defense. PLoS Genet 5: e1000562. doi:10.1371/journal.pgen.1000562

Benhar, M., Forrester M.T., Stamler J.S. (2009) Protein denitrosylation: enzymatic mechanisms and cellular functions. Nat Rev Mol Cell Biol;10: 721–32

Benhar, M., Forrester, M.T., Hess, D. T., and Stamler, J. S. (2008) Regulated protein denitrosylation by cytosolic and mitochondrial thioredoxins. Science 320, 1050–1054.

Benhar, M, Thompson J.W, Moseley M.A, Stamler J.S (2010) Identification of S-nitrosylated targets of thioredoxin using a quantitative proteomic approach. Biochemistry, 49:6963-6969.

Birch, P.R., Boevink, P.C., Gilroy, E.M., Hein, I., Pritchard, L., and Whisson, S.C. (2008). Oomycete RXLR effectors: delivery, functional redundancy and durable disease resistance. Curr Opin Plant Biol 11, 373-379.

Boerjan, W., Ralph, J. and Baucher, M. (2003) Lignin Biosynthesis. Annu. Rev. Plant Biol. 54, 519–546.

Boyle, P., Le Su, E., Rochon, A., Shearer, H.L., Murmu, J., Chu, J.Y., Fobert, P.R., and Després, C. (2009) The BTB/POZ domain of the *Arabidopsis* disease resistance protein NPR1 interacts with the repression domain of TGA2 to negate its function. Plant Cell 21, 3700-3713.

Canton, B, Labno A, Endy D, (2008) Refinement and standardization of synthetic biological parts and devices. *Nat Biotechnol* 26: 787–793

Cao, H, Bowling S.A, Gordon S, Dong X. (1994) Characterization of an *Arabidopsis* mutant that is nonresponsive to inducers of systemic acquired resistance. Plant Cell, 6:1583-1592.

Cao, H., Glazebrook, J., Clarke, J. D., Volko, S. and Dong, X. (1997) The *Arabidopsis* NPR1 gene that controls systemic acquired resistance encodes a novel protein containing ankyrin repeats. Cell 88, 57–63.

Cao, H, Li X, Dong X. (1998) Generation of broad-spectrum disease resistance by overexpression of an essential regulatory gene in systemic acquired resistance. Proc Natl Acad Sci USA, 95:6531-6536.

Carr, P.A and Church G.M. (2009) Genome engineering. *Nat Biotechnol*. 27:1151-1162.

Chaturvedi, R, Krothapalli K, Makandar R, Nandi A, Sparks A.A, Roth MR, Welti R, Shah J (2008) Plastid v3-fatty acid desaturase dependent accumulation of a systemic acquired resistance inducing activity in petiole exudates of *Arabidopsis* thaliana is independent of jasmonic acid. Plant J, 54:106-117.

Chen, L, Xie Q.W, and Nathan C. (1998) Alkyl Hydroperoxide Reductase Subunit C (AhpC) Protects Bacterial and Human Cells against Reactive Nitrogen Intermediates *Mol Cell 1:795–805, pmid:9660963.*

Chen, M.T, and Weiss R., (2005) Artificial cell-cell communication in yeast *Saccharomyces cerevisiae* using signaling elements from *Arabidopsis thaliana*. Nature Biotech. 23, 1551 - 1555

Chen, F. and Dixon RA. (2007) Lignin modification improves fermentable sugar yields for biofuel production. Nat Biotechnol, 25:759-761

Chen, R. Sun S, Wang C, Li Y, Liang Y, An F, Li C, Dong H, Yang X, Zhang J, Zuo J (2009) The *Arabidopsis* PARAQUAT RESISTANT2 gene encodes an S-nitrosoglutathione reductase that is a key regulator of cell death. Cell Res 19:1377–1387

Chern, M.S., Fitzgerald, H.A., Yadav,R.C., Canlas, P.E., Dong, X., and Ronald, P.C. (2001) Evidence for a disease-resistance pathway in rice similar to the NPR1-mediated signaling pathway in *Arabidopsis*. Plant J. 27:101-113.

Chern, M., Fitzgerald, H.A., Canlas, P.E., Navarre, D.A. and Ronald, P.C. (2005) Over-expression of a rice NPR1 homolog leads to constitutive activation of defense response and hypersensitivity to light. Mol. Plant Microbe Interact. 18, 511–520.

Chinchilla, D., Zipfel, C., Robatzek, S., Kemmerling, B., Nurnberger, T., Jones, J. D. G., Felix, G. and Boller, T. (2007) A flagellin-induced complex of the receptor FLS2 and BAK1 initiates plant defence. Nature 448, 497–500.

Coleman, S.T., Epping, E.A., Steggerda, S.M., and Moye-Rowley, W.S. (1999) Yap1p activates gene transcription in an oxidant-specific fashion. Mol. Cell. Biol. 19, 8302–8313.

Coppinger, P, Repetti P.P, Day B, Dahlbeck D, Mehlert A, et al. (2004) Overexpression of the plasma membrane-localized NDR1 protein results in enhanced bacterial disease resistance in *Arabidopsis thaliana*. *Plant J.* 40:225–37

Creissen, G., Firmin, J., Fryer, M., Kular, B., Leyland, M., Reynolds, H., Pastori, G., Wellburn, F., Baker, N.R., Wellburn, A., and Mullineaux, P. (1999) Elevated glutathione biosynthetic capacity in the chloroplasts of transgenic tobacco paradoxically causes increased oxidative stress. The Plant Cell 11, 1277–1291

Dangl, J.L., and Jones, J.D. (2001) Plant pathogens and integrated defence responses to infection. Nature 411, 826-833.

Dawson, B.R, (1985) Data for biochemical research (3rd Ed.) Oxford: Clarendon Press. P. 122

Day, B., Dahlbeck, D. and Staskawicz, B. J. (2006) NDR1 interaction with RIN4 mediates the differential activation of multiple disease resistance pathways in *Arabidopsis. Plant Cell* 18, 2782–2791

de Lorenzo, V and Danchin A, (2008) Synthetic biology: discovering new worlds and new words, EMBO reports, Vol 9, No 9

Delaney, TP, Uknes S, Vernooij B, Friedrich L,Weymann K, et al. (1994) A central role of salicylic acid in plant disease resistance. *Science* 266:1247–50

Delaney, T.P., Friedrich, L., and Ryals, J.A. (1995) *Arabidopsis* Signal Transduction Mutant Defective in Chemically and Biologically Induced Disease Resistance. Proc.Natl.Acad.Sci. U.S.A 92:6602-6606.

Delaunay, A., Isnard, A.D., and Toledano, M.B. (2000) H_2O_2 sensing through oxidation of the Yap1 transcription factor. EMBO J. 19, 5157–5166.

Delaunay, A., Pflieger, D., Barrault, M.B., Vinh, J., and Toledano, M.B. (2002) A thiol peroxidase is an H_2O_2 receptor and redox-transducer in gene activation. Cell 111, 471–481.

Delledonne, M., Xia, Y., Dixon, R.A., and Lamb, C. (1998) Nitric oxide functions as a signal in plant disease resistance. Nature 394, 585-588.

Delledonne, M., Zeier, J., Marocco, A., and Lamb, C. (2001) Signal interactions between nitric oxide and reactive oxygen intermediates in the plant hypersensitive disease resistance response. Proc Natl Acad Sci U S A 98, 13454-13459.

Desikan, R, A-H Mackerness S, Hancock JT, Neill SJ. (2001) Regulation of the *Arabidopsis* transcriptome by oxidative stress. *Plant Physiol.* 127:159–72

Després, C, DeLong C, Glaze S, Liu E, Fobert P.R (2000) The *Arabidopsis* NPR1/NIM1 protein enhances the DNA binding activity of a subgroup of the TGA family of bZIP transcription factors. Plant Cell, 12:279-290.

Diaz, M, Achkor H, Titarenko E, Martinez MC. (2003) The gene encoding glutathione-dependent formaldehyde dehydrogenase/ GSNO reductase is responsive to wounding, jasmonic acid and salicylic acid. FEBS Letters 543, 136–139.

Dodd, A.N., Salathia, N., Hall, A., Kevei, E., Toth, R., Nagy, F., Hibberd, J.M., Millar, A.J., and Webb, A.A. (2005) Plant circadian clocks increase photosynthesis, growth, survival, and competitive advantage. Science 309, 630–633.

Dodds, P.N. and Rathjen, J.P. (2010) Plant immunity: Towards an integrated view of plant-pathogen interactions. *Nature 11*, 539–548.

Durrant, WE, Dong X. (2004) Systemic acquired resistance. *Annu. Rev. Phytopathol.* 42:185–209

Durrant, W.E., Wang, S., and Dong, X. (2007) *Arabidopsis* SNI1 and RAD51D regulate both gene transcription and DNA recombination during the defense response. Proc. Natl. Acad. Sci. USA 104, 4223-4227.

Edgerton, M.D (2009) Increasing Crop Productivity to Meet Global Needs for Feed, Food, and Fuel Plant Physiology , Vol. 149, pp. 7–13,

Elowitz, M. B. & Leibler, S. (2000). A synthetic oscillatory network of transcriptional regulators. Nature 403, 335–-338

Elowitz, M and Lim W.A. (2010) Build life to understand it. *Nature.*; 468 (7326):889–890. doi: 10.1038/468889a.

Endy D, (2005) Foundations for engineering biology. *Nature* 438: 449–453

Enserink, M. (2005) Infectious diseases: Source of new hope against malaria is in short supply. Science 307, 33

Erwin, P. A., Lin, A. J., Golan, D. E. & Michel, T. (2005) Receptor-regulated dynamic *S*-nitrosylation of endothelial nitric-oxide synthase in vascular endothelial cells. *J. Biol. Chem.* 280, 19888–19894

Falk, A., Feys, B.J., Frost, L.N., Jones, J.D., Daniels, M.J. and Parker, J.E. (1999) EDS1, an essential component of R gene-mediated disease resistance in *Arabidopsis* has homology to eukaryotic lipases. Proc. Natl Acad. Sci. USA, 96(6), 3292–3297.

Fan, W. and Dong, X. (2002). In vivo interaction between NPR1 and transcription factor TGA2 leads to salicylic acid-mediated gene activation in Arabidopsis. The Plant Cell 14, 1377–1389.

FAO - Food and Agriculture Organization of the United Nations (2009) http://www.fao.org/news/story/en/item/35571/

Feechan, A, Kwon E, Yun B.W, Wang Y, Pallas J.A. and Loake G. J. (2005) A central role for *S*-nitrosothiols in plant disease resistance. *Proc Natl Acad Sci USA* 102:8054-8059.

Feys, BJ, Moisan LJ, Newman MA, Parker JE (2001) Direct interaction between the *Arabidopsis* disease resistance signaling proteins, EDS1 and PAD4. Embo J 20: 5400–5411.

Feys, BJ, Wiermer M, Bhat RA, Moisan LJ, Medina-Escobar N, et al. (2005) *Arabidopsis* SENESCENCE-ASSOCIATED GENE101 stabilizes and signals within an ENHANCED DISEASE SUSCEPTIBILITY1 complex in plant innate immunity. Plant Cell 17: 2601–2613.

Foster, M.W, Liu L, Zeng M, Hess D.T, Stamler J.S. (2009) A genetic analysis of nitrosative stress. *Biochemistry.* 48:792–799

Fox, J.E, Bridgham J.T, Bovee T.F, Thornton J.W. (2007) An evolvable oestrogen receptor activity sensor: development of a modular system for integrating multiple genes into the yeast genome. *Yeast*, 24:379-390.

Fu C, Mielenz J.R, Xiao X, Ge Y, Hamilton C.Y, Rodriguez M, Chen F, Foston M, Ragauskas A, Bouton J, Dixon R. A, and Wang Z.Y (2011) Genetic manipulation of lignin reduces recalcitrance and improves ethanol production from switchgrass. Proceedings of the National Academy of Sciences 108(9):3803-3808.

Fidock, D.A. (2010) Priming the antimalarial pipeline. Nature, 465:297-298.

Fritz-Laylin, L.K, Krishnamurthy N, Tor M, Sjolander K.V, Jones J.D.G (2005) Phylogenomic analysis of the receptor-like proteins of rice and *Arabidopsis*. Plant Physiol, 138:611-623.

Gaffney, T, Friedrich L, Vernooij B, Negrotto D, Nye G, et al. (1993). Requirement of salicylic acid for the induction of systemic acquired resistance. *Science* 261:754–56

García, A.V., Blanvillain-Baufumé, S., Huibers, R.P., Wiermer, M., Li, G., Gobbato, E., Rietz, S., and Parker, J.E. (2010) Balanced nuclear and cytoplasmic activities of EDS1 are required for a complete plant innate immune response. PLoS Pathog. 6, e1000970.

Garcion, C, Lohman A, Lamodiere E, Catinot J, Buchala A, et al. (2008) Characterization and biological function of the *ISOCHORISMATE SYNTHASE 2* gene of *Arabidopsis thaliana*. *Plant Physiol.* 147:1279–87

Gardner, T.S., Cantor, C.R. and Collins, J.J. (2000) Construction of a genetic toggle switch in *Escherichia coli*. Nature 403, 339–-342

Garreton, V, Carpinelli J, Jordana X, Holuigue L. (2002) The as-1 promoter element is an oxidative stress-responsive element and salicylic acid activates it via oxidative species. *Plant Physiol.* 130:1516–26

Gasch, A.P., Spellman, P.T., Kao, C.M., Carmel-Harel, O., Eisen, M.B., Storz, G., Botstein, D., and Brown, P.O. (2000) Genomic expression programs in the response of yeast cells to environmental changes. Mol. Biol. Cell 11, 4241– 4257.

Gelhaye, E., Rouhier, N. and Jacquot, J. P. (2004) The thioredoxin *h* system of higher plants. Plant Physiol. Biochem. 42 ,265-271.

Gibson, D.G., Benders G.A., Andrews-Pfannkoch C., Denisova E.A. , Baden-Tillson H., Zaveri J., Stockwell T. B.,.Brownley A, Thomas D. W., Algire M. A., Merryman C., Young L., Noskov V. N., Glass J. I., Venter J. C., Hutchison C. A. III, Smith H. O., (2008) Complete Chemical Synthesis, Assembly, and Cloning of a Mycoplasma genitalium Genome, *Science* 319, 1215.

Gibson, D. G., Glass, J. I., Lartigue, C., Noskov, V. N., Chuang, R. Y., Algire, M. A., Benders, G. A., Montague, M. G., Ma, L., Moodie, M. M., et al. (2010) Creation of a bacterial cell controlled by a chemically synthesized genome. Science 329, 52–56.

Gietz, R.D. and R.A. Woods. (2002) Transformation of yeast by lithium acetate/single-stranded carrier DNA/polyethylene glycol method. Methods in Enzymology 350: 87-96.

Hart, T.W. (1985) Some observations concerning the S-nitroso and S-phenylsulphonyl derivatives of L-cysteine and glutathione. Tetrahedron Lett., 26, 2013-2016.

Glazebrook, J., Rogers, E.E., and Ausubel, F.M. (1996) Isolation of *Arabidopsis* mutants with enhanced disease susceptibility by direct screening. Genetics 143:973-982.

Grant, C.M, MacIver F.H, Dawes I.W . (1997) Glutathione synthetase is dispensable for growth under both normal and oxidative stress conditions in the yeast *Saccharomyces cerevisiae* due to an accumulation of the dipeptide gamma-glutamylcysteine. Mol Biol Cell 8(9):1699-707

Grant, C.M. (2001) Role of the glutathione/glutaredoxin and thioredoxin systems in yeast growth and response to stress conditions. Mol. Microbiol.39:533–541

Gingerich, D.J, Gagne J.M, Salter D.W, Hellmann H, Estelle M, Ma L, Vierstra R.D. (2005) Cullins 3a and 3b assemble with members of the broad complex/tramtrack/bric-a-brac (BTB) protein family to form essential ubiquitin-protein ligases (E3s) in *Arabidopsis*. *J Biol Chem*, 280:18810-18821.

Greco, T.M, Hodara R, Parastatidis I, Heijnen HF, Dennehy M.K, Liebler D.C, et al. (2006) Identification of S-nitrosylation motifs by site-specific mapping of the S-nitrosocysteine proteome in human vascular smooth muscle cells. Proc Natl Acad Sci U S A;103:7420–5.

Gridley, H.E, Jones M.P and Wopereis-Pura M (2002) Development of New Rice for Africa (NERICA) and participatory varietal selection. West Africa Rice Association (WARDA), Bouake, Côte d'Ivoire.

Gygi, S., Rochon, Y., Franza, B. R. & Aebersold, R. Correlation between protein and mRNA abundance in yeast. *Mol. Cell. Biol.* 19, 1720–1730 (1999).

Hager, G.L., McNally, J.G., and Misteli, T. (2009). Transcription dynamics. Mol. Cell 35, 741-753.

Hao, G. Derakhshan B, Shi L, Campagne F, Gross SS. (2006) SNOSID, a proteomic method for identification of cysteine S-nitrosylation sites in complex protein mixtures. Proc Natl Acad Sci 103:1012–7.

Hanson, G. T., Aggeler, R., Oglesbee, D., Capaldi, R. A., Tsien, R. Y., and Remington, S. J. (2004) Investigating Mitochondrial Redox Potential with Redox-sensitive Green Fluorescent Protein Indicators *J. Biol. Chem.* 279, 13044-13053

Hess, D.T, Matsumoto A, Kim S.O, Marshall H.E, Stamler J.S (2005). Protein S-nitrosylation: purview and parameters. Nat Rev Mol Cell Biol, 6:150-166.

Higashi, K, Ishiga Y, Inagaki Y, Toyoda K, Shiraishi T, Ichinose Y (2008) Modulation of defense signal transduction by flagellin-induced WRKY41 transcription factor in *Arabidopsis thaliana*. Mol Genet Genomics 279: 303–312

Horan, S., Bourges, I., Meunier, B., (2006). Transcriptional response to nitrosative stress in *Saccharomyces cerevisiae*. Yeast 23, 519–535.

Hwang, C, Sinskey, A.J., and H.F. Lodish. (1992). Oxidized redox state of glutathione in the endoplasmic reticulum. *Science.* 257:1496–1502.

Ikeda, R., G.S. Khush and R.E. Tabien, (1990) A new resistance gene to bacterial blight derived from *O. longistaminata*. Jpn. J. Breed. 40: 280-281.

Ingle, R.A., Carstens, M., and Denby, K.J. (2006) PAMP recognition and the plantpathogen arms race. Bioessays 28, 880-889.

Into, T. Inomata M, Nakashima M, Shibata K, Häcker H, Matsushita K. (2008) Regulation of MyD88-dependent signalling events by *S* nitrosylation retards toll-like receptor signal transduction and initiation of acute-phase immune responses. *Mol. Cell. Biol.* 28, 1338–1347

Ishihara, T., Sekine, K.-T., Hase, S., Kanayama, Y., Seo, S., Ohashi, Y., Kusano, T., Shibata, D., Shah, J. and Takahashi, H. (2008) Overexpression of the *Arabidopsis thaliana* EDS5 gene enhances resistance to viruses. Plant Biology 10, 451–461.

Iwai, K, Naganuma A, and Kuge S (2010) Peroxiredoxin Ahp1 Acts as a Receptor for Alkylhydroperoxides to Induce Disulfide Bond Formation in the Cad1 Transcription Factor. *J. Biol. Chem*. 285, 10597–10604.

Izawa, S., Inoue, Y., and Kimura, A. (1995) Oxidative stress response in yeast: effect of glutathione on adaptation to hydrogen peroxide stress in *Saccharomyces cerevisiae.* FEBS Lett. *368*, 73–76.

Jaffrey, S. R. & Snyder, S. H. (2001) The biotin switch method for the detection of *S*-nitrosylated proteins. Sci. STKE, Issue 86, p. pl1.

Jakoby, M., Weisshaar, B., Droge-Laser, W., Vicente-Carbajosa, J., Tiedemann, J., Kroj, T. and Parcy, F. (2002) bZIP transcription factors in *Arabidopsis*. Trends in Plant Science. 7, 106–111.

Jiang, K., Schwarzer, C., Lally, E., Zhang, S., Ruzin, S., Machen, T., Remington, S.J. and Feldman, L. (2006) Expression and characterization of a redox-sensing green fluorescent protein (reduction-oxidation-sensitive green fluorescent protein) in *Arabidopsis*. Plant Physiol. 141, 397–403.

Jirage, D., Tootle, T.L., Reuber, T.L., Frost, L.N., Feys, B.J., Parker, J.E., Ausubel, F.M. and Glazebrook, J. (1999) *Arabidopsis thaliana* PAD4 encodes a lipase-like gene that is important for salicylic acid signaling. Proc. Natl Acad. Sci. USA, 96(23), 13583–13588.

Johnson, C., Boden, E. and Arias, J. (2003) Salicylic acid and NPR1 induce the recruitment of trans-activating TGA factors to a defense gene promoter in *Arabidopsis*. Plant Cell 15, 1846–1858.

Johnson, C., Mhatre A., Arias J., (2008) NPR1 preferentially binds to the DNA-inactive form of *Arabidopsis* TGA2, Biochimica et Biophysica Acta 1779 583–589

Jones, J.D. & Dangl, J.L. (2006) The plant immune system. Nature. 444, 323–329

Jung, H. W., Tschaplinski, T. J., Wang, L., Glazebrook, J. and Greenberg, J. T. (2009) Priming in systemic plant immunity. Science 324, 89–91.

Kale, S.D., Gu, B., Capelluto, D.G., Dou, D., Feldman, E., Rumore, A., Arredondo, F.D., Hanlon, R., Fudal, I., Rouxel, T., Lawrence, C.B, Shan, W., Tyler, B.M. (2010). External lipid PI3P mediates entry of eukaryotic pathogen effectors into plant and animal host cells. Cell 142, 284–295.

Kang, H.G, and Klessig D.F (2005) Salicylic acid-inducible *Arabidopsis* CK2-like activity phosphorylates TGA2. Plant Mol Biol 57: 541–557

Kaminaka, H., Nake, C., Epple, P., Dittgen, J., Schutze, K., Chaban, C., Holt, B.F., 3rd, Merkle, T., Schafer, E., Harter, K., and Dangl, J.L. (2006) bZIP10-LSD1 antagonism modulates basal defense and cell death in *Arabidopsis* following infection. Embo J 25, 4400- 4411.

Keasling, J.D. (2010). Manufacturing Molecules through Metabolic Engineering. *Science* 330 (6009):1355–1358.

Kesarwani, M., Yoo, J., and Dong, X. (2007) Genetic interactions of TGA transcription factors in the regulation of pathogenesis-related genes and disease resistance in *Arabidopsis*. Plant Physiol. 144, 336-346.

Khalil, A.S and Collins J.J. (2010) Synthetic biology: applications come of age. Nat Rev Genet.;11 (5):367–379.

Khush, G.S., E. Bacalangco and T. Ogawa, (1990) A new gene for resistance to bacterial blight from *O. longistaminata*. Rice Genetics Newsletter 7: 121-122.

Kim, H.S, and Delaney T.P, (2002) Over-expression of TGA5, which encodes a bZIP transcription factor that interacts with NIM1/NPR1, confers SAR independent resistance in *Arabidopsis thaliana* to *Peronospora parasitica*. Plant J 32: 151–163

Kim, K.-C., Lai, Z., Fan, B. and Chen, Z. (2008) *Arabidopsis* WRKY38 and WRKY62 transcription factors interact with histone deacetylase 19 in basal defense. The Plant Cell 20, 2357–2371.

Kinkema, M, Fan W, Dong X. (2000) Nuclear localization of NPR1 is required for activation of PR gene expression. Plant Cell, 12:2339-2350.

Knoth, C, Ringler J, Dangl JL, Eulgem T (2007) *Arabidopsis* WRKY70 is required for full RPP4-mediated disease resistance and basal defense against Hyaloperonospora parasitica. Mol Plant Microbe Interact 20: 120–128

Kobayashi, H, Kaern M, Araki M, Chung K, Gardner T.S, Cantor C.R, Collins J.J, (2004) Programmable cells: interfacing natural and engineered gene networks. Proc Natl Acad Sci USA 101: 8414–8419

Kodadek, T, Sikder D, Nalley K. (2006) Keeping transcriptional activators under control. Cell 127: 261–264.

Kohler, A., Schwindling, S., and Conrath, U. (2002) Benzothiadiazole-induced priming for potentiated responses to pathogen infection, wounding, and infiltration of water into leaves requires the NPR1/NIM1 gene in *Arabidopsis*. Plant Physiol. 128, 1046-1056.

Koornneef, A, Leon-Reyes A, Ritsema T, Verhage A, Den Otter FC, Van Loon LC, Pieterse CMJ: (2008) Kinetics of salicylate-mediated suppression of jasmonate signalling reveal a role for redox modulation. Plant Physiol, 147:1358-1368.

Kuge, S., and Jones, N. (1994) YAP1 dependent activation of TRX2 is essential for the response of *Saccharomyces cerevisiae* to oxidative stress by hydroperoxides. EMBO J. 13, 655–664.

Kuge, S., Jones, N., and Nomoto, A. (1997) Regulation of yAP-1 nuclear localization in response to oxidative stress. EMBO J. 16, 1710–1720.

Kuge, S., Toda, T., Iizuka, N., and Nomoto, A. (1998) Crm1 (XpoI) dependent nuclear export of the budding yeast transcription factor yAP-1 is sensitive to oxidative stress. Genes Cells 3, 521–532.

Laloi, C., Mestres-Ortega D., Marco Y., Meyer Y. and Reichheld J.P. (2004) The *Arabidopsis* cytosolic thioredoxin *h5* gene induction by oxidative stress and its W-Box-mediated response to pathogen elicitor. *Plant Physiology* 134, 1006–1016.

Lawton, K, Weymann K, Friedrich L, Vernooij B, Uknes S, et al. (1995) Systemic acquired resistance in *Arabidopsis* requires salicylic acid but not ethylene. *Mol. Plant-Microbe Interact.* 8:863–70

Lawton, K.A., Friedrich, L., Hunt, M., Weymann, K., Delaney, T., Kessmann, H., Staub, T., and Ryals, J. (1996) Benzothiadiazole induces disease resistance in *Arabidopsis* by activation of the systemic acquired resistance signal transduction pathway. Plant J 10, 71-82.

Le Novère, N, Hucka, M, Mi, H, Moodie, S, Schreiber, F, Sorokin, A, Demir, E, Wegner, K, Aladjem, M.I, Wimalaratne, S.M, et al. (2009) The Systems Biology Graphical Notation. *Nature Biotechnology*. 27:735–741.

Lebel, E., Heifetz, P., Thorne, L., Uknes, S., Ryals, J., and Ward, E. (1998) Functional analysis of regulatory sequences controlling *PR-1* gene expression in *Arabidopsis*. Plant J. 16, 223-233.

Lee, C., Lee, S.M., Mukhopadhyay, P., Kim, S.J., Lee, S.C., Ahn, W.S., Yu, M.H., Storz, G., and Ryu, S.E. (2004) Redox regulation of OxyR requires specific disulfide bond formation involving a rapid kinetic reaction path. Nat. Struct. Mol. Biol. 11, 1179–1185.

Lee, E. K. Jin Y. W. Park J. H. Yoo Y. M. Hong S. M. Amir R. Yan Z. Kwon E. Elfick A. Tomlinson S.; Halbritter F. Waibel T. Yun B. W. & Loake G. J. (2010) Cultured Cambial Meristematic Cells as a Source of Plant Natural Products. Nature Biotechnology, Vol.28, No.11, pp 1213-1217

Lehti-Shiu, M. D., Zou, C., Hanada, K. & Shiu, S.-H. (2009) Evolutionary history and stress regulation of plant receptor-like kinase/pelle genes. *Plant Physiol.* 150, 12–26

Leskinen, P., Virta M., and Karp M. (2003) One-step measurement of firefly luciferase activity in yeast. *Yeast*; 20: 1109–1113.

Levskaya, A., Weiner, O.D., Lim, W.A., and Voigt, C.A. (2009) Spatiotemporal control of cell signalling using a light-switchable protein interaction. Nature 461, 997–1001.

Lillig, C.H., and Holmgren, A. (2007) Thioredoxin and related molecules from biology to health and disease. Antioxid. Redox Signal. 9, 25–47.

Lillig, CH, Berndt C, Holmgren A. (2008) Glutaredoxin systems.. Biochimica et Biophysica Acta;1780:1304-17.

Lin, W.C., Lu, C.F., Wu, J.W., Cheng, M.L., Lin, Y.M., Yang ,N.S., Black, L., Green, S.K., Wang, J.F., and Cheng, C.P. (2004) Transgenic tomato plants expressing the *Arabidopsis* NPR1 gene display enhanced resistance to a spectrum of fungal and bacterial diseases. Transgenic Res. 13:567-581.

Lindermayr, C, Saalbach G, Durner J. (2005) Proteomic identification of S-nitrosylated proteins in *Arabidopsis*. Plant Physiology 137, 921–930.

Li, X., Zhang, Y., Clarke, J.D., Li, Y., and Dong, X. (1999) Identification and cloning of a negative regulator of systemic acquired resistance, SNI1, through a screen for suppressors of npr1-1. Cell 98, 329-339.

Li, J., Brader, G. and Palva, E. T. (2004) The WRKY70 transcription factor: A node of convergence for jasmonate-mediated and salicylate-mediated signals in plant defense. The Plant Cell 16, 319–331.

Li, J., Brader, G., Kariola, T. and Palva, E. T. (2006) WRKY70 modulates the selection of signaling pathways in plant defense. The Plant Journal 46, 477–491.

Lindermayr, C., Sell, S., Muller, B., Leister, D., and Durner, J. (2010) Redox regulation of the NPR1-TGA1 system of *Arabidopsis thaliana* by nitric oxide. Plant Cell 22, 2894-2907.

Lipke, P. N. and R. Ovalle, (1998) Cell wall architecture in yeast: new structure and new challenges. J. Bacteriol. 180:3735-3740

Liu, L., Zeng, M., Hausladen, A., Heitman, J., and Stamler, J. S. (2000) Protection from nitrosative stress by yeast flavohemoglobin. *Proc. Natl. Acad. Sci. U.S.A. 97*, 4672–4676.

Liu, L., Hausladen A, Zeng M, Que L, Heitman J, Stamler JS. (2001) A metabolic enzyme for S-nitrosothiol conserved from bacteria to humans. Nature 410, 490–494.

Liu, P.P, Yang Y, Pichersky E, Klessig D.F. (2010) Altering expression of benzoic acid/salicylic acid carboxyl methyltransferase 1 compromises systemic acquired resistance and PAMP-triggered immunity in *Arabidopsis*. Mol Plant Microbe Interact 23: 82–90

Liu, P.P, von Dahl C.C, Park S.W, and Klessig D.F (2011) Interconnection between Methyl Salicylate and Lipid-Based Long-Distance Signaling during the Development of Systemic Acquired Resistance in *Arabidopsis* and Tobacco. Plant Physiology Vol. 155, pp. 1762–1768

Locke, J.C., Millar, A.J., and Turner, M.S. (2005) Modelling genetic networks with noisy and varied experimental data: the circadian clock in *Arabidopsis thaliana*. J. Theor. Biol. 234, 383–393.

Locke, J.C., Kozma-Bognar, L., Gould, P.D., Feher, B., Kevei, E., Nagy, F., Turner, M.S., Hall, A., and Millar, A.J. (2006) Experimental validation of a predicted feedback loop in the multi-oscillator clock of *Arabidopsis thaliana*. Mol. Syst. Biol. 2, 59.

Lushchak, O., Nykorak, N., Ohdate, T., Inoue, Y., Lushchak, V. (2009) Inactivation of Genes Encoding Superoxide Dismutase Modifies Yeast Response to S-Nitrosoglutathione-Induced Stress, *Biochemistry (Mosc)*, 74: 445-451.

Mackey, D., Belkhadir, Y., Alonso, J. M., Ecker, J. R. & Dangl, J. (2003) *Arabidopsis* RIN4 is a target of the type III virulence effector AvrRpt2 and modulates RPS2-mediated resistance. *Cell* 112, 379–389

Mackey, D., Holt, B. F., Wiig, A. & Dangl, J. L. (2002) RIN4 interacts with *Pseudomonas syringae* type III effector molecules and is required for RPM1-mediated resistance in *Arabidopsis. Cell* 108, 743–754

Madeo, F., Frohlich, E., Ligr, M., Grey, M., Sigrist, S. J., Wolf, D. H., and Frohlich, K. U. (1999) Oxygen stress: a regulator of apoptosis in yeast. J. Cell Biol. *145*, 757–767.

Maier, F, Zwicker S, Huckelhoven A, Meissner M, Funk J, Pfitzner A.J.P. and Pfitzner U.M. (2011) NONEXPRESSOR OF PATHOGENESIS-RELATED PROTEINS1 (NPR1) and some NPR1-related proteins are sensitive to salicylic acid. Mol. Plant Pathol. 12:73–91

Malamy, J. Carr J.P, Klessig D.F, Raskin I. (1990) Salicylic acid: a likely endogenous signal in the resistance response of tobacco to viral infection. *Science* 250:1002–4

Maldonado, A.M, Doerner P, Dixon R.A, Lamb C.J, Cameron R.K: (2002) A putative lipid transfer protein involved in systemic resistance signalling in *Arabidopsis*. Nature, 419:399-403.

Mao, P., Duan, M., Wei, C., and Li, Y. (2007) WRKY62 transcription factor acts downstream of cytosolic NPR1 and negatively regulates jasmonate-responsive gene expression. Plant Cell Physiol. 48 833–842.

Marino, S.M. and Gladyshev V.N. (2010) Structural analysis of cysteine S-nitrosylation: a modified acid-based motif and the emerging role of trans-nitrosylation, J. Mol. Biol. 395 844–859.

Marín, I (2009) Diversification of the cullin family. BMC Evolutionary Biology, 9:267

Maris, A. F., Kern, A. L., Picada, J. N., Boccardi, F., Brendel, M., and Henriques, J. A. (2000) Glutathione, but not transcription factor Yap1, is required for carbon source-dependent resistance to oxidative stress in *Saccharomyces cerevisiae.* Curr. Genet. *37*, 175–182.

Marshall, H. E. & Stamler, J. S. (2001) Inhibition of NF-κB by *S*-nitrosylation. *Biochemistry* 40, 1688–1693

Martin, V. J., Pitera, D. J., Withers, S. T., Newman, J. D. & Keasling, J. D. (2003) Engineering a mevalonate pathway in *Escherichia coli* for production of terpenoids. Nature Biotech. 21, 796–802

Martínez, A.T., Ruiz-Dueñas, F.J., Martínez, M.J., del Río, J.C., and Gutiérrez, A. (2009) Enzymatic delignification of plant cell wall: from nature to mill. *Curr Opin Biotechnol* 20: 348–357.

Marty, L, Siala W, Schwarzlander M, Fricker M.D, Wirtz M, Sweetlove L.J, Meyer Y, Meyer A.J, Reichheld J.P and Hell R: (2009) The NADPH-dependent thioredoxin system constitutes a functional backup for cytosolic glutathione reductase in *Arabidopsis*. Proc Natl Acad Sci USA, 106:9109-9114.

Mateo, A, Funck D, Mulhlenbock P, Kular B, Mullineaux P.M, Karpinski S. (2006) Controlled levels of salicylic acid are required for optimal photosynthesis and redox homeostasis. J Exp Bot, 57:1795-1807

McBean, G.J. (2011) The transsulfuration pathway: a source of cysteine for glutathione in astrocytes Amino Acids. DOI: 10.1007/s00726-011-0864-8

Melcher, K., B. Sharma, W. V. Ding and Nolden M., (2000) *Zero background yeast reporter plasmids*. Gene 247: 53–61

Meyer, A.J. and Brach, T. (2009) Dynamic redox measurements with redox-sensitive GFP in plants by confocal laser scanning microscopy. Methods Mol. Biol. 479, 93–107

Meyer, Y, Buchanan BB, Vignols F, Reichheld JP. (2009) Thioredoxins and glutaredoxins: Unifying elements in redox biology. Annu Rev Genet 43:335–367.

Mishina, T.E., and Zeier, J. (2007) Pathogen-associated molecular pattern recognition rather than development of tissue necrosis contributes to bacterial induction of systemic acquired resistance in *Arabidopsis*. Plant J. 50: 500–513.

Moershbacher, B., Noll, U., Gorrichon, L. and Reisener, H. J. (1990) Specific Inhibition of Lignification Breaks Hypersensitive Resistance of Wheat to Stem Rust *Plant Physiol.* 93, 465–470.

Moore, J.W, Loake, G.J, Spoel, S.H. (2011) Transcription dynamics in plant immunity. Plant Cell, 28, 2809-2820

Mosher, R.A., Durrant, W.E., Wang, D., Song, J., and Dong, X. (2006) A comprehensive structure-function analysis of *Arabidopsis* SNI1 defines essential regions and transcriptional repressor activity. Plant Cell 18, 1750-1765.

Mou, Z., Fan, W., and Dong, X. (2003) Inducers of plant systemic acquired resistance regulate NPR1 function through redox changes. Cell 113, 935-944.

Mukhtar, M. S, Carvunis A.R, Dreze M, Epple P, Steinbrenner J, Moore J, Tasan M, Galli M, Hao T. *et al.,* (2011) Independently Evolved Virulence Effectors Converge onto Hubs in a Plant Immune System Network. *Science* 333, 596 DOI: 10.1126/science.1203659

Mur, L.A.J, Kenton P, Atzorn R, Miersch O,Wasternack C. (2006) The outcomes of concentration-specific interactions between salicylate and jasmonate signaling include synergy, antagonism, and oxidative stress leading to cell death. *Plant Physiol.* 140:249–62

Mustacich, D. and Powis G., (2000) Thioredoxin reductase. Biochem. J. 346, 1-8

Ndamukong, I., Al Abdallat, A., Thurow, C., Fode, B., Zander, M., Weigel, R. and Gatz, C. (2007) SA-inducible *Arabidopsis* glutaredoxin interacts with TGA factors and suppresses JA-responsive PDF1.2 transcription. The Plant Journal 50, 128–139.

Nandi, A, Welti R, Shah J (2004) The *Arabidopsis thaliana* dihydroxyacetone phosphate reductase gene SUPPRESSOR OF FATTY ACID DESATURASE DEFICIENCY 1 is required for glycerolipid metabolism and for the activation of systemic acquired resistance. Plant Cell, 16:465-477.

Nawrath, C. and Me´traux, J.-P. (1999) Salicylic acid induction-deficient mutants of *Arabidopsis* express PR-2 and PR-5 and accumulate high levels of camalexin after pathogen inoculation. The Plant Cell 11, 1393–1404.

Nawrath, C., Heck, S., Parinthawong, N. and Metraux, J.-P. (2002) EDS5, an essential component of salicylic acid-dependent signaling for disease resistance in *Arabidopsis*, is a member of the MATE transporter family. The Plant Cell 14, 275–286.

Noctor, G, Gomez L, Vanacker H, Foyer CH. (2002) Interactions between biosynthesis, compartmentation and transport in the control of glutathione homeostasis and signalling. Journal of Experimental Botany 53, 1283–1304.

Nurnberger, T., and Lipka, V. (2005) Non-host resistance in plants: new insights into an old phenomenon. Mol Plant Pathol 6, 335-345.

Oerke, E.C., Dehne H.W. (2004) Safeguarding production—losses in major crops and the role of crop protection Crop Protection 23 275–285

Ohtake, Y and Yabuuchi S. (1991) Molecular cloning of the gamma-glutamylcysteine synthetase gene of *Saccharomyces cerevisiae*. Yeast 7(9):953-61

Østergaard, H, Tachibana C, Winther JR. (2004). Monitoring disulfide bond formation in the eukaryotic cytosol. *J. Cell Biol.* 166:337–45

Pandey, SP, Somssich IE. (2009) The role of WRKY transcription factors in plant immunity. *Plant Physiol*, 150(4):1648-55.

Pape, S., Thurow C., and Gatz C. (2010a) Exchanging the *as-1*-like element of the *PR-1* promoter by the *as-1* element of the CaMV *35S* promoter abolishes salicylic acid responsiveness and regulation by NPR1 and SNI1. Plant Signaling & Behavior 5:12, 1669-1671

Pape, S., Thurow, C., and Gatz, C. (2010b) The *Arabidopsis PR-1* promoter contains multiple integration sites for the coactivator NPR1 and the repressor SNI1. Plant Physiol. 154, 1805-1818.

Park, S. W., Kaimoyo, E., Kumar, D., Mosher, S. and Klessig, D. F. (2007) Methyl salicylate is a critical mobile signal for plant systemic acquired resistance. Science 318, 113–116.

Peng, Y., Bartley, L.E., Chen, X., Dardick, C., Chern, M., Ruan, R., *et al*. (2008) OsWRKY62 is a negative regulator of basal and Xa21-mediated defense against *Xanthomonas oryzae* pv. *oryzae* in rice. *Mol Plant* 1: 446–458.

Peng, Y., Bartley, L.E., Canlas, P., and Ronald, P.C. (2010) OsWRKY IIa transcription factors modulate rice innate immunity. *Rice* 3: 36–42.

Pérez-Mato, I., Castro, C., Ruiz, F. A., Corrales, F. J. & Mato, J. M. (1999) Methionine adenosyltransferase *S*-nitrosylation is regulated by the basic and acidic amino acids surrounding the target thiol. *J. Biol. Chem.* 274, 17075–17079

Pieterse, C.M.J., Leon-Reyes, A., Van der Ent, S., and Van Wees, S. C.M. (2009) Networking by small-molecule hormones in plant immunity. Nat. Chem. Biol. 5: 308–316.

Pontier, D., Miao, Z.-H., and Lam, E. (2001) Trans-dominant suppression of plant TGA factors reveals their negative and positive roles in plant defense responses. Plant J. 27, 529–538.

Pogány, M., von Rad, U., Grün, S., Dongó, A., Pintye, A., Simoneau, P., Bahnweg, G., Kiss, L., Barna, B., Durner, J. (2009) Dual Roles of Reactive Oxygen Species and NADPH Oxidase RBOHD in an *Arabidopsis-Alternaria* Pathosystem. *Plant Physiol.* 151:1459-1475.

Purnick, P, and Weiss R. (2009) The second wave of synthetic biology: from modules to systems. *Nature Reviews Molecular Cell Biology*, 10(6):410-422.

Quentin, M., Allasia, V., Pegard, A., Allais, F., Ducrot, P.-H., Favery, B., Levis, C., Martinet, S., Masur, C., Ponchet, M., Roby, D., Schlaich, N. L., Jouanin, L., and Ketter, H. (2009). Imbalanced lignin biosynthesis promotes the sexual reproduction of homothallic oomycete pathogens. PLoS Pathog. 5:e1000264.

Ragauskas, A.J, Nagy M, Kim D.H, Eckert C.A, Hallet J.P, Liotta C.L (2006) From wood to fuels. Integrating biofuels and pulp production. Ind Biotechnol, 2:55-65.

Riechmann, J.L. *et al.* (2000) *Arabidopsis* transcription factors: genome-wide comparative analysis among eukaryotes. *Science* 290, 2105–2110

Rizzo MA, Springer GH, Granada B, Piston DW (2004) An improved cyan fluorescent protein variant useful for FRET. Nat Biotechnol, 22:445-449.

Reichheld, J.P., Mestres-Ortega D., Laloi C., Meyer Y., (2002) The multigenic family of thioredoxin *h* in *Arabidopsis thaliana*: specific expression and stress response, Plant Physiol. Biochem. 40 685–690.

Ro, D.K, Paradise E.M, Ouellet M, Fisher K.J, Newman K.L, Ndungu J.M, Ho K.A, Eachus R.A, Ham T.S, Kirby J, Chang M.C.Y, Withers S.T, Shiba Y, Sarpong R, Keasling J.D. (2006) Production of the antimalarial drug precursor artemisinic acid in engineered yeast. Nature, 440(7086):940-943.

Rochon, A., Boyle, P., Wignes, T., Fobert, P.R., and Després, C. (2006) The coactivator function of *Arabidopsis* NPR1 requires the core of its BTB/POZ domain and the oxidation of C-terminal cysteines. Plant Cell 18, 3670-3685.

Ryals, J, Weymann K, Lawton K, Friedrich L, Ellis D, Steiner H-Y, Johnson J, Delaney TP, Jesse T, Vos P et al. (1997) The *Arabidopsis* NIM1 protein shows homology to the mammalian transcription factor inhibitor IkB. Plant Cell, 9:425-439.

Ross, A. F. (1961). Systemic acquired resistance induced by localized virus infections in plants. Virology 14, 340–358.

Sadowski, I., T.C. Su, and J. Parent. (2007) Disintegrator vectors for single copy yeast chromosomal integration. Yeast ; 24: 447–455.

Salazar, JD, Saithong T, Brown PE, Foreman J, Locke JC, Halliday KJ, Carre IA, Rand DA, Millar AJ. (2009) Prediction of photoperiodic regulators from quantitative gene circuit models. *Cell.*; 139: 1170–9

Sakamoto, A, Ueda M, Morikawa H. (2002) *Arabidopsis* glutathione- dependent formaldehyde dehydrogenase is an S-nitrosoglutathione reductase. FEBS Letters 515, 20–24.

Sambrook, J. and Russell D. (2001) Molecular Cloning: A Laboratory Manual (*Third Edition)*. Cold Spring Harbor Laboratory Press.

Schulze, B. *et al.* (2010) Rapid heteromerization and phosphorylation of ligand-activated plant transmembrane receptors and their associated kinase BAK1. *J. Biol. Chem.* 285, 9444–9451

Sengupta, T., Mukherjee, M., Mandal, C., Das, A., and Majumder, H. K. (2003) Functional dissection of the C-terminal domain of type II DNA topoisomerase from the kinetoplastid hemoflagellate *Leishmania donovani*. *Nucleic Acids Res*. 31, 5305-5316

Sengupta, R., Ryter, S. W., Zuckerbraun, B. S., Tzeng, E., Billiar, T. R., and Stoyanovsky, D. A. (2007) Thioredoxin catalyzes the denitrosation of low-molecular mass and protein S-nitrosothiols. Biochemistry 46, 8472–8483.

Sengupta, R., Billiar, T. R., Atkins, J. L., Kagan, V. E., and Stoyanovsky, D. A. (2009) Nitric oxide and dihydrolipoic acid modulate the activity of caspase 3 in HepG2 cells. FEBS Lett. 583, 3525–3530.

Sorokina, O., Kapus, A., Terecskei, K., Dixon, L.E., Kozma-Bognar, L., Nagy, F., and Millar, A.J. (2009) A switchable light-input, light-output system modelled and constructed in yeast. J. Biol. Eng. 3, 15.

Shah, D.M, (1997), Genetic engineering for fungal and bacterial diseases, Current Opinion in Biotechnology, Volume 8, Issue 2, Pages 208-214

Shah, J., Tsui,F., and Klessig,D.F. (1997) Characterization of a salicylic acid-insensitive mutant (sai1) of *Arabidopsis thaliana*, identified in a selective screen utilizing the SA- inducible expression of the tms2 gene. Mol.Plant Microbe Interact. 10:69-78.

Shearer, H.L., Wang, L., DeLong, C., Després, C., and Fobert, P. (2009) NPR1 enhances the DNA binding activity of the *Arabidopsis* bZIP transcription factor TGA7. Botany 87, 561–570.

Sikorski, R S, Hieter P. (1989) A system of shuttle vectors and yeast host strains designed for efficient manipulation of DNA in *Saccharomyces cerevisiae*. Genetics.;122:19–27.

Silva-Rocha, R, de Lorenzo V, (2008) Mining logic gates in prokaryotic transcriptional regulation networks. FEBS Letters 582: 1237–1244

Sinclair, D A, Mills K, Guarente L. (1997) Accelerated aging and nucleolar fragmentation in yeast *sgs1* mutants. Science. 277:1313–1316

Song, W.Y., Wang, G.L., Chen, L.L., Kim, H.S., Pi, L.Y.,Holsten, T., *et al*. (1995) A receptor kinase-like protein encoded by the rice disease resistance gene, Xa21. *Science* 270: 1804–1806.

Song, J., Durrant, W.E., Wang, S., Yan, S., Tan, E.H., and Dong, X. (2011) DNA repair proteins are directly involved in regulation of gene expression during plant immune response. Cell Host Microbe 9, 115-124.

Spadaro, D.; Yun, B. W.; Spoel, S. H.; Chu, C.; Wang, Y. Q.; Loake, G. J. (2010) The Redox Switch: Dynamic regulation of protein function by cysteine modifications. Physiol. Plant., 138, 360- 371.

Spoel, S.H., Koornneef, A., Claessens, S.M.C., Korzelius, J.P., Van Pelt, J.A., Mueller, M.J., Buchala, A.J., Métraux, J.-P., Brown, R., Kazan, K., Van Loon, L.C., Dong, X., and Pieterse, C.M.J. (2003) NPR1 modulates cross-talk between salicylate and jasmonate-dependent defense pathways through a novel function in the cytosol. Plant Cell 15, 760-770.

Spoel, S. H., Mou, Z., Tada, Y., Spivey, N. W., Genschik, P. and Dong, X. (2009) Proteasome-mediated turnover of the transcription coactivator NPR1 plays dual roles in regulating plant immunity. Cell 137, 860–872.

Spoel SH, Tada Y, and Loake GJ (2009) Post-translational protein modification as a tool for transcription reprogramming. New Phytol 186: 333–339

Spoel, S.H., Tada, Y., and Loake, G.J. (2010) Post-translational modification as a tool for transcription reprogramming. New Phytol 186, 333-339.

Spoel, S.H and Loake G.J (2011) Redox-based protein modifications: the missing link in plant immune signalling Current Opinion in Plant Biology, 14:1–7

Stamler, J S, Simon D.I, Osborne J.A, Mullins M.E, Jaraki O, Michel T, Singel D.J, Loscalzo J. (1992) *S*-nitrosylation of proteins with nitric oxide: synthesis and characterization of biologically active compounds. Proceedings of the National Academy of Sciences, USA 89, 444–448

Stoyanovsky, D. A., Tyurina, Y. Y., Tyurin, V. A., Anand, D., Mandavia, D. N., Gius, D., Ivanova, J., Pitt, B., Billiar, T. R., and Kagan, V. E. (2005) Thioredoxin and lipoic acid catalyze the denitrosation of low molecular weight and protein S-nitrosothiols. J. Am. Chem. Soc. 127, 15815–15823.

Strawn, M.A., Marr, S.K., Inoue, K., Inada, N., Zubieta, C., and Wildermuth, M.C. (2007) *Arabidopsis* isochorismate synthase functional in pathogen-induced salicylate biosynthesis exhibits properties consistent with a role in diverse stress responses. J Biol Chem 282, 5919-5933.

Subramaniam, R., Desveaux, D., Spickler, C., Michnick, S.W., and Brisson, N. (2001) Direct visualization of protein interactions in plant cells. Nat. Biotechnol. 19, 769-772.

Sugiyama, K., Izawa, S., Inoue, Y., (2000) The Yap1p-dependent induction of glutathione synthesis in heat shock response of *Saccharomyces cerevisiae*. J. Biol. Chem. 275, 15535e15540.

Tada, Y., Spoel, S.H., Pajerowska-Mukhtar, K., Mou, Z., Song, J., and Dong, X. (2008) *S*-nitrosylation and thioredoxins regulate conformational changes of NPR1 in plant innate immunity. Science 321, 952-956.

Tachibana, T., Okazaki, S., Murayama, A., Naganuma, A., Nomoto, A., and Kuge, S. (2009) A Major Peroxiredoxin-induced Activation of Yap1 Transcription Factor Is Mediated by Reduction-sensitive Disulfide Bonds and Reveals a Low Level of Transcriptional Activation. *J. Biol. Chem.* 284, 4464–4472

Tao, K. (1999) In vivo oxidation-reduction kinetics of OxyR, the transcriptional activator for an oxidative stress-inducible regulon in Escherichia coli. FEBS Lett. 457, 90–92.

Tao, Y. Xie Z, Chen W, Glazebrook J, Chang HS, Han B, Zhu T, and Zou, G (2003). Quantitative nature of *Arabidopsis* responses during compatible and incompatible interactions with the bacterial pathogen *Pseudomonas syringae. Plant Cell* 15, 317–330

Thomas, D and Surdin-Kerjan, Y. (1997) Metabolism of sulfur amino acids in *Saccharomyces cerevisiae*. *Microbiol Mol Biol Rev* 61(4):503-32

Tigges, M., Marquez-Lago T. T., Stelling J., and Fussenegger M., (2009) A tunable synthetic mammalian oscillator. Nature, Vol 457.

Toenniessen, G.H., J.C. O'Toole, and J. DeVries. (2003) Advances in plant biotechnology and its adoption in developing countries. Curr. Opin. Plant Biol. 6:191–198.

Torres, MA, Dangl JL, Jones JD (2002) *Arabidopsis* gp91phox homologues AtrbohD and AtrbohF are required for accumulation of reactive oxygen intermediates in the plant defense response. Proc Natl Acad Sci USA 99: 517–522

Torres, MA, Jones DGJ, Dangl JL (2005) Pathogen-induced, NADPH oxidase-derived reactive oxygen intermediates suppress spread of cell death in *Arabidopsis thaliana*. Nat Genet 37: 1130–1134

Tramier M, Zahid M, Mevel JC, Masse MJ, Coppey-Moisan M (2006) Sensitivity of CFP/YFP and GFP/mCherry pairs to donor photobleaching on FRET determination by fluorescence lifetime imaging microscopy in living cells. Microsc Res Tech 69:933–939

Trotter, E.W and Grant C.M (2005) Overlapping roles of the cytoplasmic and mitochondrial redox regulatory systems in the yeast *Saccharomyces cerevisiae*. *Eukaryot Cell* 4(2):392-400

Truman, W., Bennett, M.H., Kubigsteltig, I., Turnbull, C., and Grant, M. (2007) *Arabidopsis* systemic immunity uses conserved defense signaling pathways and is mediated by jasmonates. Proc. Natl. Acad. Sci. USA 104, 1075-1080.

Truman, W.M., Bennett, M.H., Turnbull, C.G., and Grant, M.R. (2010) *Arabidopsis* auxin mutants are compromised in systemic acquired resistance and exhibit aberrant accumulation of various indolic compounds. Plant Physiol. 152, 1562-1573.

Tsuda, K., Sato, M., Glazebrook, J., Cohen, J.D., and Katagiri, F. (2008) Interplay between MAMP-triggered and SA-mediated defense responses. Plant J. 53: 763–775.

Tsuda, K., Sato, M., Stoddard, T., Glazebrook, J. & Katagiri, F. (2009) Network properties of robust immunity in plants. *PLoS Genet.* 5, e1000772.

Uknes, S., Mauch-Mani,B., Moyer,M., Potter,S., Williams,S., Dincher,S., Chandler,D., Slusarenko,A., Ward,E., and Ryals,J. (1992) Acquired resistance in *Arabidopsis*. Plant Cell 4:645-656.

Van Loon, L.C, Van Strien E.A (1999). The families of pathogenesis-related proteins, their activities, and comparative analysis of PR-1 type proteins. Physiol Mol Plant Pathol 55:85–97.

Van Noorden, R. (2010) Demand for malaria drug soars. Nature. Vol 466 pg 672-673

Verberne, M.C, Verpoorte R, Bol J.F, Mercado-Blanco J, Linthorst H.J.M. (2000). Overproduction of salicylic acid in plants by bacterial transgenes enhances pathogen resistance. *Nat. Biotech.* 18:779–83

Vernooij, B, Friedrich L, Goy PA, Saub T, Kessmann H, et al. (1995) 2,6-Dichloroisonicotinic acid induced resistance to pathogens without the accumulation of salicylic acid. *Mol. Plant-Microbe Interact.* 8:228–34

Vignols, F., Bréhélin, C., Surdin-Kerjan, Y., Thomas, D., and Meyer, Y. (2005) A yeast two-hybrid knockout strain to explore thioredoxin-interacting proteins *in vivo.* Proc. Natl. Acad. Sci. U. S. A. 102, 16729-*16734*

Vlot, AC, Klessig DF, Park S-W. (2008) Systemic acquired resistance: the elusive signal(s). *Curr. Opin. Plant Biol.* 11:436–42

Vlot, A.C, Dempsey D.A and Klessig D.F. (2009) Salicylic acid, a multifaceted hormone to combat disease. *Annu Rev Phytopathol*, 47:177-206

Voth, WP, Richards JD, Shaw JM, Stillman DJ. (2001) Yeast vectors for integration at the HO locus. *Nucleic Acids Res* 29: E59.

Wang, G.L., Song, W.Y., Ruan, D.L., Sideris, S., and Ronald, P.C. (1996) The cloned gene, Xa21, confers resistance to multiple *Xanthomonas oryzae* pv. *oryzae* isolates in transgenic plants. *Mol Plant Microbe Interact* 9: 850–855

Wang, D., Weaver, N.D., Kesarwani, M., and Dong, X. (2005) Induction of protein secretory pathway is required for systemic acquired resistance. Science 308, 1036-1040.

Wang, D., Amornsiripanitch, N., and Dong, X. (2006a) A genomic approach to identify regulatory nodes in the transcriptional network of systemic acquired resistance in plants. PLoS Pathog 2, e123.

Wang, Y., Yun, B.W., Kwon, E., Hong, J.K., Yoon, J., and Loake, G.J. (2006b) *S*-nitrosylation: an emerging redox-based post-translational modification in plants. J Exp Bot 57, 1777-1784.

Wang, G. Ellendorff U, Kemp B, Mansfield JW, Forsyth A, Mitchell K, Bastas K, Liu CM, Woods-Tor A, Zipfel C, de Wit PJ, Jones JD, Tor M, Thomma BP (2008) A genome-wide functional investigation into the roles of receptor-like proteins in *Arabidopsis. Plant Physiol.* 147, 503–517

Wang, Y.Q, Feechan A, Yun B.W, Shafiei R, Hofmann A, et al. (2009) S-nitrosylation of AtSABP3 antagonizes the expression of plant immunity. *J. Biol. Chem.* 284:2131–7

Wang, W, Barnaby JY, Tada Y, Li H, Tör M, Caldelari D, Lee DU, Fu XD, Dong X. (2011) Timing of plant immune responses by a central circadian regulator. *Nature* 470: 110.

Ward, E.R., Uknes, S.J., Williams, S.C., Dincher ,S.S., Wiederhold, D.L., Alexander, D.C., hl-Goy,P., Metraux,J.P., and Ryals,J.A. (1991) Coordinate Gene Activity in

Response to Agents That Induce Systemic Acquired Resistance. Plant Cell 3:1085-1094.

Waypa, G.B, Marks J.D, Guzy R, Mungai P.T, Schriewer J, Dokic D, Schumacker P.T. (2010) Hypoxia triggers subcellular compartmental redox signaling in vascular smooth muscle cells. Circ Res 106: 526–535

Weber, H, Bernhardt A, Dieterle M, Hano P, Mutlu A, Estelle M, Genschik P, Hellmann H. (2005) *Arabidopsis* AtCUL3a and AtCUL3b form complexes with members of the BTB/POZ-MATH protein family. *Plant Physiol,* 137:83-93

Weng, J.K, Li X, Bonawitz N.D, Chapple C. (2008) Emerging strategies of lignin engineering and degradation for cellulosic biofuel production. Curr Opin Biotechnol, 19:166-172.

Whisson, S. C., Boevink, P. C., Moleleki, L., Avrova, A. O., Morales, J. G., Gilroy, E. M., Armstrong, M. R., Grouffaud, S., van West, P., Chapman, S., Hein, I., Toth, I. K., Pritchard, L., and Birch, P. R. (2007). A translocation signal for delivery of oomycete effector proteins into host plant cells. Nature 450:115-118.

Wiermer, M., Feys, B. J. & Parker, J. E. (2005) Plant immunity: the EDS1 regulatory node. *Curr. Opin. Plant Biol.* 8, 383–389

Wildermuth, M.C, Dewdney J, Wu G, Ausubel F.M. (2001), Isochorismate synthase is required to synthesize salicylic acid for plant defence. *Nature* 414:562–71

Wojtaszek, P (1997) Oxidative burst: an early plant response to pathogen infection. Biochem J 322: 681–692

Wood, M.J., Storz, G., and Tjandra, N. (2004) Structural basis for redox regulation of Yap1 transcription factor localization. Nature 430, 917–921.

Wu, A., and Moye-Rowley, W.S. (1994) *GSH1*, which encodes g-glutamylcysteine synthetase, is a target gene for yAP-1 transcriptional regulation. *Mol Cell Biol* 14: 58332– 55839.

Wu, A.L and Moye-Rowley W.S (1994) GSH1, which encodes gamma-glutamylcysteine synthetase, is a target gene for yAP-1 transcriptional regulation. *Mol Cell Biol* 14(9):5832-9

Yan, C., Lee, L.H., and Davis, L.I. (1998) Crm1p mediates regulated nuclear export of a yeast AP-1-like transcription factor. EMBO J. 17, 7416–7429.

Yun, B.W., Feechan A., Yin M., Saidi N.B.B., Le Bihan T., Yu M., Moore J.W., Kang J.G., Kwon E.J., Spoel S.H., Pallas J.A., and Loake G.J. (2011) *S*-nitrosylation of NADPH oxidase regulates cell death in plant immunity. Nature 478: 264–268.

Zander, M, La Camera S, Lamotte O, Metraux J-P, Gatz C (2010) *Arabidopsis thaliana* class-II TGA transcription factors are essential activators of jasmonic acid/ethylene-induced defense responses. Plant J 61:200–210

Zhang, Y., Fan, W., Kinkema, M., Li, X., and Dong, X. (1999) Interaction of NPR1 with basic leucine zipper protein transcription factors that bind sequences required for salicylic acid induction of the *PR-1* gene. Proc. Natl. Acad. Sci. USA 96, 6523–6528

Zhang, Y, Tessaro MJ, Lassner M, Li X. (2003) Knockout analysis of Arabidopsis transcription factors TGA2, TGA5 and TGA6 reveals their redundant and essential roles in systemic acquired resistance. Plant Cell; 15:2647-53.

Zhang, Y., Cheng, Y.T., Qu, N., Zhao, Q., Bi, D. and Li, X. (2006) Negative regulation of defense responses in *Arabidopsis* by two NPR1 paralogs. *Plant J*. 48, 647–656.

Zheng, Z, Qamar SA, Chen Z, Mengiste T (2006) *Arabidopsis* WRKY33 transcription factor is required for resistance to necrotrophic fungal pathogens. Plant J 48: 592–605

Zheng, M., Aslund, F., and Storz, G. (1998) Activation of the OxyR transcription factor by reversible disulfide bond formation. Science 279, 1718–1721.

Zhou, N., Tootle, T.L., Tsui, F., Klessig, D.F. and Glazebrook, J. (1998) PAD4 functions upstream from salicylic acid to control defense responses in *Arabidopsis*. Plant Cell, 10(6), 1021–1030.

Zhou, JM, Trifa Y, Silva H, Pontier D, Lam E, Shah J, Klessig DF (2000) NPR1 differentially interacts with members of the TGA/OBF family of transcription factors that bind an element of the PR-1 gene required for induction by salicylic acid. Mol Plant Microbe Interact 13: 191–202

Zipfel, C. (2008). Pattern-recognition receptors in plant innate immunity. *Curr. Opin. Immunol.* 20, 10–16

Appendix A

Calculation of R_{red} and R_{ox} values of roGFP2 expressed in BY4741

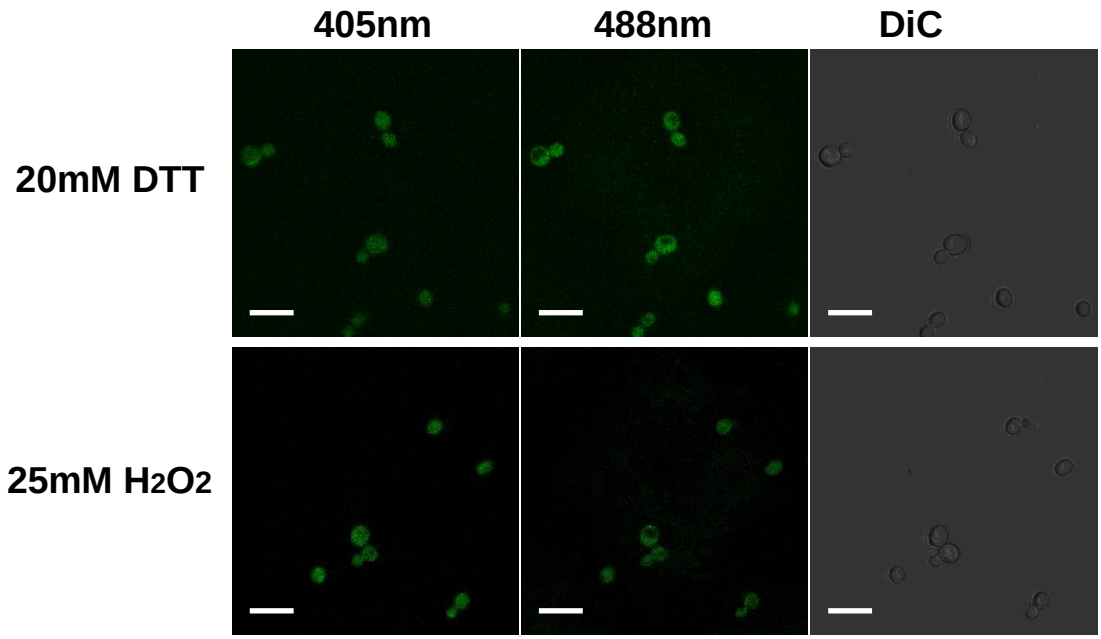

Representative image of BY4741 yeast cells expressing either fully reduced (DTT) or fully oxidised (H_2O_2) roGFP2. Images were captured simultaneously at excitation maxima of 408 and 488nm, with emission at 525nm and ratiometric imaging completed using Image-Pro Analyzer 7.0. This reveals that the addition of 20mM DTT provides a 405/488 ratio of 0.64 while the addition of 25mM H_2O_2 provides a 405/488 ratio of 1.42. White bar indicates 25µm.

Appendix B

The Kappa code and parameters used to develop the model

Parameters

System Kinetics

1. 2 hours for GSNOR/TRXH5 to appear once induced.
2. 90 minutes from cytosolic oligomer to nucleic monomer.
3. 4-5 hours for NPR1 monomer threshold to be reached.
4. 2-3 hours for LUCIFERASE protein translation.

Relative Protein Units (based on promoter strength)

400 NPR1
400 TGA3
300 GSNO (when switched on)
250 TRXH5 (when switched on)

Assumptions

1. Assume GSNO and TRXH5 function as on/off switches (respectively).
2. Equilibrium favours the NPR1 oligomer until GSNOR/TRXH5 takes action.
3. Assume that disassociation of the oligomer occurs when all NPR1 units are denitrosylated.
4. The NPR1 monomer migrates into the nucleus.
5. The NPR1-TGA3 complex is needed for transcriptional activity.
6. The number of LUCIFERASE protein units (RLU) is proportional to monomeric NPR1.
7. GSNO/TRXH5 protein is highly stable and therefore the system cannot re-switch more than once.
8. TRXH5 and GSNOR do not degrade very quickly which inhibits resetting of system.

Kappa Script

```
### Agents:
%agent: NPR1(C156~u~s,S1,S2,tga3,loc~nuc~cyt)
%agent: GSNO(x~active~inactive)
%agent: GSNOR(x)
%agent: TRXH5(x)
%agent: TGA3(npr1,dna)
%agent: DNA(type~luc,tga3)
%agent: mRNA(type~luc,loc~nuc~cyt)
%agent: LUC()

### Rules:
# GSNO action
'NPR1-GSNO binding' NPR1(C156~u), GSNO(x~active) -> NPR1(C156~u!1),
GSNO(x~active!1) @ 1.0
'NPR1-GSNO unbinding' NPR1(C156!1), GSNO(x!1) -> NPR1(C156), GSNO(x) @
1.0
'NPR1-GSNO S-nitrosylation' NPR1(C156~u!1), GSNO(x~active!1) ->
NPR1(C156~s!1), GSNO(x~active!1) @ 10.0

# GSNOR action
'GSNOR creation'  -> GSNOR(x) @ 0.0
'GSNO-GSNOR binding' GSNO(x~active), GSNOR(x) -> GSNO(x~active!1),
GSNOR(x!1) @ 1.0
'GSNO-GSNOR unbinding' GSNO(x!1), GSNOR(x!1) -> GSNO(x), GSNOR(x) @
10.0
'GSNO inactivation' GSNO(x~active) -> GSNO(x~inactive) @ 0.001
'GSNO-GSNOR inactivation' GSNO(x~active!1), GSNOR(x!1) ->
GSNO(x~inactive!1), GSNOR(x!1) @ 10.0
'GSNO activation' GSNO(x~inactive) -> GSNO(x~active) @ 0.05
'GSNOR degradation' GSNOR(x) ->  @ 0.05

# TRXH5 action
'TRXH5 creation'  -> TRXH5(x) @ 0.0
'NPR1-TRXH5 binding' NPR1(C156~s), TRXH5(x) -> NPR1(C156~s!1),
TRXH5(x!1) @ 1.0
'NPR1-TRXH5 unbinding' NPR1(C156!1), TRXH5(x!1) -> NPR1(C156), TRXH5(x)
@ 10.0
'NPR1 de-nitrosylation' NPR1(C156~s) -> NPR1(C156~u) @ 0.1
'NPR1-TRXH5 de-nitrosylation' NPR1(C156~s!1), TRXH5(x!1) ->
NPR1(C156~u!1), TRXH5(x!1) @ 10.0
'TRXH5 degradation' TRXH5(x) ->  @ 0.05

# NPR1 action
'NPR1 multimer formation' NPR1(C156~s,S1,S2,loc~cyt),
NPR1(C156~s,S1,S2,loc~cyt), NPR1(C156~s,S1,S2,loc~cyt),
NPR1(C156~s,S1,S2,loc~cyt) -> NPR1(C156~s,S1!1,S2!2,loc~cyt),
```

```
NPR1(C156~s,S1!1,S2!3,loc~cyt), NPR1(C156~s,S1!2,S2!4,loc~cyt),
NPR1(C156~s,S1!3,S2!4,loc~cyt) @ 100.0
'NPR1 oligomer disassociation' NPR1(C156~u,S1!1,S2!2,loc~cyt),
NPR1(C156~u,S1!1,S2!3,loc~cyt), NPR1(C156~u,S1!2,S2!4,loc~cyt),
NPR1(C156~u,S1!3,S2!4,loc~cyt) -> NPR1(C156~u,S1,S2,loc~cyt),
NPR1(C156~u,S1,S2,loc~cyt), NPR1(C156~u,S1,S2,loc~cyt),
NPR1(C156~u,S1,S2,loc~cyt) @ 5.0

# Transport
'NPR1 nuclear transport' NPR1(C156~u,S1,S2,loc~cyt) ->
NPR1(C156~u,S1,S2,loc~nuc) @ 10.0
'NPR1 cytosolic transport' NPR1(tga3,loc~nuc) -> NPR1(tga3,loc~cyt) @ 10.0
'mRNA cytosolic transport' mRNA(loc~nuc) -> mRNA(loc~cyt) @ 10.0

# Reporter system
'NPR1-TGA3 binding' NPR1(C156~u,tga3,loc~nuc), TGA3(npr1,dna) ->
NPR1(C156~u,tga3!1,loc~nuc), TGA3(npr1!1,dna) @ 1.0
'NPR1-TGA3 unbinding' NPR1(tga3!1,loc~nuc), TGA3(npr1!1,dna) ->
NPR1(tga3,loc~nuc), TGA3(npr1,dna) @ 10.0
'Transcription factor binding' NPR1(C156~u,tga3!1,loc~nuc), TGA3(npr1!1,dna),
DNA(type~luc,tga3) -> NPR1(C156~u,tga3!1,loc~nuc), TGA3(npr1!1,dna!2),
DNA(type~luc,tga3!2) @ 1.0
'Transcription factor unbinding' NPR1(tga3!1,loc~nuc), TGA3(npr1!1,dna!2),
DNA(type~luc,tga3!2) -> NPR1(tga3!1,loc~nuc), TGA3(npr1!1,dna),
DNA(type~luc,tga3) @ 100.0
'Transcription' DNA(type~luc,tga3!_) -> DNA(type~luc,tga3!_),
mRNA(type~luc,loc~nuc) @ 1.0
'Translation' mRNA(type~luc,loc~cyt) -> mRNA(type~luc,loc~cyt), LUC() @ 5.0
'mRNA degradation' mRNA() ->  @ 1.0
'LUC degradation' LUC() ->  @ 0.05

### Initial Conditions:
%init: 100 (NPR1(C156~u,S1!1,S2!2,tga3,loc~cyt),
NPR1(C156~u,S1!1,S2!3,tga3,loc~cyt), NPR1(C156~u,S1!2,S2!4,tga3,loc~cyt),
NPR1(C156~u,S1!3,S2!4,tga3,loc~cyt))
%init: 400 (TGA3(npr1,dna))
%init: 300 (GSNO(x~active))
%init: 1 (DNA(type~luc,tga3))
```

Appendix C - Systems Biology Graphical Notation (SBGN) diagram

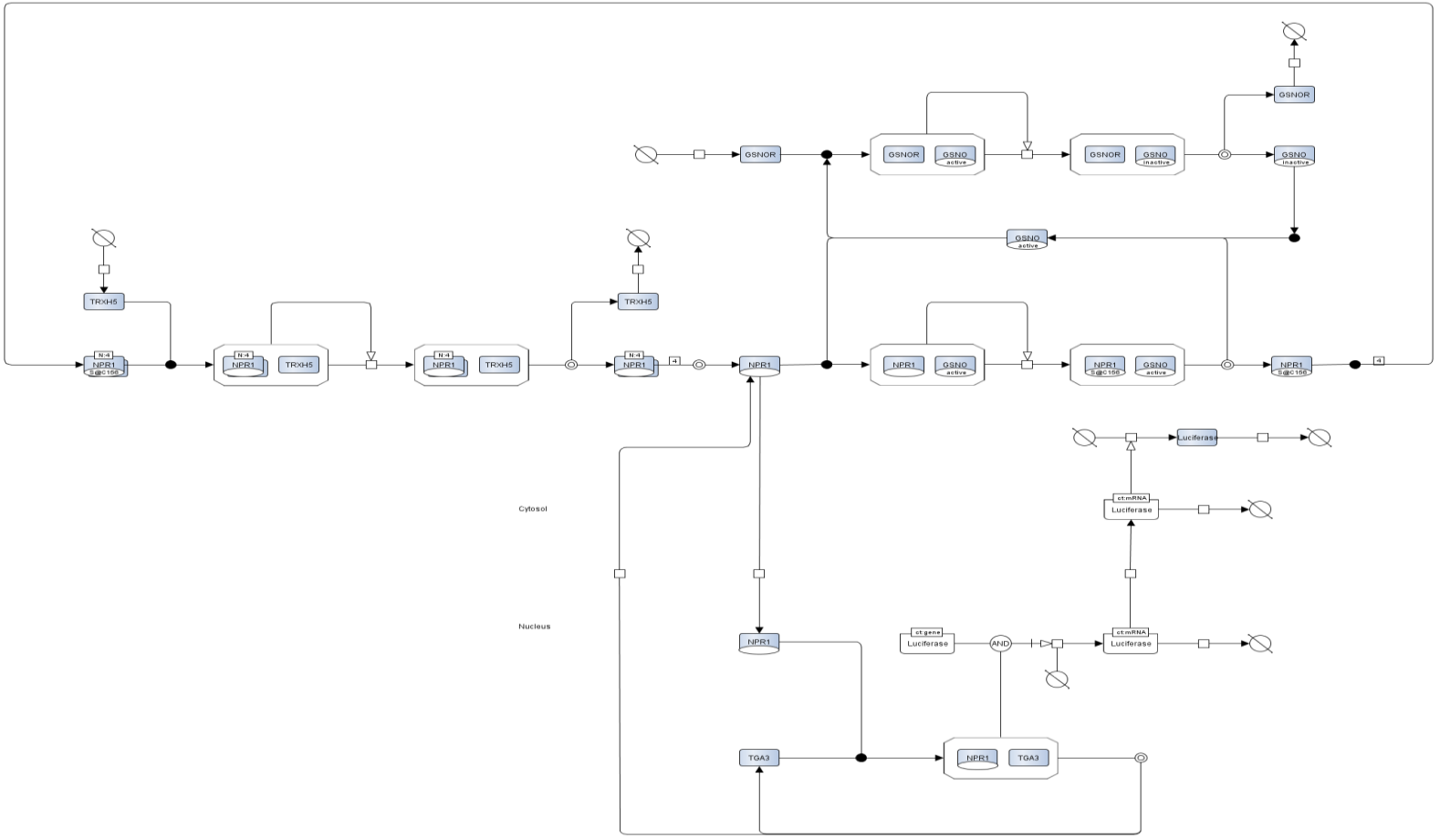

SBGN representative of the NPR1 oligomer-to-monomer switch leading to NPR1-TGA3 protein interaction and subsequent reporter gene activation. Constructed, tested and optimised by John R. Wilson-Kanamori, School of Informatics, University of Edinburgh. Nomenclature, standards and relationships are defined in accordance with Le Novère et al., (2009).

Publications

Yun, B.W., Feechan, A., Yin, M., Saidi, N.B.B., Le Bihan, T., Yu, M., **Moore, J.W**., Kang, J.G., Kwon, E.J., Spoel, S.H., Pallas, J.A., and Loake, G.J. (2011) *S*-nitrosylation of NADPH oxidase regulates cell death in plant immunity. Nature **478:** 264–268.

Moore, J.W., Loake, G.J., and Spoel, S.H. (2011) Transcription Dynamics in Plant Immunity. Plant Cell **23**: 2809-2820.